

REPUBLIQUE DU CAMEROUN

Paix-Travail-Patrie



DEPARTMENT DE GENIE CIVIL
DEPARTMENT OF CIVIL ENGINEERING

REPUBLIC OF CAMEROON

Peace-Work-Fatherland



UNIVERSITÀ
DEGLI STUDI
DI PADOVA

DEPARTMENT OF CIVIL, ARCHITECTURAL
AND ENVIRONMENTAL ENGINEERING

**DESIGN OF A RETAINING STRUCTURE AND IT'S
PUMPING SYSTEM FOR AND UNDERGROUND
STRUCTURE CONSTRUCTION
CASE STUDY: AULNAY-SOUS-BOIS TRAIN STATION**

A thesis submitted in partial fulfilment of the requirement for the degree of Master of Engineering

(MEng) in Civil Engineering

Curriculum: Geotechnical engineering

Presented by:

TCHIINDA KENGNE Franck Junior

Student Number: 16T21148

Supervised by:

Pr. Simonetta COLA

ACADEMIC YEAR: 2020-2021

REUBLIQUE DU CAMEROUN

Paix-Travail-Patrie



DEPARTMENT DE GENIE CIVIL
DEPARTMENT OF CIVIL ENGINEERING

REPUBLIC OF CAMEROON

Peace-Work-Fatherland



UNIVERSITÀ
DEGLI STUDI
DI PADOVA

DEPARTMENT OF CIVIL, ARCHITECTURAL
AND ENVIRONMENTAL ENGINEERING

**DESIGN OF A RETAINING STRUCTURE AND IT'S
PUMPING SYSTEM FOR AND UNDERGROUND
STRUCTURE CONSTRUCTION
CASE STUDY: AULNAY-SOUS-BOIS TRAIN STATION**

*A thesis submitted in partial fulfilment of the requirement for the degree of Master of Engineering
(MEng) in Civil Engineering*

Curriculum: Geotechnical engineering

Presented by:

TCHINDA KENGNE Franck Junior

Student Number: 16T21148

Supervised by:

Pr. Simonetta COLA

ACADEMIC YEAR: 2020-2021

DEDICATION

In memory of my Grand-Father,

Papa Maurice TCHINDA

(1929-2012)

ACKNOWLEDGMENTS

This thesis is a humble attempt to sketch down the contributions of all those persons who have directly or indirectly contributed by their precious time, help and guidance to the completion of this thesis.

I therefore extend my sincere thanks and gratitude to:

- The **President of the Jury**, for the honour accepting to preside this Jury
- The **Examiner of the Jury**, for accepting to examine this work through remarks and suggestions made with regards to this work
- My supervisors **Prof Simonetta COLA** and **Eng Parfait POUEMI** for their encouragement, constructive criticism, patient guidance and friendly cooperation during my research.
- **Pr. NKENG George ELAMBO**, Director of the National Advanced School of Public Works (NASPW) Yaoundé, for his unwavering commitment to providing standard engineering education.
- **Pr. MBESSA Michel**, the head of the Civil Engineering Department, for his effort to see that the work is completed on schedule and for his fatherly wise counsel.
- The **Prof Carmelo MAJORANA**, for his participation in the Master of Engineering curricula in the NASPW with the DICEA/University of Padua in Italy
- Both the **teaching and administrative staff of NASPW**, who inculcated in us moral values and knowledge in the civil engineering field and for services rendered
- All my **friends, classmates, academic elders and juniors** for the support and the memorable time spent together
- My whole **family** for the good education and encouragement during all these years
- My parents **Mr. KENGNE TCHINDA Roger** and **Mme TCHUENCHE Stephanie Diane** for the support during all these years
- My tutor **Mr. FONKOU Michel** and his wife **Mme NKACHE Anne Florence** for their financial support and permanent assistance.
- My uncle **Mr. KENGNE François** and his wife for their assistance.

LIST OF ABBREVIATIONS AND SYMBOLS

CFMS : Comité français de mécanique des sols (French Committee for Soil Mechanics)

CSTC : Centre scientifique et technique de la construction (Scientific and Technical Center for Construction)

FDM: finite difference method

FEM: finite element method

GTR : guide du terrassement routier (Guide to roadwork)

GWT : ground water table

SFEG : Syndicat national des entrepreneurs de puits et de forages pour l'eau et la géothermie (National Union of Well and Borehole Contractors for Water and Geothermal)

c: cohesion

S_u : undrained shear strength

E: young modulus

γ : unit weight of a soil

k_a : active lateral earth coefficient

q_s : eventual surcharge

Φ : friction angle

ν : Poisson's ratio

k_h : horizontal permeability

k_v : vertical permeability $(c_u)_b$: average undrained shear strength below the toe of the wall

D_f : thickness of the firm layer

D_s : thickness of the failure surface

q_s : eventual surcharge

H_0 : height of the retained earth

N_c : bearing capacity coefficient

r_p : radius of the well

h_w : height of the wet well

ABSTRACT

The main objectives of this thesis were the verification of the stability of a diaphragm wall and the determination of the flow infiltrated in the station of Aulnay-sous-Bois train station in order to design the pumping system to be set up for drainage the water from the train station. In order to solve this problem and achieve these objectives, a comparison was made between the analytical calculation allowing the verification of the wall stability and the determination of the flow rate to be pumped, and a numerical analysis carried out with the Plaxis code which is a numerical model developed within the finite elements. The finite element method used by the Plaxis model is better adapted because the interaction effect between the soil and the wall is considered. The verification of this stability involves the verification of the wall against the uplift phenomenon, the determination of the forces in the struts which are essential elements for the realization of the diaphragm wall, the determination of the displacement and the determination of the flow rate due to water seepage. For the case studied here, the struts were realized in two rows for the case studied here separated by five meters when going down and by six meters when going in horizontal direction. The analytical calculation indicated that the compression forces are equal to 3370 kN and 8729 kN in the strut on the first and second row respectively and the water flow that has to be pumped is 38.06 m³/h and this with a pump of at least 3 kW, the minimum thickness of the raft will be 5.67 m to avoid the lifting of the raft due to the water-level difference inside and outside the station and all these informations were confirmed by the Plaxis code.

KEYS WORDS: Diaphragm wall, seepage, analytical calculus, numerical analysis, underground structure.

Résumé

Ce mémoire avait pour objectif général la vérification de la stabilité d'un mur de soutènement du type paroi moulée et la détermination du débit d'eau infiltrée dans la gare d'Aulnay-sous-Bois afin de dimensionner le système de pompage qui sera mis en place pour expulser cette eau de la gare. Afin d'aborder ce problème et d'atteindre cet objectif, une comparaison a été faite entre le calcul analytique permettant la vérification de la stabilité des parois et le calcul du débit à pomper, et une analyse numérique réalisée avec le logiciel Plaxis qui est un logiciel d'éléments finis pour vérifier que les résultats obtenus avec la méthode analytique s'approchaient au maximum de la réalité. La méthode des éléments finis utilisée par le logiciel Plaxis est mieux adaptée, car l'effet d'interaction entre le sol et la paroi est mieux considéré. La vérification de cette stabilité est passée par la vérification de la résistance de la paroi au soulèvement, à la détermination des forces dans les buttons qui sont des éléments indispensables à la réalisation des parois moulées, la détermination des déplacements et la détermination du débit due à l'infiltration d'eau. Les buttons ont été réalisés en deux rangées pour le cas étudié ici séparé de 5m lorsque l'on va vers le bas et de 6m lorsque l'on sort du plan. Après avoir effectué le calcul analytique, on obtient que la force dans les buttons est de 3370 kN et 8729 kN pour les buttons de la première et deuxième rangée respectivement, le débit d'eau qui sera pompé est de 38.06 m³/h à l'aide d'une pompe d'une puissance d'au moins 3kW, l'épaisseur minimale du radier réalisé sera de 5.67m pour éviter le soulèvement de ce dernier dû à la différence de niveau de l'eau à l'intérieur et à l'extérieur de la station et toutes ces informations ont été confirmées par le logiciel Plaxis.

MOTS CLES : Paroi moulée, infiltration, calcul analytique, analyse numérique, ouvrages souterrains.

LIST OF FIGURES

Figure 1.1. Schematic diagram of sealing diaphragm wall.....	3
Figure 1.2. Installation principle of a prefabricated diaphragm wall.....	3
Figure 1.3. Schematic representation of a classic diaphragm wall (CSTC, juillet 2014).....	4
Figure 1.4. Stages of realization of the diaphragm wall (CSTC, juillet 2014).....	5
Figure 1.5. Concreting of diaphragm wall.....	7
Figure 1.6. Section of the diaphragm wall with the button (BUDHU, 2011).....	9
Figure 1.7. Lateral pressure distribution from a) coarse-grained soils; b) fine grained soil with $\gamma H_0/c_u < 4$; c) fine grained soil with $\gamma H_0/c_u > 4$ (BUDHU, 2011)	9
Figure 1.8. Abacus for the evaluation of N_c (BUDHU, 2011)	11
Figure 1.9. Decomposition of the plate (MAJORANA, 2020)	13
Figure 1.10. Coefficient use by the FDM method (MAJORANA, 2020)	14
Figure 1.11. Mode of rotational failure of embedded walls (Eurocode 7).....	15
Figure 1.12. Rotational failure of the wall section (Eurocode 7).....	15
Figure 1.13. Examples of overall instability (Eurocode 7).....	16
Figure 1.14. Example of situation where seepage might be critical (Eurocode 7).....	16
Figure 1.15. Example of confined seepage (SIMONINI, 2019).....	18
Figure 1.16. Permeameter with the same level of water in the left and right tank (COLA, 2021)	19
Figure 1.17. Permeameter with different levels of water in right and left tank (COLA, 2021)	20
Figure 1.18. Illustration of water pressure under an impermeable layer (COLA, 2021)	21

Figure 1.19. Out-of-balance water pressure on the wall. a) wall layout, b) water pressures on wall, c) Net pressure (Clayton et al., 2014).....	21
Figure 1.20. Partially penetrating trench that does not reach the aquifer bottom. (Teatini, 2019).....	23
Figure 1.21. parameter λ vs d/b (Teatini, 2019).....	23
Figure 1.22. Trench with a negligible thickness b that does not reach the impermeable rock (Teatini, 2019).....	24
Figure 1.23. C_1 and C_2 parameters (Teatini, 2019).....	25
Figure 1.24. Two trenches with a negligible thickness b that does not reach the impermeable rock (Teatini, 2019).....	25
Figure 1.25. Pumping device to avoid the cancelling of the effective stresses at the bottom of the excavation. (CFMS, 2016).....	26
Figure 1.26. Schematic section of a manual piston pump (a), centrifugal pump (b).....	27
Figure 1.27. Partial grid of a flow domain (BUDHU, 2011).....	28
Figure 1.28. Three types of boundary encountered in practice (BUDHU, 2011).....	29
Figure 1.29. Grid for the finite difference analysis. (BUDHU, 2011).....	32
Figure 2.1. Coulomb model of friction	38
Figure 2.8. lateral stress distribution on the wall.....	40
Figure 2.3. Net water pressure distribution on the wall.....	40
Figure 2.4. Partial grid of a flow domain of the station.....	42
Figure 2.5. Plaxis interface	49
Figure 2.6. Box of input dimension in Plaxis	50
Figure 2.7. Main windows of Plaxis output program.....	54

Figure 3.1. Localization of the Aulnay sous Bois town (GOOGLE MAP).....	56
Figure 3.2. Aerial view of the localization of the Aulnay station (LOMBARDI, 2019).....	56
Figure 3.3. 3D presentation of the Aulnay-sous-bois station (LOMBARDI, 2019)	57
Figure 3.4. Picture of marls with pholadomies sampling.....	59
Figure 3.5. Picture of Greensand sampling.....	59
Figure 3.6. Picture of limestone of saint ouen sampling.....	59
Figure 3.7. Picture of beauchamp sand sampling.....	60
Figure 3.8. Picture of marls and pebbles sampling.....	60
Figure 3.9. Picture of coarse limestone sampling.....	61
Figure 3.10. Cross section of the train station.....	63
Figure 3.11. Meshing system of the station on initial state soil.....	70
Figure 3.12. Phase construction of the project.....	70
Figure 3.13. Model of the constructed wall at initial state.....	71
Figure 3.14. Deformation of the model.....	71
Figure 3.15. Deformation of the wall.....	72
Figure 3.16. Force on the struts in Plaxis code.....	73
Figure 3.17. Bending moment diagram of the wall.....	74
Figure 3.18. Shear force diagram of the wall.....	75
Figure 3.19. Ground water flow in the station.....	76

LISTS OF TABLES

Table 1.1. Partial factors on action (Eurocode, 1997)	33
Table 1.2. Partial factors on materials (Eurocode, 1997)	33
Table 1.3. Partial factors on resistance (Eurocode, 1997)	34
Table 2.1. Recapitulative table of the parameter's symbols	36
Table 3.1. data of the problem (LOMBARDI, 2019)	61
Table 3.2. Properties of concrete C35/45	62
Table 3.3. Properties of the steel B500	62
Table 3.4. Recapitulative of the pressure on the wall	64
Table 3.5. Presentation of the force obtains in each button	64
Table 3.6. Presentation of the maximum displacement of the wall	65

TABLE OF CONTENTS

CHAPTER 1: LITERATURE REVIEW	2
Introduction	2
1.1. Types of diaphragm walls	2
1.1.1. Sealing diaphragm wall	2
1.1.2. Prefabricated diaphragm walls	3
1.1.3. Simple retaining diaphragm wall.....	4
1.2. Implementation method of a simple retaining diaphragm wall.....	4
1.2.1. Bentonite mud.....	6
1.2.1.1. Generalities.....	6
1.2.1.2. Behaviour of the bentonite mud in the trench	6
1.2.2. Reinforcement cage	6
1.2.3. Diaphragm wall concrete.....	7
1.2.4. Joints between panels	7
1.2.4.1. Joined tubes	7
1.2.4.2. Keyed joints.....	8
1.2.5. Anchorage.....	8
1.3. Design procedure for diaphragm walls	8
1.3.1. Stability verification	8
1.3.2. Wall displacement calculation and loads on the struts	10
1.3.3. Analytical method for determining the displacement of the wall	12
1.3.3.1. General concept	12
1.3.3.2. Squared plate simply supported at the edges.....	13
1.3.3.3. Squared plate built-in at the edges.....	14

1.3.4. Limit state for embedded wall	15
1.4. Generalities on the pumping system	16
1.4.1. Theory of seepage	16
1.4.1.1. Liquefaction under seepage	18
1.4.2. Methods of design of the drainage systems.....	22
1.4.2.1. Partially penetrating trench, confined aquifer	22
1.4.2.2. Partially penetrating trench, phreatic aquifer	23
1.5. Drainage associated to an impermeable wall	25
1.6. Type of dewatering pump	26
1.7. Calculation of the flow due to seepage in diaphragm wall	27
1.8. Eurocode recommendation for the design of the wall.....	32
1.8.1. Ultimate limit state	32
1.8.1.1. Design approach 1	32
1.8.1.2. Design approach 2	32
1.8.1.3. Design approach 3	32
1.8.2. Serviceability limit state	34
Conclusion.....	34
CHAPTER 2: METHODOLOGY	35
Introduction	35
2.1. General recognition of the site	35
2.2. Data acquisition.....	35
2.2.1. Geotechnical data	35
2.2.2. Load data	36
2.3. Input data for the design and calculation of flow in diaphragm walls	36
2.3.1. Input data for the calculation of the flow	36

2.3.1.1. Permeability	36
2.3.1.2. Water level inside and outside the diaphragm walls	37
2.3.2. Input data for the design of the wall	37
2.3.2.1. External load near the diaphragm wall	37
2.3.2.2. Friction angle and cohesion of a soil	37
2.3.3. Input data for the calculation of the displacements of the wall	38
2.3.4. Input data for the calculation of the compression force on the struts	38
2.3.5. Input data for the verification of the stability of the wall	38
2.4. Analytical design method	38
2.4.1. Semi-empirical method	39
2.4.1.1. Check the stability against bottom heave	39
2.4.1.2. Determine the lateral stress on the walls for the soil type	39
2.4.1.3. Calculate the forces on the struts at each level	41
2.4.1.4. Deformation of the wall	41
2.4.1.5. Calculate resultant forces on the struts	41
2.4.2. Determination of the flow with the finite difference method	41
2.5. Choice of the pump to drain the bottom of the excavation	43
2.6. Numerical design method	44
2.6.1. Presentation of the modelling software: Plaxis 2D	44
2.6.2. Plaxis input component	47
2.6.2.1. Input of geometry	49
2.6.2.2. Input of the dimensions of the project	49
2.6.2.3. Plaxis input program structures-modes	50
2.6.3. Material model	51
2.6.3.1. Linear elastic model	51

2.6.3.2. Mohr coulomb model	51
2.6.3.3. Hardening soil model	51
2.6.3.4. Modified cam clay model.....	51
2.6.3.5. Soft soil model	52
2.6.3.6. Soft soil creep model.....	52
2.6.3.7. Jointed rock model	52
2.6.3.8. Concrete model	52
2.6.4. Mesh	53
2.6.5. Presentation of the phase's construction of the project.....	53
2.6.6. Plaxis output program	53
Conclusion.....	54
CHAPTER 3: RESULTS AND INTERPRETATIONS	55
Introduction	55
3.1. General presentation of the site	55
3.1.1. Localization	55
3.1.2. Climate	57
3.1.3. Demography	57
3.1.4. Economic activity.....	58
3.2. Presentation of the project.....	58
3.2.1. Backfill (R).....	58
3.2.2. Marls with Pholadomies (MPH)	59
3.2.3. Greensand (SV).....	59
3.2.4. Limestone of Saint Ouen (SO)	59
3.2.5. Beauchamp sand (SB)	60
3.2.6. Marls and Pebbles (MC)	60

3.2.7. Coarse limestone (CG)	60
3.2.8. Soil parameters	61
3.2.9. Design load.....	61
3.2.10. Materials characteristics	62
3.2.11. Presentation of the geometry of the train station.....	62
3.3. Analytical results.....	63
3.3.1. Stability against bottom heave	63
3.3.2. Lateral pressure on the wall.....	63
3.3.3. Compression force on the struts	64
3.3.4. Deformation of the wall	65
3.3.5. Calculation of the flow	65
3.3.6. Determination of the power of the pump	65
3.3.7. Minimum height of the raft	66
3.4. Numerical results.....	67
3.4.1. Hypothesis	67
3.4.2. Calculation steps	67
3.4.3. Mesh generation	69
3.4.4. Principal result.....	70
3.4.4.1. Deformation of the wall.....	71
3.4.4.2. Compression force in the struts	73
3.4.4.4. Shear force diagram.....	75
3.4.4.5. Flow on the station	75
Conclusion.....	76
Bibliography	78

GENERAL INTRODUCTION

Retaining structures are essential to retain unstable soil next to a road or railway, creation of underground space, etc. When space needs to be created in the ground, it could be possible to excavate a very large area and then build retaining walls, but this is not possible when the excavation is done in unstable soils or when the working space is reduced and this implies the use of a diaphragm wall. Diaphragm wall can easily be installed near existing structures with little loss of bearing capacity of these structures. To construct it, a trench is dug in the ground and at the same time, the bentonite mixture is pumped into the ground to stabilize the trench walls. When the excavation goes beyond the water table, it is indispensable to associate to this wall a pumping system to dewater the bottom of the excavation and allow the work in dry conditions. Pumping wells plays a very important role here because they are lowering the level of the water table (WT). A numerical modelling was carried out in the Plaxis code and the results of the analytical calculation could be compared with the numerical calculation. The chapter one of this work deals with the literature review elaborating on the history of the retaining wall and the technology to install the diaphragm wall that is the wall use in the train station project in Aulnay-sous-Bois. Moreover, the chapter one also introduces the basic features of the pumping systems use in coupling to the diaphragm walls to pump the underground water in order to permit the earthwork in dry condition. Eurocode 7 is also presented in chapter 1: Eurocode is a code describes how to design geotechnical structures, using the limit state design philosophy. This norm intended to be applied to the geotechnical aspects of the design of buildings and civil engineering works and it is concerned with the requirements for strength, stability and serviceability of structures. The chapter two present analytical and numerical method use in order to come up with a reliable result. Finally, chapter three presents the result and the interpretation of the solution obtained by using the analytical method and the result obtained with the numerical method.

CHAPTER 1: LITERATURE REVIEW

Introduction

It is necessary in geotechnical to retain masses of soil. Earth-retaining structures are ubiquitous in the man-made environment. There are various types of retaining walls. By convention, these walls are grouped into five categories: Gravity walls, embedded walls, reinforced soil (MSE) structure, anchored earth, Soil nailing. Regardless of the category, a geotechnical engineer must ensure that the wall is stable under anticipated loadings. It is necessary to recall that stability refers to a condition in which a geotechnical system will not fail or collapse under any conceivable loading (static and dynamic loads, fluid pressure, seepage forces). In this work the wall that has to be used is an Embedded wall specially a diaphragm wall.

1.1. Types of diaphragm walls

Diaphragm walls are a relatively recent advance in retaining wall construction compared with steel sheet piling. According to Puller (1996), the first diaphragm walls were tested in 1948 and the first full-scale slurry wall was built by Icos in Italy in 1950, with bentonite slurry support as a cut-off wall (Clayton, Woods, Bond, & Milititsky, 2013). Diaphragm wall is a retaining structure in concrete poured into a trench and is the most use for the construction of the tunnel and underground structure in the world. Walls can be constructed to considerable depths ahead of the main excavation, so acting as support for adjacent structures. There are many types of diaphragm wall such as:

1.1.1. Sealing diaphragm wall

It creates a waterproof barrier in the ground, this type of wall does not require any earthwork after its execution. The wall is poured either with a mixture of bentonite mud (significant thickness of at least 1.5 m), or with a plastic concrete with a reduced cement dosage, introduced into the dip tube under a bentonite, cement and admixtures. This wall can be placed vertically and horizontally ensuring a durable resistance to water. The applications are as follows: excavations, tunnels, underground car parks, polluted site, etc. (Riadh)

The figure 1.1 present a cross section of a sealing diaphragm wall.

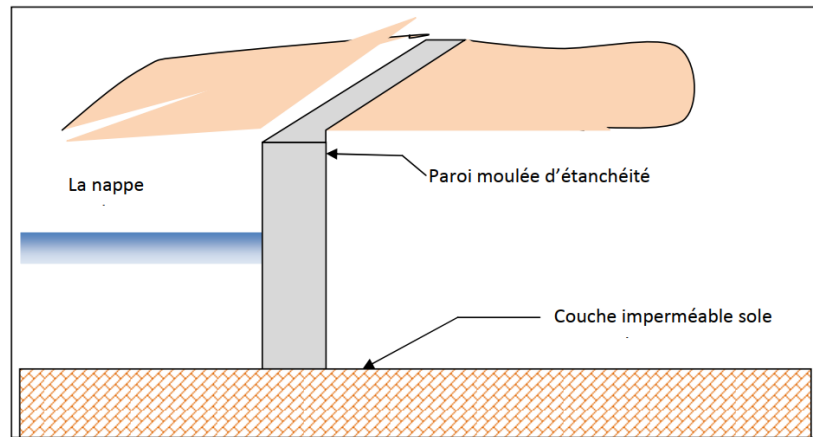


Figure 1.9. Schematic diagram of sealing diaphragm wall

1.1.2. Prefabricated diaphragm walls

The finish of a diaphragm wall always presents imperfections due to its molding in the ground: joints between imperfect panels, bad position of the reinforcement etc. The prefabricated diaphragm wall is an improvement of the diaphragm wall: the concrete no longer poured with a dip tube under a bentonite slurry but introduced into it in the form of whole reinforced concrete panels, manufactured in advance in the workshop. The drilling is as for a diaphragm wall, but a little wider than the future wall, with bentonite mud filling. The prefabricated reinforced concrete panels are lowered one after the other into the borehole and wedged on the walls of the excavation. They are centered so as to leave a thickness of mud on each side. The ends of the panels are shaped in the form of joints, so as to ensure the connection from panel to panel.

The figure 1.2 shows the installation principle of a prefabricated panel.

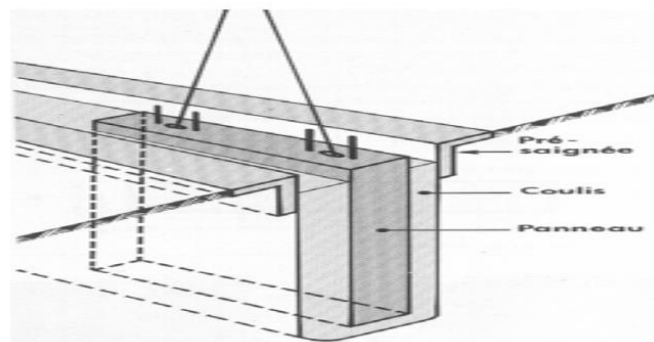


Figure 1.10. Installation principle of a prefabricated diaphragm wall

1.1.3. Simple retaining diaphragm wall

These walls are reinforced concrete walls in the ground. During their realization, individual trenches are dug in the ground by means of special rectangular grapples hanging from a cable crane to the required depth. The following picture is the cross section of the panel realize in the construction phase of diaphragm wall.

A schematic representation of a classic diaphragm wall is presented in the figure 1.3.

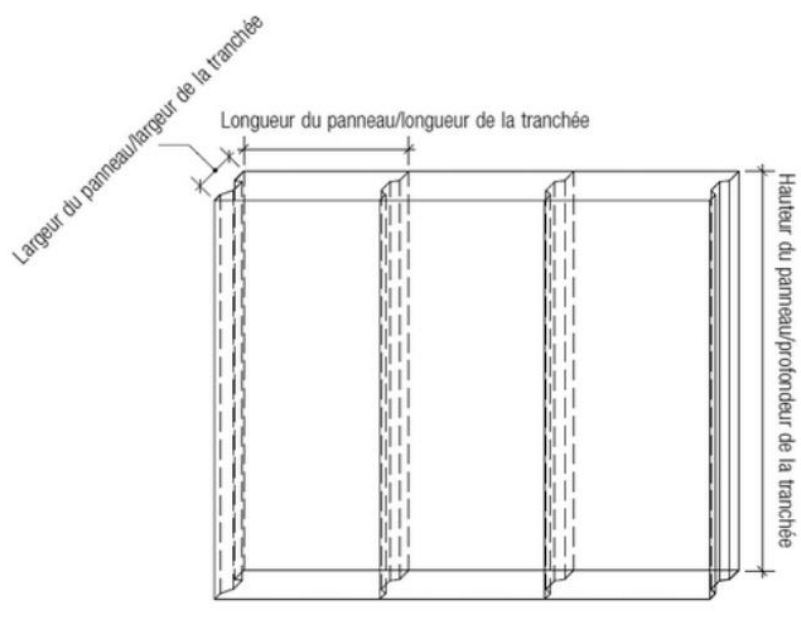


Figure 1.11. Schematic representation of a classic diaphragm wall (CSTC, juillet 2014)

1.2. Implementation method of a simple retaining diaphragm wall

Before executing the wall, the problem of stability of the trench during excavation must be solved and to overcome this problem, the use of a bentonite mud is necessary because it can be easily extracted after pouring concrete.

- First of all, the guide wall is executed, which consists of two smalls and temporary reinforced concrete walls.
- Then we move on to the perforation phase which is carried out using a support fluid so as to excavate the panels. The length of each excavated panel being adjusted according to the type of soil so as to guarantee the stability of the trench each time during the works. During excavation, the ground is gradually replaced by the carrier fluid known as drilling mud. Bentonite mixed with water is generally used to forms a waterproof deposit on the

DESIGN OF A RETAINING STRUCTURE AND ITS PUMPING SYSTEM FOR AN UNDERGROUND STRUCTURE

CONSTRUCTION Presented by TCHINDA KENGNE Franck Junior

walls of the excavation which also has the role to keeping the walls stable against hydrostatic pressure and earth pressure. The density of the mud has to be rightly chosen in order to maintain workable for the machine and sustain the earth pressure and the hydrostatic pressure during the excavation.

- When the excavation of a panel is finished, the reinforcing cage is placed in the panel which can be equipped with a reserve for the installation of the struts and a pipe is introduced inside the panel to introduce the concrete and as the concrete is poured, the drilling mud is recovered for recycling.

The figure 1.4 illustrates in detail the stages of realization of the diaphragm wall.

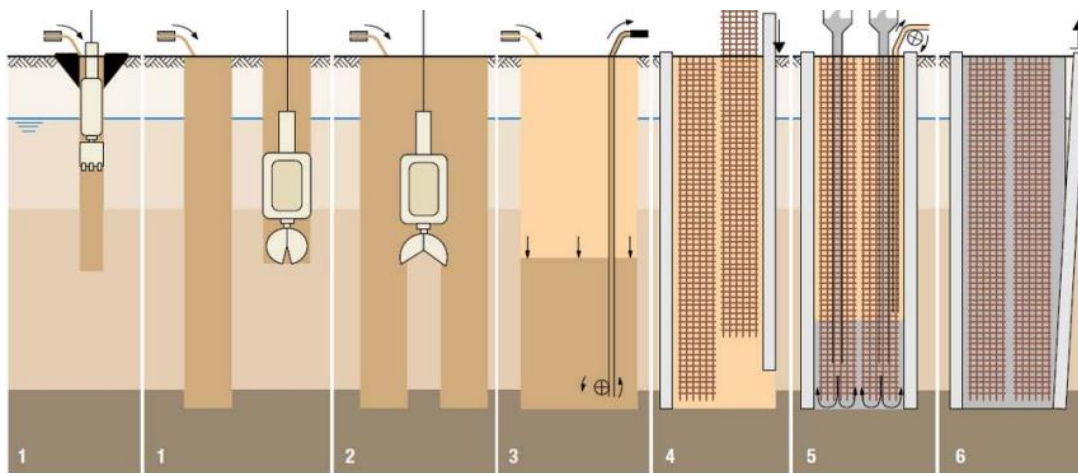


Figure 1.12. Stages of realization of the diaphragm wall (CSTC, juillet 2014)

Step 1: Excavation under excavation fluid of the two trenches at the ends of the panel, the length of which corresponds to the length of the grapple.

Step 2: Excavation under excavation fluid of the remaining pass between the two trenches

Step 3: Replacement of the soil-soiled excavation fluid with a cleaner one

Step 4: introduction of the reinforcement cages in the excavated trench

Step 5: Concreting of the panel using dip tubes.

Step 6: Extraction of joined tubes

1.2.1. Bentonite mud

Before executing the diaphragm wall, there is a problem of trench stability during excavation. If the execution is done without a precaution, the collapse of the wall inevitably occurs. In the case of the diaphragm wall, this stability is ensured by the bentonite mud which will later be replaced by concrete.

1.2.1.1. Generalities

Bentonite is an absorbent swelling clay consisting mostly of montmorillonite. It usually forms from weathering of volcanic ash in seawater, which converts the volcanic glass present in the ash to clay minerals. Bentonite beds are white or pale blue or green in fresh exposures, turning to a cream colour and then yellow, red or brown as the exposure is weathered further. As a swelling clay, bentonite has the ability to absorb large quantities of water, which increases its volume by up to a factor of eight. This makes bentonite beds unsuitable for building and road construction. However, the swelling property is used to advantage in drilling mud and groundwater sealants. The montmorillonite making up bentonite is an aluminium phyllosilicate mineral which takes the form of microscopic platy grains. These give the clay a very large total surface area, making bentonite a valuable adsorbent. The plates also adhere to each other when wet. This gives the clay a cohesiveness that makes it useful as a binder and as an additive to improve the plasticity of kaolinite clay used for pottery.

1.2.1.2. Behaviour of the bentonite mud in the trench

Bentonite sludge exhibits two phenomena:

- The mud penetrates the ground by walking between the grains, impregnates the surroundings of the trench to a thickness linked to the permeability.
- The free water dissipates through the soil and the edges of the wall is covered with a layer of bentonite.

1.2.2. Reinforcement cage

The reinforcement cages of the diaphragm walls are placed in the trench full of mud before concreting. They must be rigid enough not to deform during the handling phases. The spacing of the steels must be sufficient so that the concrete which arrives can be correctly implemented. The cages are subjected to significant pressure from the concrete during the concreting phase, reinforcement of the cage is provided at the level of the tie rods in the case

of anchored walls to ensure the distribution of the anchoring forces. In the event of the implementation of the cage in several vertical elements, the continuity of the reinforcement is generally ensured by overlapping of the elements.

1.2.3. Diaphragm wall concrete

The concrete of the diaphragm wall is never vibrated. Concreting is carried out using a dip tube from the bottom of the excavation. Concreting must be carried out in such a way that the mud is properly driven out by the concrete. The dip tube must remain engaged for several meters in the fresh concrete setting retarders are incorporated into the concrete so that the setting of the concrete implemented first does not occur before the end of the concreting of the entire panel. The concrete must be liquid enough to properly occupy the entire volume of the excavation. The concrete must be studied in terms of its formulation and workability.

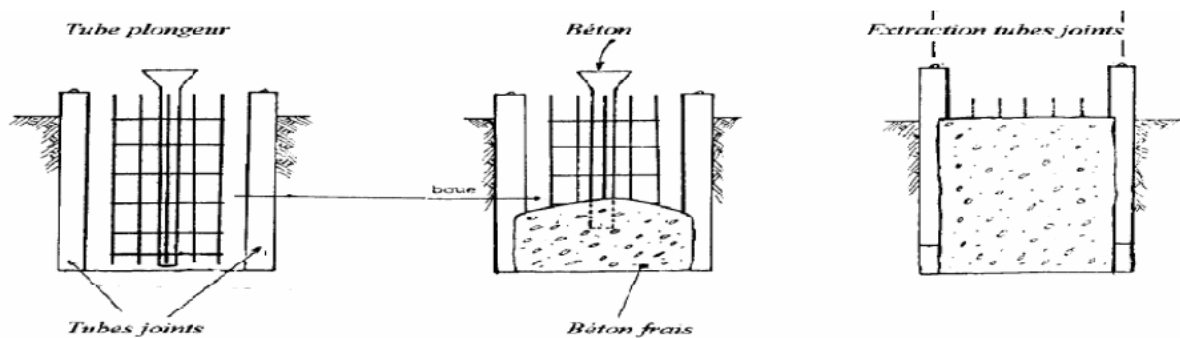


Figure 1.13. Concreting of diaphragm wall

1.2.4. Joints between panels

The joints are delicate points of junction between panels which, if they have in general no structural function, are brought to ensure a continuity with respect to the hydraulic aspects. The joined use is the following:

1.2.4.1. Joined tubes

Here, each free end of the panels is equipped with a circular tube of diameter equal to the wall thickness before concreting. This tube is used as formwork and allows to obtain a semicircular concreting stop surface ensuring a good recovery with the following panel. The tubes are extracted as soon as the concrete has reached a sufficient rigidity.

1.2.4.2. Keyed joints

This system used in addition to the joint tube consists of reserving a void in the plane of the joint between two panels for concreting and the waterproofing is reinforced by a grout. The void is created by a reservation tube or by a plastic tube used as a guide for a later perforation.

1.2.5. Anchorage

These elements are active or passive intended to take up the transverse forces resulting essentially from the thrust of the soil and water on the wall. These devices can be mobilized in traction in case of anchors or in compression in case of struts. In the case of struts, it is either a metallic element in the case of temporary works or reinforced concrete for final concreting. The element can take the form of spaced horizontal beams or a continuous slab for the case of final concreting. A continuity of reinforcement between wall and button closely associates them.

1.3. Design procedure for diaphragm walls

1.3.1. Stability verification

The conventional method of designing diaphragm walls for excavations consists in the following steps:

Step 1: Specify the given conditions and indicate all known soil data, stratification, water level.

Step 2: Compute the lateral pressure diagram using some specific method (Terzaghi and Peck method, etc.) depending on the quality of soil data and what is to be retained.

Step 3: Design the wall and struts.

As excavation proceeds within the area enclosed by the wall, button is added to keep the sheet piles in place and the following formula take place:

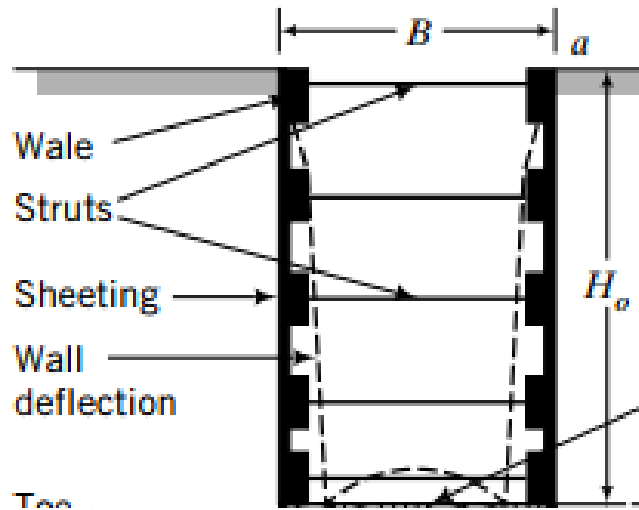


Figure 1.14. Section of the diaphragm wall with the button (BUDHU, 2011)

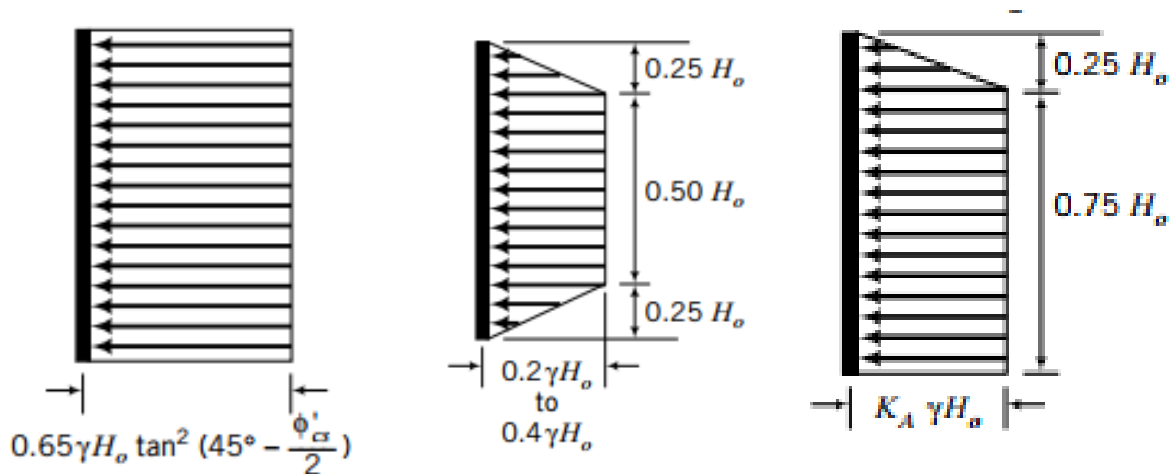


Figure 1.15. Lateral pressure distribution from a) coarse-grained soils; b) fine grained soil with $\gamma H_0/c_u < 4$; c) fine grained soil with $\gamma H_0/c_u > 4$ (BUDHU, 2011)

$$K_a = \left(1 - \frac{4c_u}{\gamma H_0 + q_s}\right) + \frac{2\sqrt{2}D_s}{H_0} * \left(1 - \frac{5.14(c_u)_b}{\gamma H_0 + q_s}\right) \quad \text{Equation 1.1.}$$

The first term of this sum represents the value of the K_a that would be calculated from the limit equilibrium, and the second term represents the lateral pressure from heaving and is neglected when $(\gamma H_0 + q_s)/(c_u)_b < 5.14$.

With:

c_u : undrained shear strength

$(c_u)_b$: average undrained shear strength below the toe of the wall

D_f : thickness of the firm layer

D_s : thickness of the failure surface and is

$D_s = B/\sqrt{2}$ if $D_f > D_s$ or $D_f = D_s$ if $D_f < D_s$

γ : unit weight of the layer

q_s : eventual surcharge

H_0 : height of the retained earth

The critical design elements to verify the stability of the wall are the struts which are usually different because of the different lateral load at different depth, the time between excavations, and the installation procedure. Failure of a single button can be catastrophic because it can lead to collapse of the whole system.

1.3.2. Wall displacement calculation and loads on the struts

The top struts are installed, followed by others at lower depths. The wall displacements before the top struts are usually very small but get larger as the excavation gets deeper. The largest wall displacement occurs at the base -bottom- of the excavation.

The critical design elements in a braced excavation are the loads on the struts, which are usually different because of different lateral loads at different depths, the time between excavations, and the installation procedure. Failure of a single strut can be catastrophic because it can lead to the collapse of the whole system. The analysis for the forces and deflection in braced excavation should ideally consider the construction sequence, and numerical methods such as the finite element method are preferred. (BUDHU, 2011)

Lateral stress distributions for use in the semi-empirical method are approximations from field measurements of strut loads in different types of soil. The lateral stress distributions used for coarse-grained and fine-grained soils are shown in Figure (1.7, 1.8, 1.9.). These lateral stress distributions are not real but average approximate stress distributions to estimate the maximum strut load.

CHAPTER 1: LITERATURE REVIEW

There are analytical and numerical method to evaluate the displacement of the wall. For the numerical method, we can use the Plaxis code and for the analytical method, Karlsruud and Andresen, 2008 showed that wall movement and struts or struts load are sensitive to $(FS)_{heave}$ and with FEM method they showed that for $(FS)_{heave} > 1.8$, the wall displacement is constant and is about 0.2% of H_0 but it's 0.5% if the $(FS)_{heave} = 1.4$. (BUDHU, 2011)

If the soil below the base of the excavation is a soft, normally consolidated soil, it is possible that heaving can occur. The soil above the base acts as a surcharge on the soil below it. (BUDHU, 2011)

$$(FS)_{heave} = N_c * \frac{C_u}{\gamma H_0 + q_s} \quad \text{Equation 1.2.}$$

If $(FS)_{heave} < 1.5$ the sheeting should be extended below the base of the excavation for stability

N_c is a bearing capacity coefficient

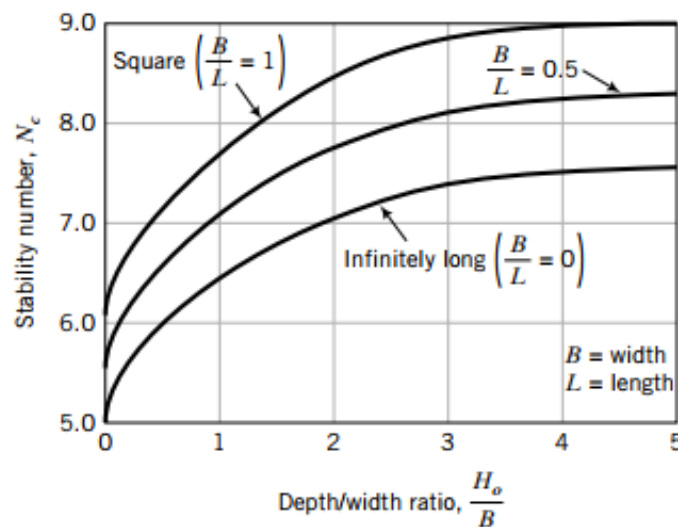


Figure 1.8. Abacus for the evaluation of N_c (BUDHU, 2011)

The struts are present because the depth of embedment of the wall is insufficient to provide fixity at the bottom end of the wall and they can also be installed to control the displacement of the wall in case of low stiffness. We will assume that our wall is like an anchored wall in order to determine his embedded depth. The button load at each level is found by assuming hinged connections of the button to the walls. A free-body diagram is drawn for each level of

excavation, and the forces imposed on the struts are determined using static equilibrium. The lateral wall displacement is dependent on:

- Dynamics loads induce by the machine on the site. The soil strength and stiffness decrease with greater levels of soil disturbance.
- Stresses from nearby structures.

To sum up, a good analysis of the diaphragm wall is done by respecting the following procedure:

- Check the stability against bottom heave by calculating $(FS)_{\text{heave}}$. If $(FS)_{\text{heave}} < 1.5$ the toe penetration should be extended.
- Determine the lateral stress on the wall for each soil type.
- Treat the connections of the wall to the struts as hinges.
- Draw a free body diagram as each level of the excavation.
- Solve for the forces in the struts by applying the static equilibrium equations for each

free-body diagram.

1.3.3. Analytical method for determining the displacement of the wall

The diaphragm wall is a plate element because two dimensions prevail on one. The plate is the section of the cylinder with a very small thickness with respect to the transversal dimensions of the system. To approximate well the displacement of the wall, the method uses here is the finite difference method (FDM).

1.3.3.1. General concept

This is a method of the solution of boundary value problems for differential equations. The essence of the FDM lies in the following:

- The middle plane of the plate is covered by a rectangular, triangular, or other reference network, depending on the geometry of the plate. This network is called a finite difference mesh and points of intersection of this mesh are referred to as mesh or nodal points.

- The governing differential equation inside the plate domain is replaced by the corresponding finite difference equations at the mesh points using the special finite difference operators.
- Boundary conditions are also formulated with the use of the above-mentioned finite difference operators at mesh points located on the plate boundary.

As a result of such replacement, we obtain a closed set of linear algebraic equations written for every nodal point within the plate. Solving this system of equations, one obtains a numerical field of the nodal displacements.

Here we distinguish the case where the squared plate is simply supported at the edges and the case where the plate is a built-in support at the edges and uniformly loaded.

1.3.3.2. Squared plate simply supported at the edges

The figure 1.9 illustrates the decomposition of a square plate element

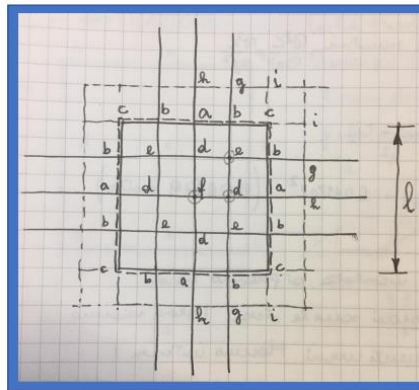


Figure 1.9. Decomposition of the plate (MAJORANA, 2020)

- We choose the desired points superposing to the plate a squared mesh.
- At the edge points we have simple support, hence there is not a displacement: $w = 0$.
- Here the boundary conditions are posed at the beginning.
- We want to know displacements in the inner points.
- We'll have as much equation as the number of points where we search displacements (i.e. 25 equations. In 25 unknowns).

CHAPTER 1: LITERATURE REVIEW

For symmetry reasons the number of equations is reduced. Taking advantage of the symmetry the problem is highly simplified.

If we double the mesh, due to symmetry, the interesting points are those marked in the upper square. We put the same letter for points characterized by the same parameters (i.e. we use the symmetry).

- We take into account the table where we have 20 in the center. We superpose it such that 20 is coincident with f point, and write the consequent equation.
- Then we displace the table with $20 \equiv e$, and finally with $20 \equiv d$.
- The real unknowns are 3, while w_g and w_h also appear in the equations.
- We eliminate them by means of boundary conditions.

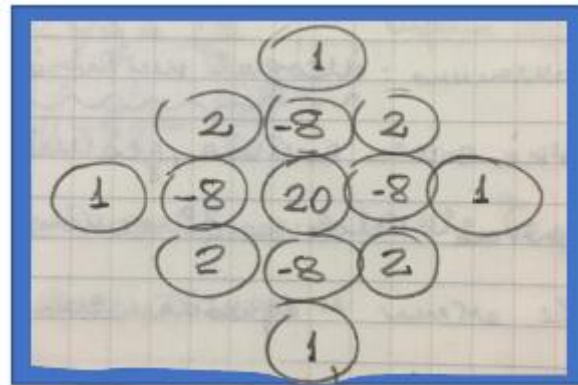


Figure 1.10. Coefficient use by the FDM method (MAJORANA, 2020)

At the end, we obtain the following displacement of the points:

$$w_f = 0.00403 \, ql^4/D, \quad \text{Equation 1.3.}$$

$$w_d = 0.00293 \, ql^4/D, \quad \text{Equation 1.4.}$$

$$w_e = 0.00214 \, ql^4/D \quad (\text{MAJORANA, 2020}) \quad \text{Equation 1.5.}$$

$$\text{With } D = E \cdot h^3 / (12 \cdot (1 - \nu^2)). \quad (\text{Ventsel \& Krauthammer, 2001}) \quad \text{Equation 1.6.}$$

1.3.3.3. Squared plate built-in at the edges

- The equations are the same as before. The values will certainly be lesser.

- Here the displacement of the points at the edges is zero

By using the new boundary condition, we can obtain the real displacement of all the nodes of the plate by resolving the following system of equation

$$\left\{ \begin{array}{l} 20w_f - 32w_d + 8w_e = q\lambda^4/D \quad \text{Equation 1.7.} \\ -8w_f + 25w_d - 16w_e = q\lambda^4/D \quad \text{Equation 1.8.} \\ 2w_f - 16w_d + 24w_e = q\lambda^4/D \quad \text{Equation 1.9.} \end{array} \right.$$

1.3.4. Limit state for embedded wall

Embedded walls can collapse for many reasons:

- Failure as a result of insufficient depth of embedment and the failure below represent the failure mode.

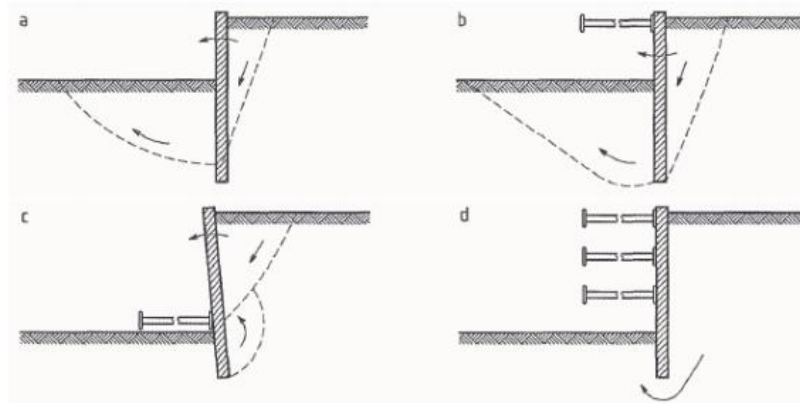


Figure 1.11. Mode of rotational failure of embedded walls (Eurocode 7)

- Failure of the wall section or struts: this result of a bad structural design and the figure below represent the mode of failure.

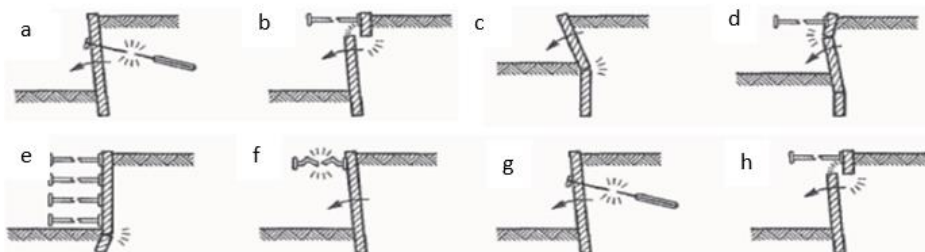


Figure 1.12. Rotational failure of the wall section (Eurocode 7)

- Overall instability: this failure occurs because all the part of the wall is in the failure surface.

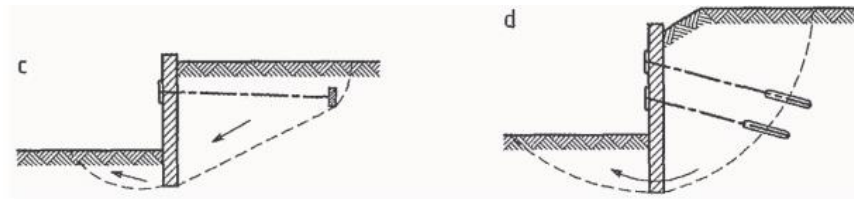


Figure 1.13. Examples of overall instability (Eurocode 7)

- Finally, failure of the wall can occur due to the seepage.

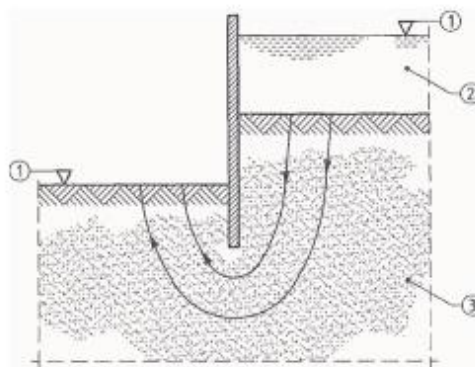


Figure 1.14. Example of situation where seepage might be critical (Eurocode 7)

1.4. Generalities on the pumping system

The level of the bottom of the structure is under the GWT this means that water will enter in the structure continuously by the effect of seepage.

1.4.1. Theory of seepage

All soil is permeable materials, water being free to flow through the interconnected pores between the solid particles. The pressure of the pore water is measured relative to atmospheric pressure and the level at which the pressure is atmospheric (i.e. zero) is defined as the water table (WT) or the phreatic surface. Below the water table the soil is assumed to be fully saturated, although it is likely that, due to the presence of small volumes of entrapped air, the degree of saturation will be marginally below 100%. The level of the water table changes according to climatic conditions but the level can also change as a consequence of constructional operations. A perched water table can occur locally, contained by soil of low

DESIGN OF A RETAINING STRUCTURE AND ITS PUMPING SYSTEM FOR AN UNDERGROUND STRUCTURE

CONSTRUCTION Presented by TCHINDA KENGNE Franck Junior

permeability, above the normal water table level. Below the water table the pore water may be static, the hydrostatic pressure depending on the depth below the water table, or may be seeping through the soil under the hydraulic gradient. (R.F.Craig, 2004)

$$\text{Thus } h = \frac{u}{\gamma_w} + z \quad \text{equation 1.10}$$

Where h is the total head

U the pore water pressure

γ_w is the unit weight of the water

z the elevation head above the chosen datum.

Above the water table, water can be held at negative pressure by capillary tension; the smaller the size of the pores the higher the water can rise above the water table. The capillary rise tends to be irregular due to the random pore sizes occurring in a soil. The soil can be almost completely saturated in the lower part of the capillary zone but in general the degree of saturation decreases with height. The negative pressure of water held above the water table results in attractive forces between the particles: this attraction is referred to as the soil suction and is a function of pore size and water content. (R.F.Craig, 2004)

The hypothesis on the equipotential and flow lines are the following:

- The points belonging to a curve along which the potential function has constant value has all the same total head: this curve is called equipotential line.
- A curve along which the flow function has constant value is called flow line.
- Equipotential and flow lines are mutually orthogonal. Flow lines could not intersect one with each other. Same for the potential lines.
- The potential lines together with the flow lines constituted the flow net.
- If the flow net is known, much information can be obtained: in every point of the space, we know the total head and, consequently we are able to determine the water pore pressure, the space between two flow lines is a flow channel.

- The flow net is drawn according to the geometry and the boundary conditions. Since the Laplace equation does not contain the permeability, the flow net is independent from the permeability of media if we are considering the flow through one only layer.
- The total flow discharge of a seepage is: $q = \Delta q * N_{\Psi}$

Where N_{Ψ} is the number of flow channels, each carry the same flow Δq .

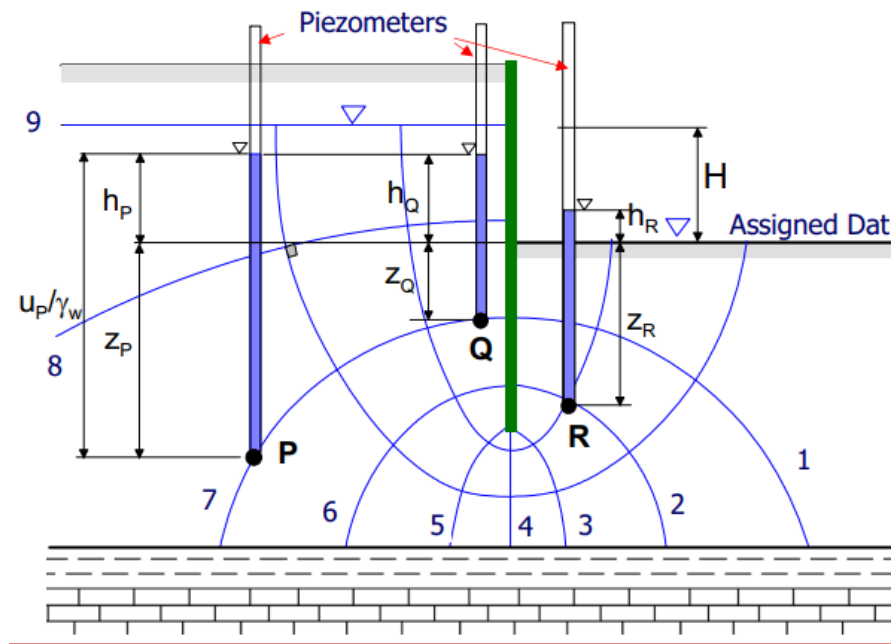


Figure 1.15. Example of confined seepage (SIMONINI, 2019)

1.4.1.1. Liquefaction under seepage

Considering the permeameter in the figure below. The left tank contains a soil sample, being L its thickness and γ_{sat} its saturated unit weight. On the top of soil, there is water for a level equal to h_w . Since the level in two tanks is the same, the water is firm (hydrostatic condition).

At a generic point P, at depth z into the soil, the total vertical stress, the pore water pressure and the vertical effective stress are:

$$\sigma_v' = (\gamma_{sat} - \gamma_w) * z \quad \text{equation 1.11}$$

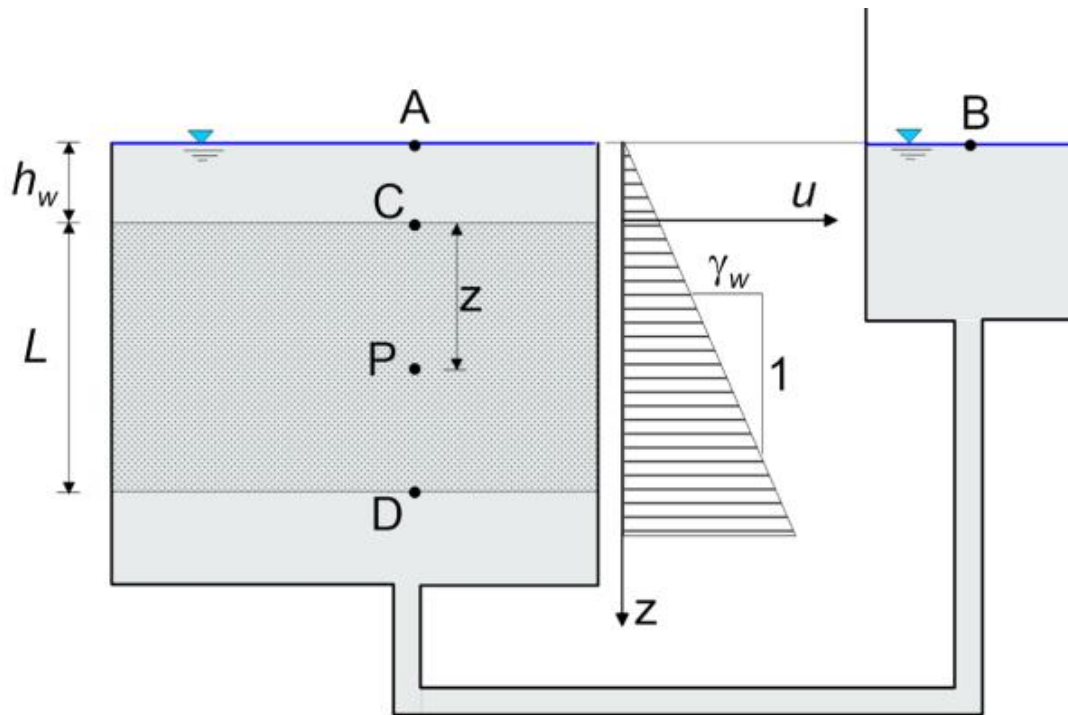


Figure 1.16. Permeameter with the same level of water in the left and right tank (COLA, 2021)

Now if the water level in the right tank increases of H , the water flows with a hydraulic gradient $i=H/L$. The total stress in P is constant but the effective stress become:

$$\sigma_v' = \gamma' * z - \gamma_w * i * z \quad \text{equation 1.12}$$

The effective stress is reduced because seepage force acts on the particles of a soil in the opposite direction of the gravitational force.

If H increases too much, the hydraulic gradient also increases and since the first term of the equation is still constant, the vertical effective stress can become 0. And in this condition, we have $i = i_c = \gamma' / \gamma_w$.

i_c is calling critical hydraulic gradient.

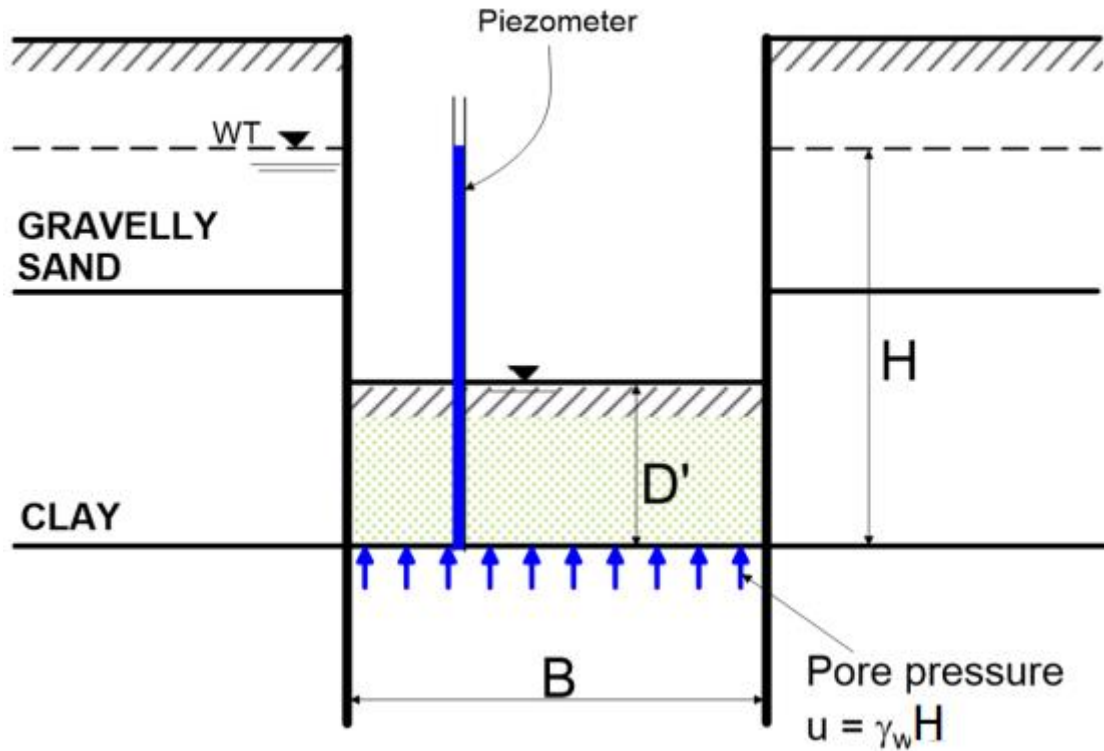


Figure 1.18. Illustration of water pressure under an impermeable layer (COLA, 2021)

The water level in the excavation being lower than the natural water table, the pressure distribution on both sides is represented by the following figure.

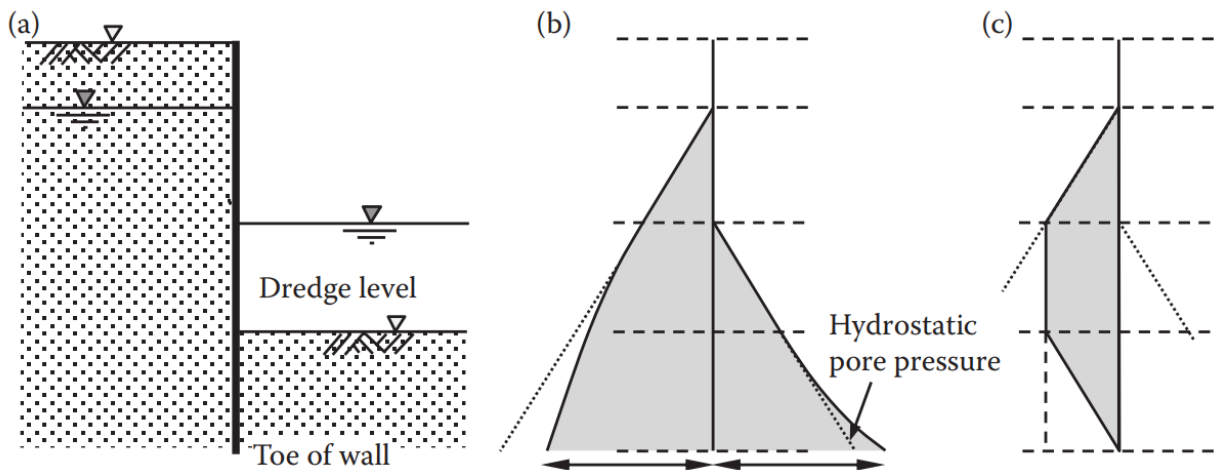


Figure 1.19. Out-of-balance water pressure on the wall. a) wall layout, b) water pressures on wall, c) Net pressure (Clayton et al., 2014)

1.4.2. Methods of design of the drainage systems

Problems related to groundwater drainage can be studied considering a transient or a steady state regime. In the transient regime, the cone of influence expands during pumping while, in steady state, the depression cone reaches a geometry that remains fixed over time. With regard to drainage works, the steady state regime is mainly considered because these works generally drain and remain active over long periods of time. In such conditions steady state is reached.

Generally, some simplifying hypotheses are used:

- The groundwater movement is laminar, thus making valid Darcy's law.
- In undisturbed conditions the groundwater does not move, i.e. the water table is horizontal.
- The aquifer thickness is constant.
- The soil forming the aquifer is continuous, homogeneous, and isotropic.
- The flow velocity does not change with depth, i.e. the equipotential lines are vertical lines.

1.4.2.1. Partially penetrating trench, confined aquifer

The unit-width discharge is computed using the relationship:

$$q = \frac{2Kb(H-h_0)}{L+\lambda b} \quad \text{Equation 1.14}$$

The elevation of the water table is computed as follows:

$$h = h_0 + (H - h_0) \left(\frac{x+\lambda b}{L+\lambda b} \right) \quad \text{Equation 1.15}$$

with:

λ = dimensionless factor depending on the ratio d/b as provided the figure to the right;

d = depth of the trench into the aquifer;

L = distance of the recharge from the trench (or distance at which the piezometric head can be assumed undisturbed)

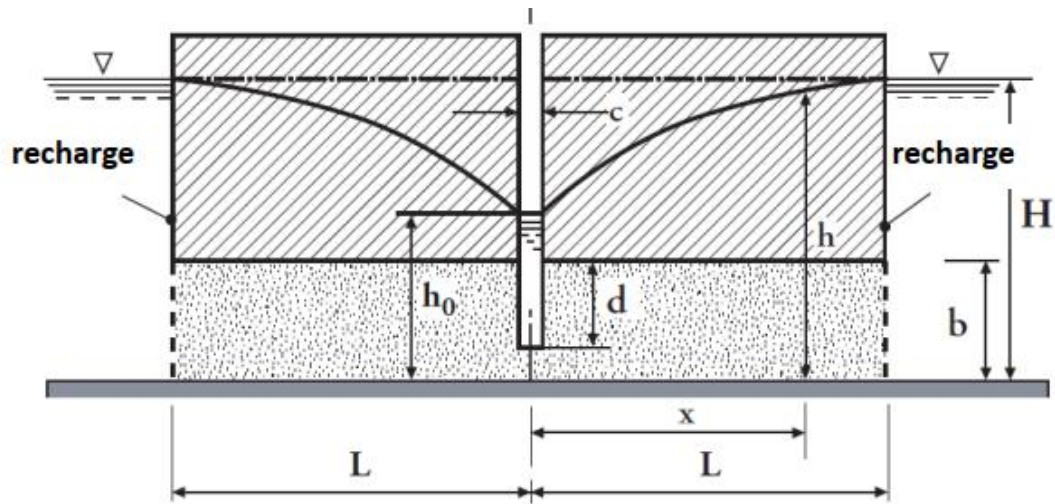


Figure 1.20. Partially penetrating trench that does not reach the aquifer bottom. (Teatini, 2019)

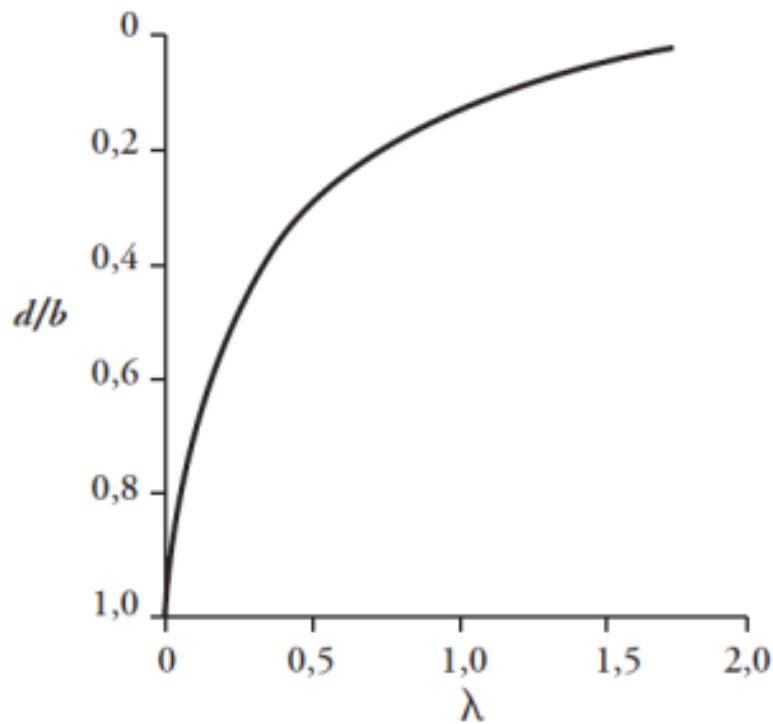


Figure 1.21. parameter λ vs d/b (Teatini, 2019)

1.4.2.2. Partially penetrating trench, phreatic aquifer

If the recharge occurs from one side, the unit-width discharge is computed using the Chapman (1956) relationship:

$$q = \frac{\left(0.73 + \frac{0.27(H-h_0)}{H}\right)K(H^2-h_0^2)}{2L} \quad \text{Equation 1.16}$$

The maximum elevation of the water table downstream the trench h_D is estimated as:

$$h_D = h_0 \left(\frac{1.48(H-h_0)}{L} + 1 \right) \quad \text{Equation 1.17}$$

The total discharge amounts to: $Q = ql$ with l the trench length.

L = distance from the recharge (m); if the recharge is placed at a distance from the trench greater than the distance of influence provided by Sichardt, this latter value is used;

H = thickness of the undisturbed aquifer (m);

h_0 = aquifer thickness at the trench (m);

h_s = difference between the dynamic levels inside the trench and in the aquifer at the trench wall a (m) – usually negligible.

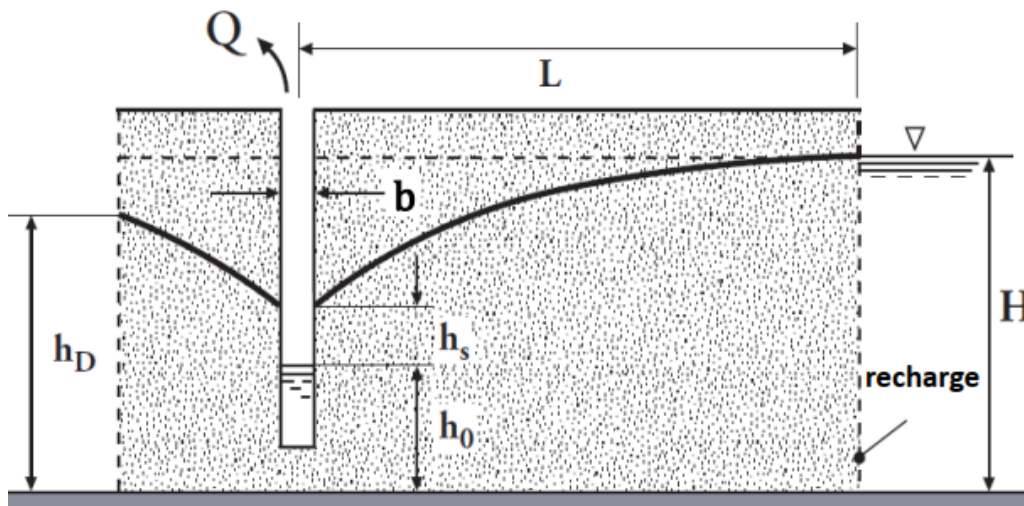


Figure 1.22. Trench with a negligible thickness b that does not reach the impermeable rock (Teatini, 2019)

If the recharge occurs from both the sides: $q_c = 2q$ and h_D loses the meaning.

If the trenches are two, parallel to each other, the discharge rate is obtained from the single trench formula with h_D computed as:

$$h_D = h_0 \left(\frac{C_1 C_2 (H-h_0)}{L} + 1 \right) \quad \text{Equation 1.18.}$$

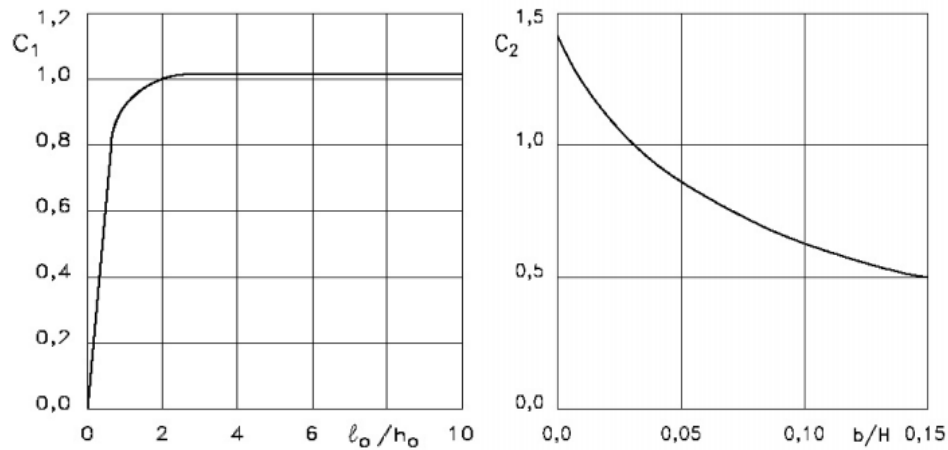


Figure 1.23. C_1 and C_2 parameters (Teatini, 2019)

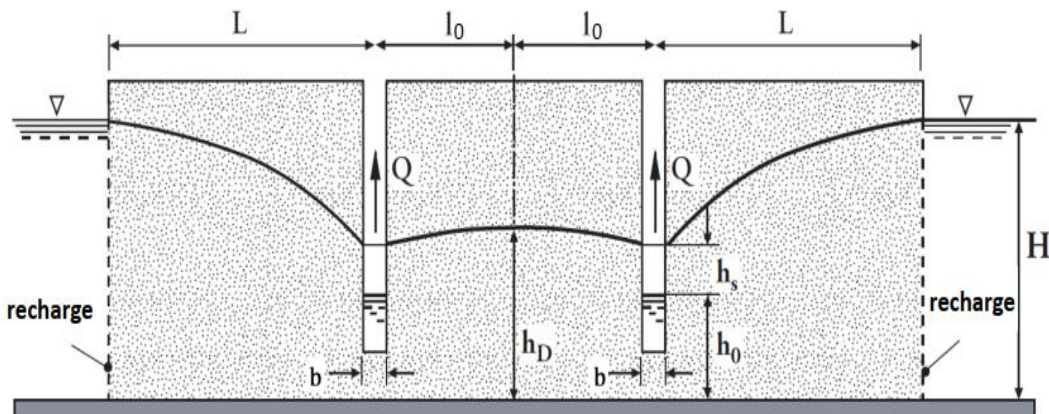


Figure 1.24. Two trenches with a negligible thickness b that does not reach the impermeable rock (Teatini, 2019)

1.5. Drainage associated to an impermeable wall

Here can arise the phenomenon of buoyancy which is the phenomenon by which the vertical component of the forces of the ascending flow opposes the weight of the ground until cancelling the vertical effective stress. This results in a hydrostatic lifting of the soil particles. The rupture then occurs by boiling. To avoid the risk of boiling, it is therefore necessary to avoid upward flow and prefers to collect the water by deep wells.

The figure 1.25. illustrate the direction of the flow line induced by the well which avoid the cancelling of the effective stress at the bottom of excavation.

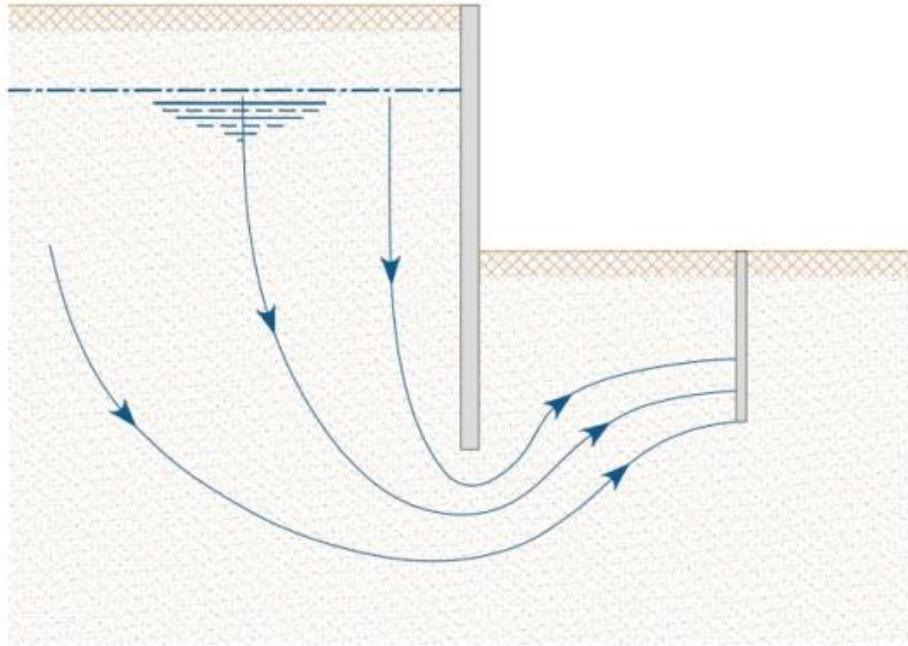


Figure 1.25. Pumping device to avoid the cancelling of the effective stresses at the bottom of the excavation. (CFMS, 2016)

1.6. Type of dewatering pump

The choice of pump characteristics is one of the critical points of their use in the water table drawdown system as it can determine the success or the failure of the operation. To achieve this, a pump is connected to the well and its characteristics are calculated according to the flow rate of the well and the pressure required for discharge.

There are several types of pumps among which:

- Hand pumps with piston located on the surface: these pumps are usable for water levels lower than 5 m and their priming is generally essential. These pumps are fixed directly on the well.
- Manual submerged piston pumps: the piston and its cylinder are lowered below the water level, as soon as the piston is activated the reciprocating movement is given by a lever, their flow rate is comparable to that of surface piston pumps but priming is not necessary.

- The centrifugal pump: this type of pump can cover a very wide range of flow rates, thus theoretically meeting all needs. This type of pump can be driven by an electric or thermal motor.

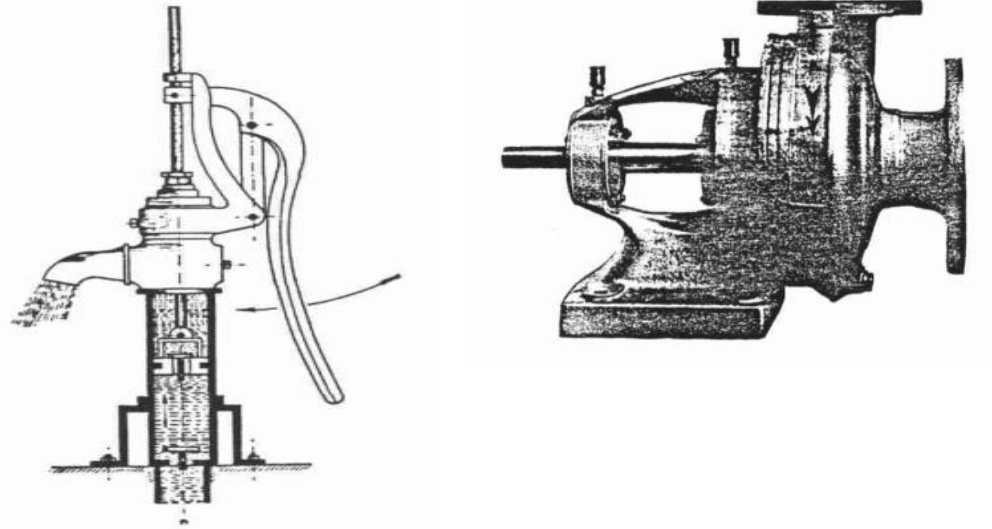


Figure 1.166. Schematic section of a manual piston pump (a), centrifugal pump (b)

1.7. Calculation of the flow due to seepage in diaphragm wall

In reality, seepage takes place in both directions, so it would be wise to calculate the equivalence of all the quantities that will be used in the process of determining the dewatering flow. Let's consider a grid of a flow domain, as shown in Figure 1.12, where (i, j) is a nodal point.

Using Taylor's theorem, we have:

$$k_x \frac{\partial^2 H}{\partial x^2} + k_z \frac{\partial^2 H}{\partial z^2} = \frac{k_x}{\Delta x^2} (h_{i+1,j} + h_{i-1,j} - 2h_{i,j}) + \frac{k_z}{\Delta z^2} (h_{i,j+1} + h_{i,j-1} - 2h_{i,j}) = 0$$

Equation 1.19.

Let $a = K_x/K_z$ and $\Delta x = \Delta z$ (ie we subdivide the flow domain into a square grid), then solving from $h_{i,j}$ from the previous equation give:

$$h_{i,j} = \frac{a \cdot h_{i+1,j} + a \cdot h_{i-1,j} + h_{i,j+1} + h_{i,j-1}}{2 \cdot (1+a)}$$

Equation 1.20.

For isotropic conditions, $a=1$ the equation become:

$$h_{i,j} = \frac{h_{i+1,j} + h_{i-1,j} + h_{i,j+1} + h_{i,j-1}}{4} \quad \text{Equation 1.21.}$$

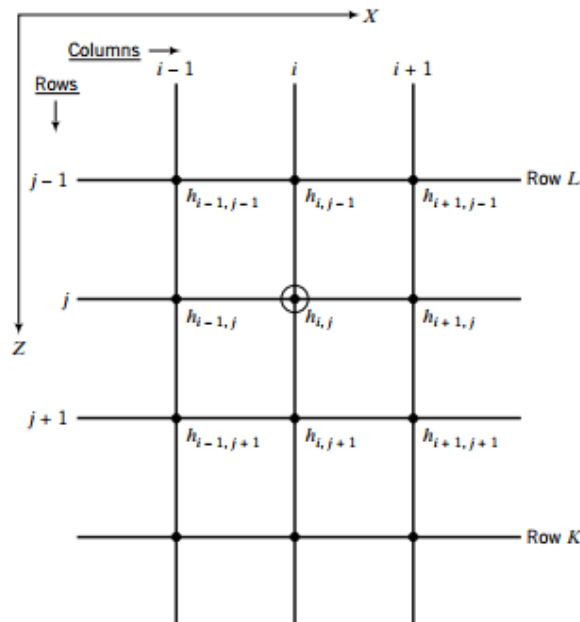


Figure 1.27. Partial grid of a flow domain (BUDHU, 2011)

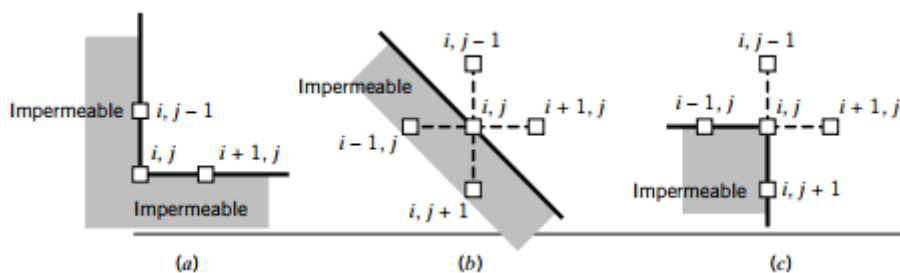
Since we are considering confined flow, one or more of the boundaries would be impermeable. Flow cannot cross impermeable boundaries and, therefore, for a horizontal impermeable surface

$$\frac{h_{i,j+1} + h_{i,j-1}}{2\Delta x} = 0 \quad \text{Equation 1.22.}$$

Therefore, $h_{i,j+1} = h_{i,j-1}$ and we can write the following equation

$$h_{i,j} = \frac{h_{i+1,j} + h_{i-1,j} + 2h_{i,j-1}}{4} \quad \text{Equation 1.23.}$$

Various types of geometry of impermeable boundaries are encountered in practice, three of which are shown in Figure 1.



DESIGN OF A RETAINING STRUCTURE AND ITS PUMPING SYSTEM FOR AN UNDERGROUND STRUCTURE
CONSTRUCTION Presented by TCHINDA KENGNE Franck Junior

Figure 1.28. Three types of boundary encountered in practice (BUDHU, 2011)

For the fig1. a, the finite difference equation is:

$$h_{i,j} = \frac{h_{i+1,j} + h_{i,j-1}}{2} \quad \text{Equation 1.24.}$$

for the fig1. c, the finite difference equation is:

$$h_{i,j} = \frac{h_{i,j-1} + h_{i+1,j} + h_{i,j+1} + 0.5*h_{i-1,j} + 0.5*h_{i,j+1}}{3} \quad \text{Equation 1.25.}$$

Contours of potential heads can be drawn from discrete values of $h_{i,j}$. The finite difference equations for flow lines are analogous to the potential lines.

The horizontal velocity of flow at any node ($v_{i,j}$) is given by Darcy's law:

$$V_{i,j} = k_x * i_{i,j} \quad \text{Equation 1.26.}$$

Where $i_{i,j}$ is the hydraulic gradient express as:

$$i_{i,j} = \frac{h_{i+1,j} + h_{i-1,j}}{2 * \Delta x} \quad \text{Equation 1.27.}$$

Therefore

$$V_{i,j} = \frac{k_x * (h_{i+1,j} + h_{i-1,j})}{2 * \Delta x} \quad \text{Equation 1.28.}$$

The flow rate, q , is obtained by considering a vertical plane across the flow domain. Let L be the top row and K be the bottom row of a vertical plane defined by column i . Then the expression for q is:

$$q = \frac{k_x}{4} \left(h_{i+1,L} - h_{i-1,L} + 2 \sum_{j=L+1}^{K-1} (h_{i+1,j} - h_{i-1,j}) + h_{i+1,K} - h_{i-1,K} \right) \quad \text{Equation 1.29.}$$

Let L be the top row and K be the bottom row of a vertical plane defined by column i (figure 1.27).

CHAPTER 1: LITERATURE REVIEW

In this work the area will be divided in small part to have the flow in each part. To better estimate the total flow, the sum of the flow in each part will be done. The procedure to do this is the following:

- First of all, we determine the equivalent permeability of the layer under the water level: it's the permeability associated with a soil composed by heterogeneous layers.

$$K_{eq} = \sqrt{K_{h,eq} * K_{v,eq}} \quad \text{Equation 1.30.}$$

- Equivalent horizontal permeability:

$$K_{h,eq} = \sum_i^n K_i * \frac{A_i}{A} \quad \text{Equation 1.31.}$$

- Equivalent vertical permeability:

$$K_{v,eq} = H * \frac{1}{t} \quad \text{Equation 1.32.}$$

$$t = \sum_i^n H_i / K_i \quad \text{Equation 1.33.}$$

- The flow: we will use the FDM here to determine the flow. The procedure is the following:
 - Divide the flow domain into a square grid. The finer grids give more accurate solutions than coarser grids, but are more tedious to construct and require more computational time. If the problem is symmetrical, only one half of the flow domain needs to be considered. The total flow domain should have a width of at least four times the thickness of the soil layer. For example, if D is the thickness of the soil layer, then the minimum width of the left half of the flow domain is $2D$.
 - Identify boundary conditions, for example, impermeable boundaries -flow lines- and permeable boundaries -equipotential lines-.
 - Determine the heads at the permeable or equipotential boundaries. For example, the head along the equipotential boundary is ΔH . Therefore, all the nodes along this boundary will have a constant head of ΔH . Because of symmetry, the head along nodes directly under the sheet pile wall is $\Delta H/2$.

CHAPTER 1: LITERATURE REVIEW

- Apply the known heads to corresponding nodes and assume reasonable initial values for the interior nodes. The linear interpolation for the potential heads of the interior nodes can be used.
- To each node except to impermeable boundaries, we apply the following equation:

$$h_{i,j} = (a \cdot h_{i+1,j} + a \cdot h_{i-1,j} + h_{i,j+1} + h_{i,j-1}) / (2 \cdot (1+a)) \quad \text{Equation 1.34.}$$

and at impermeable node, we use

$$h_{i,j} = (h_{i+1,j} + h_{i-1,j} + 2h_{i,j-1}) / 4 \quad \text{Equation 1.35.}$$

$a = k_h/k_v$ is anisotropy

- Repeat the 5 previous items until the new value at a node differs from the old value by a small numerical tolerance, for example, 0.001 m.
- Arbitrarily select a sequential set of nodes along a column of nodes and calculate the flow, q , using the following equation. It is best to calculate $q' = q$ for a unit permeability value to avoid too many decimal points in the calculations.

$$q = k (h_{i+1,L} - h_{i-1,L} + 2 \cdot \sum_{L+1}^{k-1} (h_{i+1,j} - h_{i-1,j}) + h_{i+1,k} - h_{i-1,k}) / 4 \quad \text{Equation 1.36.}$$

The flow is calculated with the following formula

$$Q = q \cdot L \cdot 2 \quad \text{Equation 1.37.}$$

L is the length of the station

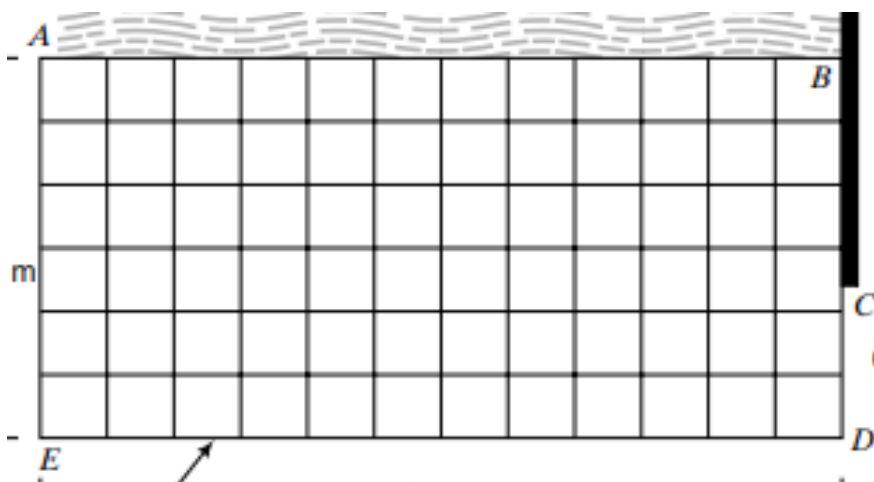


Figure 1.29. Grid for the finite difference analysis. (BUDHU, 2011)

1.8. Eurocode recommendation for the design of the wall

Geotechnical investigations shall be planned in such a way as to ensure that relevant geotechnical information and data are available at the various stages of the project. Geotechnical information shall be adequate to manage identified and anticipated project risks. For intermediate and final building stages, information and data shall be provided to cover risks of accidents, delays and damage. To ensure this the ultimate and the serviceability limit state will be studied.

1.8.1. Ultimate limit state

To avoid the failure of the wall due to excessive deformation, we have the following design approaches with their combinations of sets of partial factors:

1.8.1.1. Design approach 1

Except for the design of axially loaded piles and anchors, it shall be verified that a limit state of rupture or excessive deformation will not occur with either of the following combinations of sets of partial factors: (Eurocode, 1997).

Combination 1: A1 “+” M1 “+” R1

Combination 2: A2 “+” M2 “+” R1

where “+” implies: “to be combined with”.

1.8.1.2. Design approach 2

It shall be verified that a limit state of rupture or excessive deformation will not occur with the following combination of sets of partial factors:

Combination: A1 “+” M1 “+” R2

1.8.1.3. Design approach 3

It shall be verified that a limit state of rupture or excessive deformation will not occur with the following combination of sets of partial factors:

Combination: ($A1^*$ or $A2^\dagger$) “+” $M2$ “+” $R3$

*on structural actions

†on geotechnical actions

Table 1.1. Partial factors on action (Eurocode, 1997)

CHAPTER 1: LITERATURE REVIEW

Action		Symbol	Set	
			A1	A2
Permanent	Unfavourable	γ_G	1,35	1,0
	Favourable		1,0	1,0
Variable	Unfavourable	γ_Q	1,5	1,3
	Favourable		0	0

Table 1.2. Partial factors on materials (Eurocode, 1997)

Resistance	Symbol	Set		
		R1	R2	R3
Bearing	$\gamma_{R,v}$	1,0	1,4	1,0
Sliding	$\gamma_{R,h}$	1,0	1,1	1,0

Table 1.3. Partial factors on resistance (Eurocode, 1997)

Soil parameter	Symbol	Set	
		M1	M2
Angle of shearing resistance ^a	$\gamma_{\phi'}$	1,0	1,25
Effective cohesion	γ_c	1,0	1,25
Undrained shear strength	γ_{cu}	1,0	1,4
Unconfined strength	γ_{qu}	1,0	1,4
Weight density	γ	1,0	1,0
^a This factor is applied to $\tan \phi'$			

1.8.2. Serviceability limit state

Verification for serviceability limit states in the structural section, element or connection, shall either require that: $E_d \leq C_d$. Value of partial factors for serviceability limit states should normally be taken equal to 1 and the possibility of deformations due to changes in the groundwater conditions should be taken into account.

Conclusion

In this chapter, it was a question to explain what is the phenomenon of seepage which will be very useful in the continuation of this work for the study of the stability and the displacements of the diaphragm walls and the determination of the flow rates to be pumped due to the seepage phenomenon. In the continuation of this work, the verification necessary for the stability, the displacements of the diaphragm walls and the estimation of the flows will be carried out in the excel software and deepened in the Plaxis software which is a finite element software.

CHAPTER 2: METHODOLOGY

Introduction

The design of the diaphragm walls like any retaining wall respects a very precise methodology defined by the Eurocode 7. This work specifically deals with the diaphragm walls made at the Aulnay Sous train Bois station. In this chapter, we will present the geographical area around the station and the parameters of the different soil layers under the project, the modelling of the wall and the determination of the flow rates to be pumped will be done using Plaxis 2D

2.1. General recognition of the site

The site recognition passes through a documentary research, in order to determine the physical characteristics of the site used for the case study. The geographical location, the climate, the demography and the main economic activity of the city are presented in this work.

2.2. Data acquisition

The soil parameters are required for the representation of the soil model in a finite element software. Since the geotechnical investigation was already done on the site, and the constructions started, the analysis is done using the results of different tests made by the Société du Grand Paris.

2.2.1. Geotechnical data

The soil parameters symbols and units are in the following table 2.1

Table 2.1. Recapitulative table of the parameter's symbols

Parameters	Symbol
Unsaturated unit weight	γ (kN/m ³)
Saturated soil weight	γ_{sat} (kN/m ³)
Friction angle	ϕ (°)
Young's modulus	E (MPa)
Poisson's ratio	ν (-)
Cohesion	c (kPa)
Vertical permeability	k_h (m/s)
Horizontal permeability	k_v (m/s)
Undrained shear strenght	S_u (kPa)

2.2.2. Load data

The loads concerning the site charges due to the machinery and all the equipment necessary for the proper completion of the work.

2.3. Input data for the design and calculation of flow in diaphragm walls

The input data are data that permit to better understand and analyze the problem in order to come up with a reliable solution.

2.3.1. Input data for the calculation of the flow

- Permeability (m/h)
- Thickness of the ground layers (m)
- Station size
- Water level inside and outside the diaphragm walls at different stage of the work

2.3.1.1. Permeability

The permeability is the measure of the soil ability to permit water to flow through its pores or voids. (SIMONINI, 2019)

It is one of the most important soil properties of interest for geotechnical engineers, because it influences the design of many geotechnical structures -earth dams, embankments, excavations underground water level, stability of slopes, etc.- (SIMONINI, Seepage in porous media, 2019)

2.3.1.2. Water level inside and outside the diaphragm walls

Due to the difference of total head between the sides outer and inside the excavation the water flow toward the excavation moving below the sheet-wall. (SIMONINI, 2019)

2.3.2. Input data for the design of the wall

- External load near the diaphragm wall
- Friction angle and cohesion of the different soil layer
- Unit weight of the different soil

2.3.2.1. External load near the diaphragm wall

External load on the construction site is due to the traffic road, the construction machinery, the equipments -stair, mechanical elevator, etc-. The design approach 1 combination 1 of the Eurocode 7 is used to obtain the design load.

2.3.2.2. Friction angle and cohesion of a soil

The friction angle is a geotechnical parameter that provides information on the shear strength of a soil. The cohesion is the force that unites the particles which forms the ground.

The figure 2.1. present the coulomb model for the determination of the friction angle between two elements.

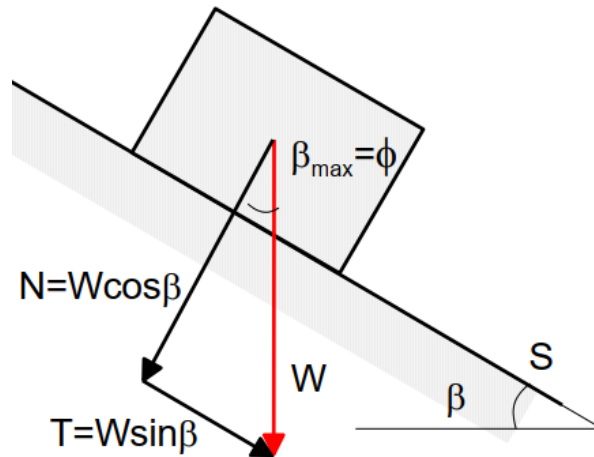


Figure 2.1. Coulomb model of friction

2.3.3. Input data for the calculation of the displacements of the wall

- The Young modulus
- The poisson coefficient
- The dimension of a panel of the wall
- The load on the panel of the wall

2.3.4. Input data for the calculation of the compression force on the struts

- The distance between the button
- The load on the influence surface of the button

2.3.5. Input data for the verification of the stability of the wall

- The stability number N_c
- The undrained cohesion of the soil at the base of the wall

2.4. Analytical design method

The realization of the diaphragm walls passes first by adequate design. For this, two methods have been proposed, in particular the semi-empirical method and the numerical method.

2.4.1. Semi-empirical method

The design of any type of retaining wall consists in evaluating its level of stress in accordance with Eurocode 7 which permit to design the wall and to be in the safety conditions. The procedure for analysis of braced excavation is as follows:

2.4.1.1. Check the stability against bottom heave

About the stability of the diaphragm wall, one was proposed by Bjerrum and Eide (1956), and the other was proposed by Henkel (1971). Bjerrum and Eide suggested that the excavation could be viewed as a footing of width B and embedment depth H_0 . They calibrated their failure mechanism using observations of bottom heave in soft clays and showed that the apparent factor of safety against bottom heave is (BUDHU, 2011):

$$(\text{FS})_{\text{heave}} = N_c * \frac{C_u}{\gamma H_0 + q_s} \quad \text{Equation 2.1.}$$

If $(\text{FS})_{\text{heave}} < 1.5$, the sheeting should be extended below the base of the excavation for stability. (BUDHU, 2011)

To get N_c we calculate the ratio H_0/B and the ratio B/L

C_u , γ and q_s are an input data

2.4.1.2. Determine the lateral stress on the walls for the soil type

Lateral stress distributions for use in the semi-empirical method are approximations from field measurements of strut loads. These lateral stress distributions are not real but average approximate stress distributions to estimate the maximum strut load.

The lateral pressure diagram on the wall is presented in the figure 2.2.

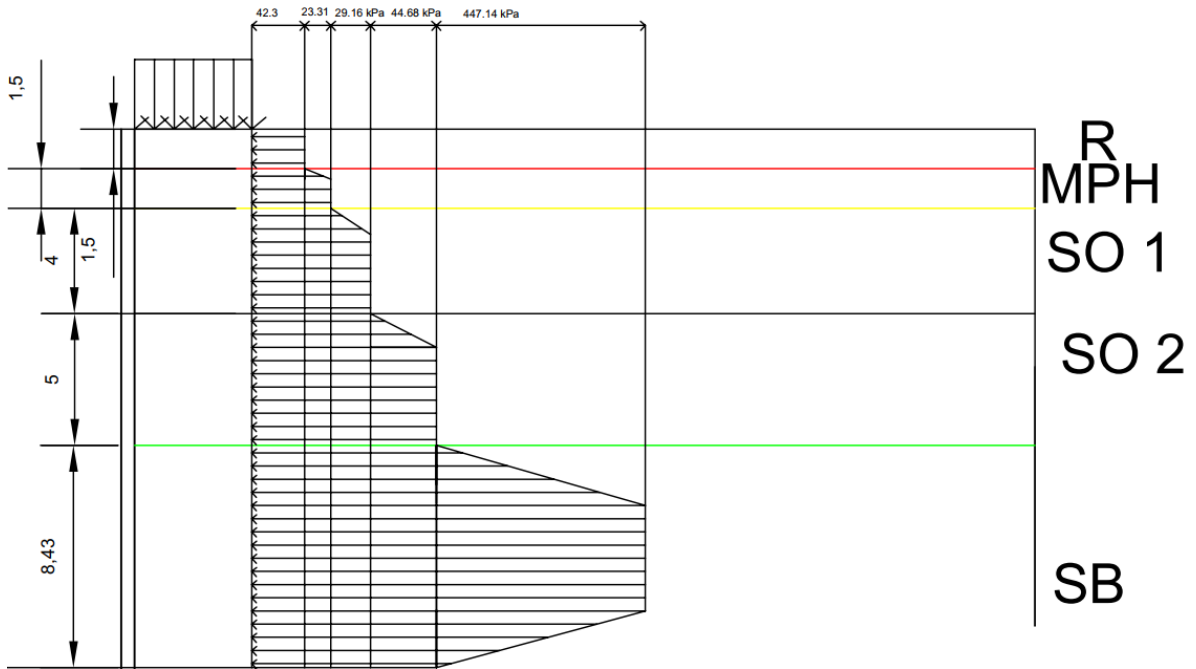


Figure 2.2. lateral stress distribution on the wall

The net water pressure on the wall is shown in the figure 2.3.

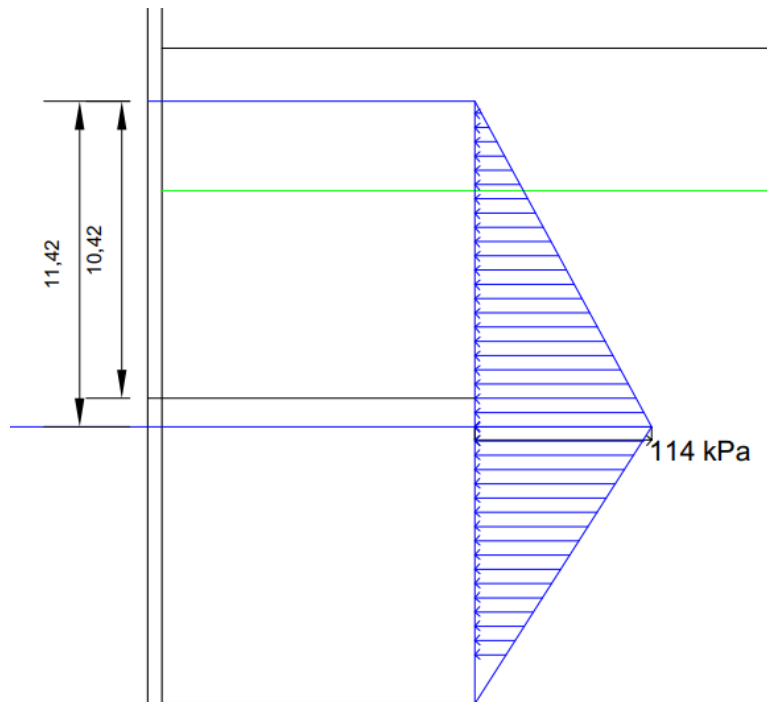


Figure 2.3. Net water pressure distribution on the wall

- For the first layer “Remblai” that is a cohesionless soil, the pressure at the base is

$$Pa = 0.65 * \gamma * H_0 * \left(\tan\left(45 - \frac{\Phi}{2}\right)\right)^2 \quad \text{Equation 2.2.}$$

- For the second layer “Marnes à Pholadomies”, the pressure at the base is

$$Pa = (0.2-0.4) \gamma H_0 \quad \text{Equation 2.3.}$$

- For the third layer “Sables vert, the pressure at the base is calculated by using the equation 2.3

- For the fourth layer “Calcaire de saint Ouen”, the pressure at the base is also calculated by using equation 2.3

- For the fifth layer “Sable de Beauchamp”, the pressure at the base is

$$Pa = K_a * \gamma * H_0 \text{ with } K_a = \left(1 - 4 * \frac{S_u}{\gamma H_0 + q_s}\right) \quad \text{Equation 2.4.}$$

2.4.1.3. Calculate the forces on the struts at each level.

The force on the button is obtained by applying the static equilibrium equations for each free-body diagram.

2.4.1.4. Deformation of the wall

The deformation of the wall is approximate with the equations 1.3, 1.4 and 1.5 discussed in the chapter 1:

2.4.1.5. Calculate resultant forces on the struts

The resultant force on the button is obtain by summing the force obtain at each level.

2.4.2. Determination of the flow with the finite difference method

- First of all, we need to divide the flow domain into a grid, because of the symmetry of the problem, we need only to consider one half of the flow domain and here, the square grid has a size of 3 m*3 m and the size of the model is 30m height and 60 m long.

The figure 2.4. presents the grid section used to determine the flow with the finite difference method.

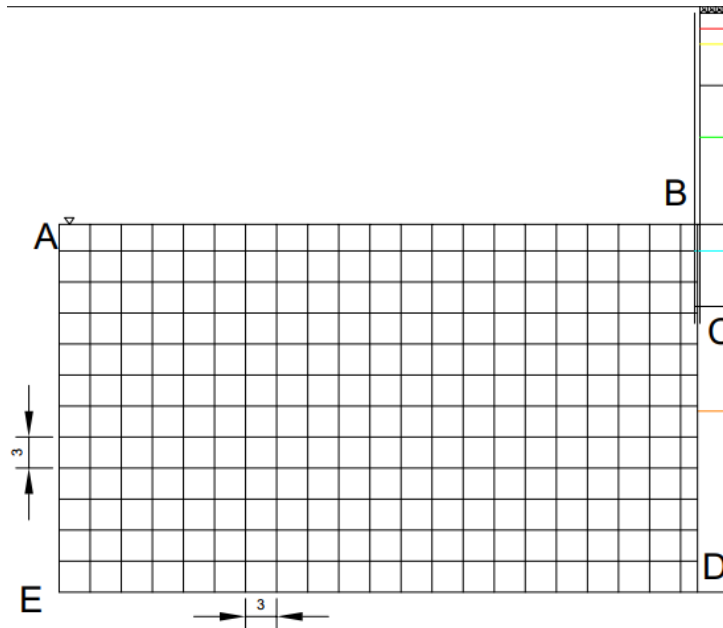


Figure 2.4. Partial grid of a flow domain of the station

- Secondly, we go to the identification of the boundary condition like the impermeable boundary that is flow line -represent the path of flow along which the water will seep through the soil- and the permeable boundary that is equipotential line -that is formed by connecting the points of equal total head-.

Permeable boundaries: AB and CD are equipotential lines.

Impermeable boundaries: BC, AE, and DE are flow lines.

- Determine the heads at the permeable or equipotential boundaries. For example, the head along the equipotential boundary AB is ΔH . Therefore, all the nodes along this boundary will have a constant head of ΔH . Because of symmetry, the head along nodes directly under the sheet pile wall (CD) is $\Delta H/2$.

In our case $\Delta H = 47 - 35.57$,

- With an excel file we apply equation 1.20 to each node except at impermeable boundaries, where we should use equation 1.21, at corners, we should use equation 1.24.
- Calculate q by using equation

$$q = k (h_{i+1, L} - h_{i-1, L} + 2 * \sum_{L+1}^{k-1} (h_{i+1, j} - h_{i-1, j}) + h_{i+1, k} - h_{i-1, k}) / 4 \quad \text{Equation 2.8}$$

- Finally, we calculate the flow in the station by applying equation 2.9

$$Q = 2 * 3600 * q * (L + l) \quad \text{Equation 2.9}$$

L is the length of the station

l is the width of the station

The factor 2 is present for the symmetry reason

The factor 3600 is present to convert the flow into m³/h Choice of the pump to drain the bottom of the excavation

2.5. Choice of the pump to drain the bottom of the excavation

To make the correct choice of the pump and the position of the well, we need to determine the influence surface of the well, the maximum elevation of the water table downstream the well and use the flow to choose the power of the pump.

- First of all, the Sichardt formula is used to determine the influence surface of each well: $L = C_r (H - h_0) \sqrt{K}$

- Secondly, the maximum elevation of the water table downstream the well is

determined with the following formula: $h_d = h_0 \left(\frac{C_1 C_2 (H - h_0)}{L} + 1 \right)$.

- Thirdly, the flow of each well is determined with the Sichardt formula and the number of wells is determined by divided the total flow by the nominal flow of a well.

$Q_n = 2\pi * r_p * h_w * \frac{(k)^{0.5}}{15}$ (CFMS & SFEG, Guide méthodologique pour le rabattement de nappe, 2016)

r_p is the radius of the well

h_w is the wet height of the well that is approximate to $\Delta h / 3$.

- Finally, the flow is used to choose the power of the pump necessary to drain the bottom of the excavation. The following formula can help to determine the power of the pump: $P = \gamma \cdot H \cdot Q$

Where P is the power of the pump in kW

γ the unit weight of the fluid in kN/m^3

H the total head of the fluid in m

Q the flow of the fluid in m^3/s

2.6. Numerical design method

Numerical calculation tools have been used in the engineering field for decades. One of the most widely used numerical tools in engineering is the finite element method which can be implemented through the use of numerous calculation codes.

The advantages of this method are the following: the non-linear material behaviour can be considered for the whole area under analysis, the modelling of excavation sequences including the installation of reinforcement and structural support is possible, the material behaviour as function of time can be introduced, the method has been widely applied to solve practical problems and therefore a lot of experience is already available. And this method presents a disadvantage due to large equation systems execution time and disk storage requirements can be excessive.

This finite element software used in this work is the Plaxis software.

2.6.1. Presentation of the modelling software: Plaxis 2D

Plaxis is a computer program that performs finite element analyses within the realm of geotechnical engineering, including deformation, stability and water flow. The input procedures enable the enhanced output facilities provide a detailed presentation of computational results. It has been developed with the principal aim to find solutions to various aspects of complex geotechnical structures and construction processes using robust and theoretically computational procedures.

Finite element analysis (FEA) is the use of calculations, models and simulations to predict and understand how an object might behave under various physical conditions. Engineers use FEA to find vulnerabilities in their design prototypes. FEA uses the finite element method (FEM), a numerical technique that cuts the structure of an object into several pieces, or elements, and then reconnects the elements at point-called nodes. The FEM creates a set of algebraic equations which engineers, developers and other designers can use to perform finite

element analysis. Frequently, the physical experiences of a product (such as its structural or fluid behaviour and thermal transport) are described using partial differential equations (PDEs). Finite element analysis emerged as a way for computers to solve both linear and nonlinear partial differential equations. However, it is important to note that FEA only provides an approximate solution; it is a numerical approach to finding the real results of partial differential equations. Various different types of tests are used during finite element analysis, such as:

- Structural static analysis. This type of FEA analyzes a scaled model based on proportions. The test maintains that any structure that is sound on a small scale will be able to handle the same interactions with the full-scale structure and produce the same results.
- Thermal engineering analysis. This test explores variations in temperature and how it affects the design structure.
- Modal analysis. Every object vibrates at a frequency, so it is important to use modal analysis to test how disruptive external vibrations affect the product's structure. This form of finite element analysis also allows users to adjust for vibrations throughout the design stage, thus creating a strong final product.
- Engineering seismic calculations. This test helps developers understand the product's performance when dealing with various ground frequencies and vibrations, ensuring a sturdy location for the final structure.

Finite element analysis is based on principles that include boundary conditions, such as forces and pressures, as well as three governing equations:

- Equilibrium equations, which find when the opposing forces or influences are balanced.
- Strain-displacement relations, which measure the deformation that the design experiences under any given external impacts.
- Constitutive equations, which are relations between two physical quantities, specific to the given metal or substance, which predicts the material's response to external stimuli.

For finite element analysis to perform its necessary simulations, a mesh -containing millions of small elements that together form the shape of a structure- must be created. Calculations must be performed on every single element; the combination of each of these individual answers provides the final result for the full structure.

This process can be further broken into three steps: the preprocess, process and postprocess.

During the preprocess step, the user is asked to select the analysis type -such as modal analysis or structural static analysis- as well as the element type. Next, the material properties must be defined and nodes must be made. The elements are then built by assigning connectivity at the nodes. Finally, boundary conditions and loads are applied.

The computer performs the second step, the process. During this step, the computer solves the boundary value problem and then presents the results to the user.

During the postprocess step, the user reviews the generated results and notes factors such as: Displacement, Temperature, Time history, Stress, Strain, Natural frequency.

Designers using finite element analysis should be aware of inherent errors that can be found in this process, such as the simplification of geometry in the finite element method and use of basic integration techniques; errors in computing stemming from numerical difficulties or the limited number of digits available in computers; and common user mistakes, such as selecting the wrong type of element or providing inconsistent units of measurement.

Finite element analysis provides the safe simulation of potentially dangerous or destructive load conditions and failure modes, allowing engineers to discover a system's physical response at any location. Other benefits include:

- Increased accuracy due to the analysis of any physical stress that might affect the design.
- Improved design because developers can observe how stresses within one element will affect the materials in another connected element.

- Earlier testing in the development process. Virtual prototyping allows the designer to model various designs and materials in a matter of hours, rather than the days or weeks it takes to produce hard prototypes.
- Increased productivity and revenue because FEA software allows developers to produce higher quality products in a shorter design cycle while also using less material.
- Enhanced insight into critical design parameters as the result of being able to model both the design's interior and the exterior. This allows designers to determine how critical factors affect the structure as a whole, as well as why and where failures might occur.
- Optimized use of models because one common model can be used to test several failure modes or physical events
- Fast calculation times and relatively low investment costs.
- Access to existing experimental results, which can be pulled from the parametric analyses of already validated models and applied to the new model.

2.6.2. Plaxis input component

The analysis of a new project with the software must start by the creation of a geometry model. This geometry model is a 2D representation of the real three-dimensional and consists of the following components: points, lines and clusters. A geometry model should include a representative division of subsoil into distinct soil layers, structural objects, construction stage and loadings. Points are from the start and end of lines, it can also be used for the positioning of anchors, point forces and point fixities. Lines are used to define the physical boundaries of the geometry, the model boundaries and discontinuities in the geometry such as walls, separations of distinct soil layers or construction stages. A line can have several functions or properties. Clusters are areas that are fully enclosed by lines. PLAXIS automatically recognizes clusters based on the input of geometry lines. Within a cluster the soil properties are homogeneous. After the creation of a geometry model, a finite element model is automatically be generated. In a finite element mesh the components that can be identified is described as follows:

- Elements: during the generation of the mesh, clusters are divided into triangular elements. A choice can be made between 15-node elements and 6-node elements. The powerful 15-node element provides an accurate calculation of stresses and failure loads. In addition, 6-node triangles are available for a quick calculation of serviceability states. Considering the same element distribution, the meshes composed of 15-nodes elements are actually much finer and much more flexible than meshes composed of 6-node elements, but calculations are also more time consuming. In addition to the triangular elements, which are generally used to model the soil, compatible plate elements and interface elements may be generated to model structural behaviour and soil-structure interaction.

In Plaxis, the following model can be defined:

- The plane strain model that is used with a (more or less) uniform cross section and corresponding stress state and loading scheme over a certain length perpendicular to the cross section (z-direction). Displacements and strains in z-direction are assumed to be zero. However, normal stresses in z-direction are fully taken into account. In earthquake problems the dynamic loading source is usually applied along the bottom of the model resulting in shear waves that propagate upwards. This type of problem is generally simulated using a plane strain model.
- The axisymmetry model that is used for circular structures with a (more or less) uniform radial cross section and loading scheme around the central axis, where the deformation and stress state are assumed to be identical in any radial direction. Note that for axisymmetric problems the x coordinate represents the radius and the y-axis corresponds to the axial line of symmetry. Negative x-coordinates cannot be used. Single-source vibration problems are often modelled with axisymmetric models. This is because waves in an axisymmetric system radiate in a manner similar to that in a three-dimensional system. In this case, the energy disperses leading to wave attenuation with distance. Such effect can be attributed to the geometric damping (or radiation damping), which is by definition included in the axisymmetric model.

2.6.2.1. Input of geometry

After applying the general setting, the input window appears. The creation of a geometry is done through the uses of points and lines procedure but also several geometry object available from the menu or from the toolbar. At the following figure it can be observed a view of the Plaxis interface.

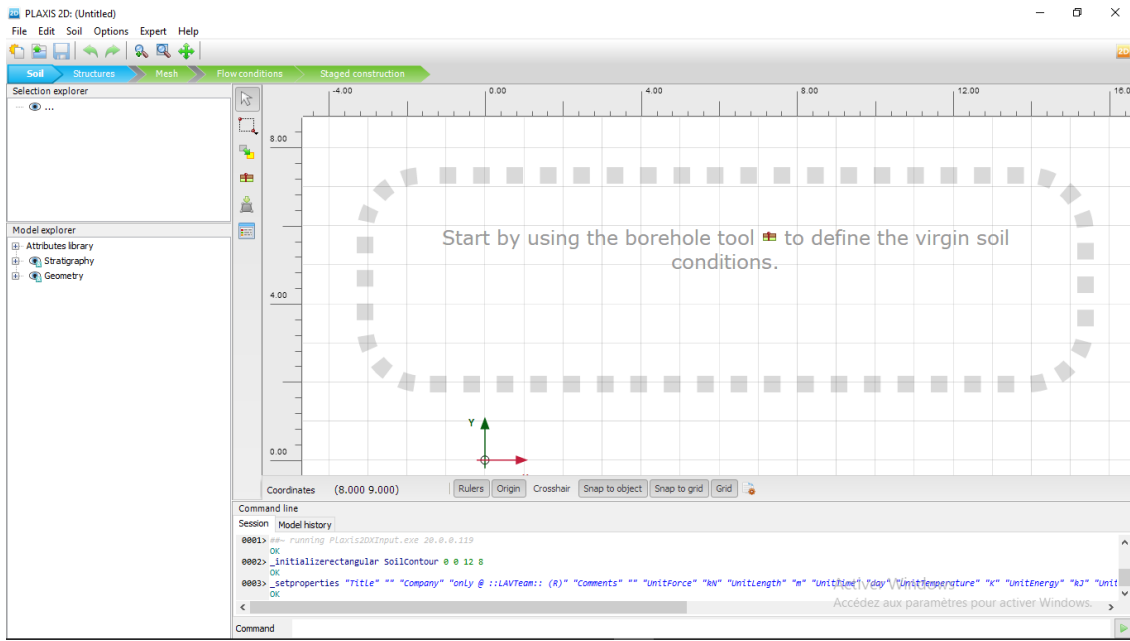


Figure 2.5. Plaxis interface

2.6.2.2. Input of the dimensions of the project

Plaxis software required the input of the dimensions of the project. The required input is specified in the edit boxes. The box of the input dimensions in Plaxis is show in the following figure.

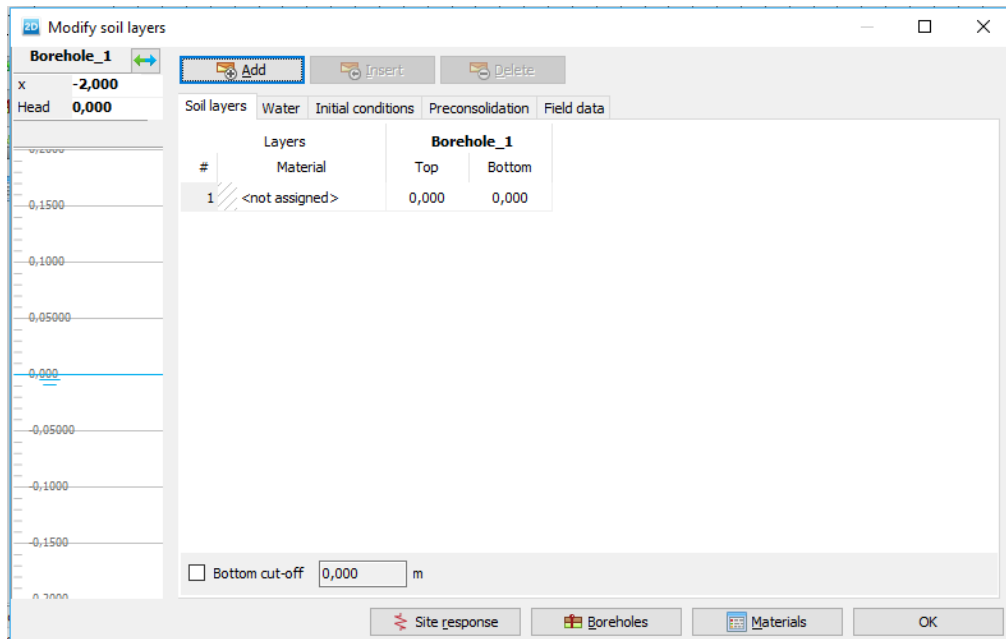


Figure 2.6. Box of input dimension in Plaxis

2.6.2.3. Plaxis input program structures-modes

The modelling process is completed in fives modes. The mode tabs are shown in the mode bar. The modes are separated into geometry and calculation modes.

- The geometry configuration of the project is defined in the geometry mode which are indicated by blue coloured type in the input program. All the changes in geometry are only possible in the geometry mode. Features such as structures, interface or loads, can be assigned in the geometric entities only in the structure mode. The geometry modes are the soil -the soil stratigraphy, the general water levels and the initial conditions of the soil layers are defined in the soil mode- and the structures -the geometry entities as well as the structural elements and forces in the project are defined in the structure mode-.
- The calculation process is defined in the calculation modes which are indicated by green coloured type in the input program. In these modes' entities cannot be created and new features cannot be assigned to existing geometry entities. The calculation modes are mesh -the geometry model is discretized and the finite element mesh is generated in the mesh mode. The geometry configuration cannot be modified in this mode. The mesh should be regenerated whenever the geometry of the project is

modified. -, flow conditions -besides water levels generated from the water conditions defined in the soil mode, user-defined water level can be specified and modified in this mode. -, staged construction -part of the geometry model can be activated/deactivated and properties can be modified. The project is calculated in the staged construction mode. –

2.6.3. Material model

The mechanical behaviour of soils may be modelled at various degrees of accuracy. Various material models are available to enable simulation of different geotechnical problems, each material model has specific parameters which are required.

2.6.3.1. Linear elastic model

This model is considered as the Hooke's law of isotropic linear elasticity. It involves two elastic stiffness parameters which are: The Young's modulus (E) and Poisson's ratio (ν). Following this, it can be said that it is very limited for the simulation of the soil behaviour. It is primarily used for stiff structures in the soil.

2.6.3.2. Mohr coulomb model

The linear elastic Mohr-Coulomb model involves five input parameters, i.e., E and ν for soil elasticity; ϕ and c for soil plasticity and ψ as an angle of dilatancy. This Mohr Coulomb model represents a 'first order' approximation of soil or rock behaviour. It is recommended to use this model for a first analysis of the problem considered. For each layer one estimates a constant average stiffness or a stiffness that increases linearly with depth. Due to this constant stiffness, computations tend to be relatively fast and one obtains a first estimate of deformations.

2.6.3.3. Hardening soil model

The Hardening Soil model is an advanced model for the simulation of soil behaviour. As for the Mohr-Coulomb model, limiting states of stress are described by means of the friction angle, ϕ , the cohesion, c, and the dilatancy angle, ψ .

2.6.3.4. Modified cam clay model

The modified cam-clay model is a well-known modelling literature. It is meant primarily for the modelling of near normally consolidated clay type soils. This model has been added to PLAXIS to compare with other codes.

2.6.3.5. Soft soil model

It is presented as a Cam-clay type model. This model can be used to simulate the behaviour of the soft soils such as normally consolidated clay and peat. The model performs best only in case of primary compression. This model is not recommended for use for excavation problems.

2.6.3.6. Soft soil creep model

The Hardening Soil model is generally suitable for all soils, but it does not account for viscous effects, i.e., creep and stress relaxation. In fact, all soils exhibit some creep and primary compression is thus followed by a certain amount of secondary compression. The latter is most dominant in soft soils, i.e., normally consolidated clays, silts and peat, and PLAXIS thus implemented a model under the name Soft Soil Creep model. The Soft Soil Creep model has been developed primarily for application to settlement problems of foundations, embankments, etc. For unloading problems, as normally encountered in tunneling and other excavation problems, the Soft Soil Creep model hardly supersedes the simple Mohr-Coulomb model. As for the Hardening Soil model, proper initial soil conditions are also essential when using the Soft Soil Creep model. This also includes data on the pre-consolidation stress, as the model accounts for the effect of over consolidation. Note that the initial over-consolidation ratio also determines the initial creep rate.

2.6.3.7. Jointed rock model

The Jointed Rock model is an anisotropic elastic-plastic model, especially meant to simulate the behaviour of rock layers involving stratification and particular fault directions. Plasticity can only occur in a maximum of three shear directions (shear planes). Each plane has its own strength parameters ϕ and c . The intact rock is considered to behave fully elastic with constant stiffness properties E and ν . Reduced elastic properties may be defined for the stratification direction.

2.6.3.8. Concrete model

The Concrete model is an advanced elasto-plastic model for concrete and shotcrete structures. It simulates the time-dependent strength and stiffness of concrete, strain hardening softening in compression and tension as well as creep and shrinkage. The failure criterion involves a Mohr-Coulomb yield surface for deviatoric loading, which is combined with a

DESIGN OF A RETAINING STRUCTURE AND ITS PUMPING SYSTEM FOR AN UNDERGROUND

STRUCTURE CONSTRUCTION Presented by TCHINDA KENGNE Franck Junior

Rankine yield surface in the tensile regime. The Concrete model employs 25 input parameters, but most of them can be derived from standard uniaxial tensile and compression tests and are generally familiar to structural engineers.

2.6.4. Mesh

When the geometry model is fully defined, the geometry has to be divided into finite elements in order to perform finite element calculations. The mesh is created in the mesh mode. PLAXIS 2D uses fully automatic generation of the finite element meshes. The generation meshes is based on robust triangulation procedures. The mesh generation process takes into account the soil stratigraphy as well all structural objects, load and boundary conditions.

2.6.5. Presentation of the phase's construction of the project

The model of this project in Plaxis was done in 7 main steps:

- The first step that is the initial phase is the installation of the wall: it's the phase during which Plaxis generates the initial stress state in the ground before installing the wall and load.

2.6.6. Plaxis output program

The main output quantities of a finite element calculation are the displacements and the stresses. In addition, when a finite element model involves structural elements, the structural forces in these elements are calculated. An extensive range of facilities exist within the PLAXIS 2D Output program to display the results of a finite element analysis. The figure 2.8 presents the windows of Plaxis output program.

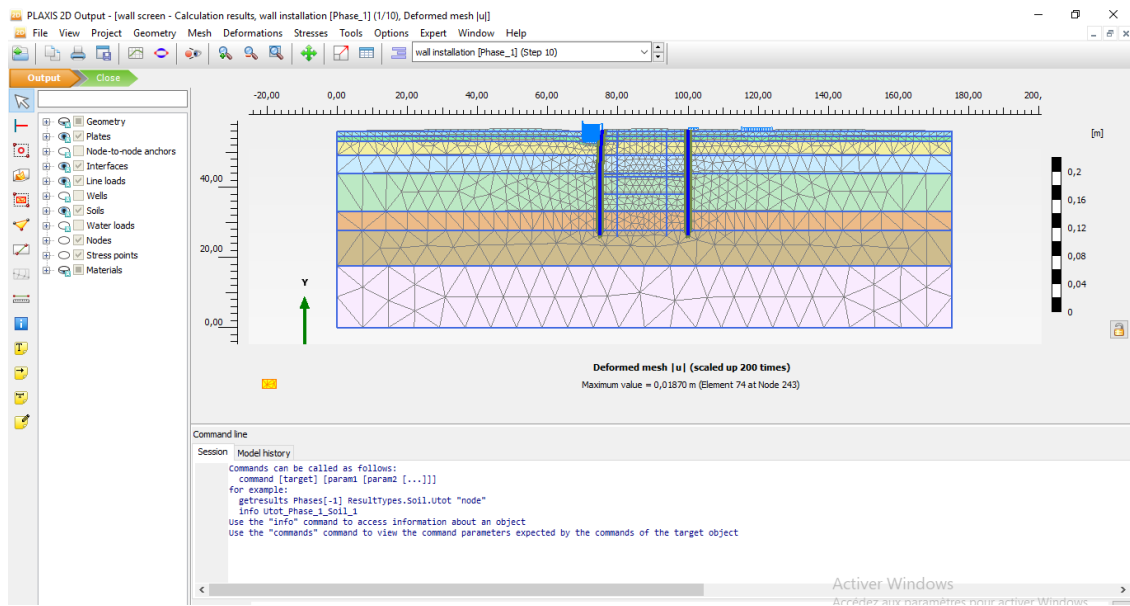


Figure 2.7. Main windows of Plaxis output program

Conclusion

The main goal of this chapter was to establish the procedure to obtain the best parameter to use in the calculation procedure, to do this a site recognition was done in order to assess the geographical localization, climatic conditions and this followed by a collection of geometric and geotechnical data to have the parameter of the study. With this parameter the verification of the stability of the wall will be verified using analytical and numerical method with the Plaxis code.

CHAPTER 3: RESULTS AND INTERPRETATIONS

Introduction

This chapter reveals the results of the research carried out during this work. It goes from the presentation of the site using project documentation to the analytical and numerical analysis of the diaphragm wall and its pumping system. The wall is embedded in the ground and supported by the struts, the water flow in the station by effect of seepage. The Plaxis program analysis has been used to provide all the valuable information which is required to confirm the result obtained by the analytical method. In the following section, the modelling of the wall and the interpretation of the results of the necessary parameters that confirm the stability of the wall are presented.

3.1. General presentation of the site

3.1.1. Localization

Aulnay station is located on the open ground of the former national road number two between boulevard Marc Chagall and Rue Paul Cézanne, in the town of Aulnay-sous-Bois and Aulnay-sous-Bois town is located in the île de France region. The station consists of a deep underground box with 3 levels, an outgrowth on the mezzanine -surface box-, and an emerging passenger building. The Aulnay station is rectangular in shape, 60.6 m long and 25.4 m wide. The rails are located around 16.3 m deep, i.e., at level 41.5 NGF.

CHAPTER 3: RESULTS AND INTERPRETATIONS

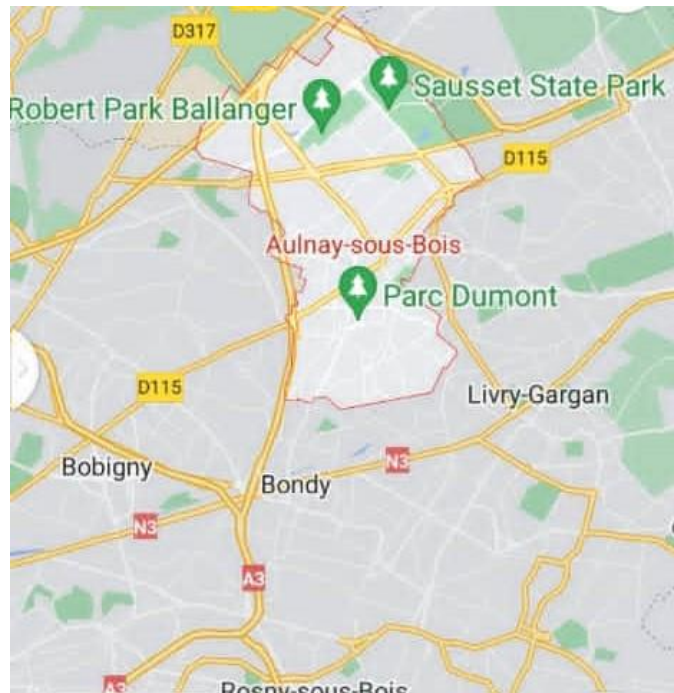


Figure 3.1. Localization of the Aulnay sous Bois town (GOOGLE MAP)

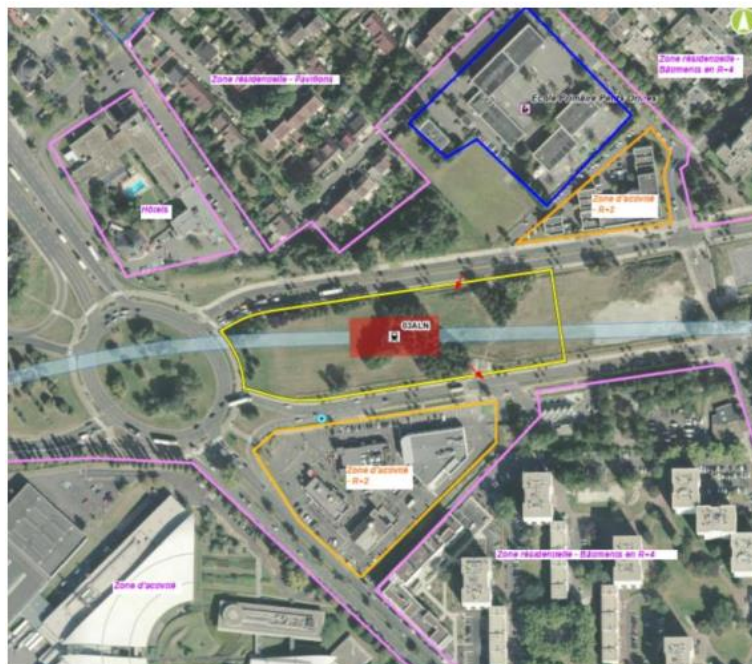


Figure 3.2. Aerial view of the localization of the Aulnay station (LOMBARDI, 2019)

DESIGN OF A RETAINING STRUCTURE AND ITS PUMPING SYSTEM FOR AN UNDERGROUND
STRUCTURE CONSTRUCTION Presented by TCHINDA KENGNE Franck Junior

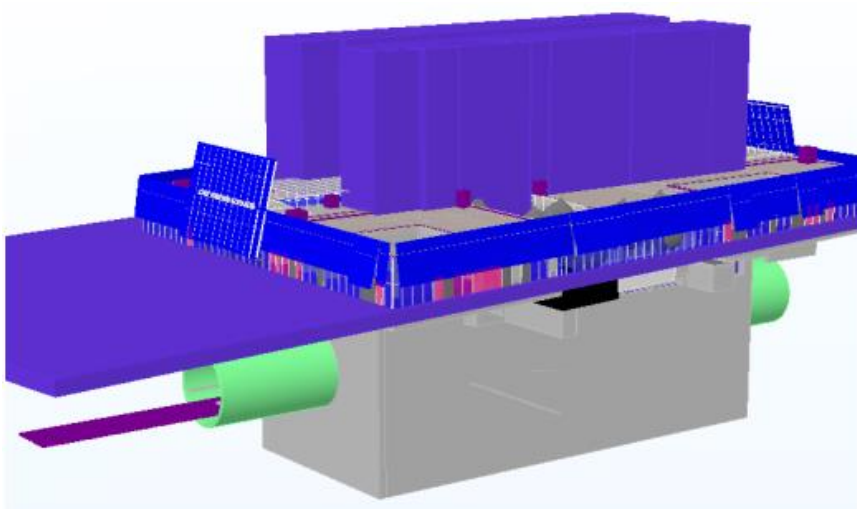


Figure 3.3. 3D presentation of the Aulnay-sous-bois station (LOMBARDI, 2019)

3.1.2. Climate

In Aulnay-sous-Bois, the summers are short, warm, and partly cloudy and the winters are very cold, windy and mostly cloudy. During the year, the temperature generally varies from 2°C to 25°C and is rarely lower than -2°C and higher than 31°C. The warm season lasts for 2.9 months, from June 13 to September 10 with an average daily temperature above 22°C. The hottest month in Aulnay-sous-Bois is July with the average high temperature of 25°C and low of 15°C. The cool season lasts for 3.7 months from November 16 to March 7 with an average daily high temperature below 11°C. The coldest month in Aulnay-sous-Bois is January with an average minimum temperature of 2°C and maximum of 7°C.

3.1.3. Demography

There are 88 166 inhabitants in Aulnay sous Bois in 2021, the official legal population of Aulnay sous Bois is however 85 740 inhabitants because the last official figure dates from 31/12/2016. The number of inhabitants for 2021 is calculated from the average annual growth rate of the population of Aulnay sous Bois over the period from 2011 to 2016, i.e., 0.7%. The population of Aulnay sous Bois is therefore on the rise. It is a population that is getting much younger with an aging index of 1 person aged 65 or over for 41.8 inhabitants under the age of 20. (ville-data.com, 2022)

CHAPTER 3: RESULTS AND INTERPRETATIONS

3.1.4. Economic activity

The development of economic life in Aulnay sous Bois is based on two main axes: the creation and establishment of new businesses, including the revitalization of current activity areas, and the establishment of training to promote the professional integration and entry into the world of employment. To confirm its economic position at the heart of the Grand Roissy/Le Bourget airport axis, Aulnay-sous-Bois is strengthening its territorial marketing action to maintain and renew its economic potential around a new business real estate offer. It encourages, through concrete actions, the creation and implementation of new activities. The city is also emphasizing the revitalization of economic activity zones. In addition, as part of the arrival of the Grand Paris Express station in 2025, it is working to improve internal service and access to motorway networks. Its ongoing dialogue and exchanges with companies lead to the establishment of new service for local economic players and their employees. By relying on the know-how of local structures and actors, the City is investing in promoting the integration of young people, professional training and support for project leaders in their procedures and the search for premises. (Aulnay-sous-bois.fr, 2022)

3.2. Presentation of the project

The project is the design of the diaphragm wall of the station of Aulnay-sous-Bois and the pumping system of the underground water which will permit the earthworks in the dry conditions before the realization of the raft. The geotechnical field investigation made to recognize the soil type permit to do the following stratigraphy of the soil. The diaphragm wall of the project has a width of 1 m and the water table is 9 m below the ground.

The diaphragm wall of this project is 30m depth and 1m width, the wall is symmetric and the problem will. The soil will be excavated under 21 m and the water will be pump 1 m below this level.

3.2.1. Backfill (R)

It is a formation generally of anthropic origin. This formation is made of a set of fine clay-sand deposits.

CHAPTER 3: RESULTS AND INTERPRETATIONS

3.2.2. Marls with Pholadomies (MPH)

These are yellowish-beige marls located between 1 and 3 m deep. They are often altered and may contain various gravels. The “Guide du terrassement routier” (GTR) classifies them as low plastic clays and marls



Figure 3.4. Picture of marls with Pholadomies sampling

3.2.3. Greensand (SV)

They are Greenish-Brown Clayey sands present on a very weak thickness and in a discontinuous way between the MPH and the SO. The GTR classifies them as low plastic silt and low pollution fine sand.



Figure 3.5. Picture of Greensand sampling

3.2.4. Limestone of Saint Ouen (SO)

It is mainly constituted of a dominant carbonate facies of marly limestone, whitish beige and slightly pink. It presents unstructured, friable and very fragmented passes as well as firmer and compact whites. The GTR classifies them as low plastic silt.



Figure 3.6. Picture of limestone of Saint Ouen sampling

DESIGN OF A RETAINING STRUCTURE AND ITS PUMPING SYSTEM FOR AN UNDERGROUND
STRUCTURE CONSTRUCTION Presented by TCHINDA KENGNE Franck Junior

CHAPTER 3: RESULTS AND INTERPRETATIONS

3.2.5. Beauchamp sand (SB)

They are a sandy clay formation of about ten meters. The GTR classifies them as low plastic silt.



Figure 3.7. Picture of Beauchamp Sand sampling

3.2.6. Marls and Pebbles (MC)

They consist mainly of a beige to whitish carbonate facies in the form of compact marl or semi rocky limestone with diffuse gypsum. The GTR classifies them as fine clayey sand.



Figure 3.8. Picture of Marls and Pebbles sampling

3.2.7. Coarse limestone (CG)

In the upper part of the coarse limestone, one facies observed is a sometimes-fragmented shell-like rocky limestone.

CHAPTER 3: RESULTS AND INTERPRETATIONS



Figure 3.9. Picture of Coarse Limestone sampling

3.2.8. Soil parameters

The soil parameters are reported in the table below

Table 3.1. data of the problem (LOMBARDI, 2019)

Layer	c (kPa)	Phi (°)	E (MPa)	v (-)	K _h (m/s)	K _v (m/s)	Y _{sat} (kN/m ³)	S _u (kPa)
R	0	28	27	0,3	1.0E-05	1.0E-05	19	0
MPH	5	34	60	0,3	1.0E-05	1.0E-05	19	15
SO1	10	33	60	0,3	2.9E-5	1.2E-5	18	20
SO2	10	33	120	0,3	2.9E-5	1.2E-5	18	20
SB	5	33	200	0,3	3.1E-4	4,1E-06	21	5
MC1	20	30	120	0,3	1.3E-4	5.2E-5	20	50
MC2	50	35	800	0,3	1.3E-5	5.2E-5	20	50
CG	100	35	1493	0,3	2,1E-05	8,4E-07	21	100

3.2.9. Design load

Site loads are of variable and permanent types. The variables loads are due to equipment (10 kPa for all the intermediate slab), road traffic (20 kPa) the minimum distance between the

CHAPTER 3: RESULTS AND INTERPRETATIONS

diaphragm wall and the road is 15 m and the load due to the excavator machine is estimate at 85 kPa.

The permanent loads are due to the structure and its permanent equipment.

3.2.10. Materials characteristics

The characteristics of the materials used to build the diaphragm wall of the station in Aulnay-sous-Bois are summarized in the table 3.2 and 3.3.

Table 3.2. Properties of concrete C35/45

Concrete characteristics	
f_{ck} (MPa)	35
f_{cd} (MPa)	23.33
γ (kN/m ³)	23.5

f_{ck} is characteristics of compressive strength of concrete, is measured in MPa by CTM machine after casting of 28 days of curing and f_{cd} is the value of design compressive strength.

Table 3.3. Properties of the steel B500

Steel characteristics	
f_{yk} (MPa)	500
f_{yd} (MPa)	434.8

f_{yk} is the characteristic yield strength of a steel reinforcement and f_{yd} is the design yield strength.

3.2.11. Presentation of the geometry of the train station

In this work, the retaining wall that is considered is a diaphragm wall and the figure 3.10. show the geometry of the train station.

CHAPTER 3: RESULTS AND INTERPRETATIONS

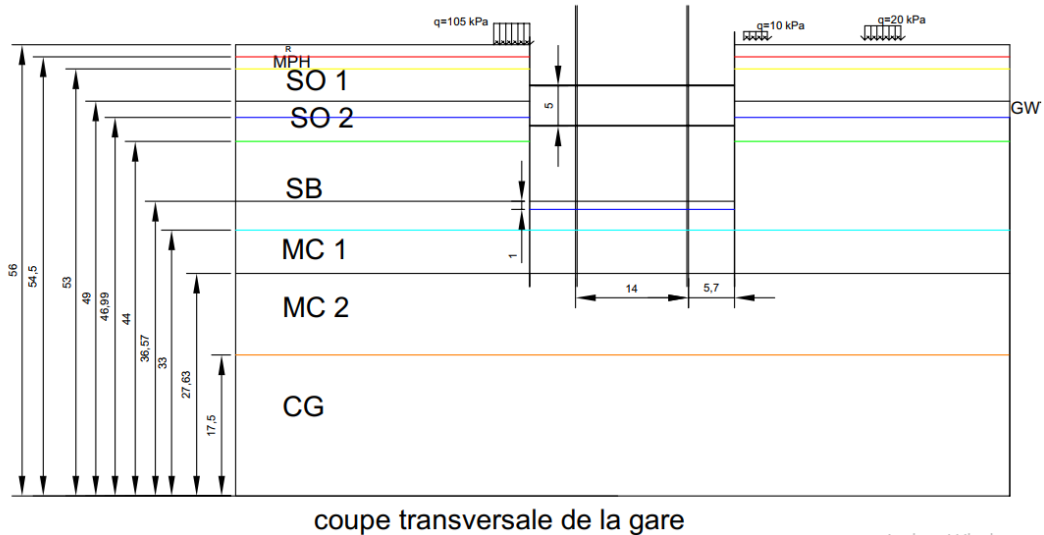


Figure 3.10. Cross section of the train station

3.3. Analytical results

3.3.1. Stability against bottom heave

The verification of the stability against bottom heave is done by the use of the equation 2.1 and the calculation is done by the excel software.

H/B	0,765		
B/L	0,423	Nc	6,4
FS heave	1,56		

The value of the safety coefficient of the bottom heave is greater than 1,5 and this means that the toe penetration is satisfactory.

3.3.2. Lateral pressure on the wall

The lateral pressure on the wall is obtained with the design load obtain by using the design approach 1 combination 1 describe by the Eurocode 7 and by using the resultant pressure diagram of the figure 2.1 implemented in the excel software. The following pressure presented the recapitulated of the pressure on the wall.

CHAPTER 3: RESULTS AND INTERPRETATIONS

Table 3.4. Recapitulative of the pressure on the wall

	$\gamma \cdot H_0 / S_u$	$(\gamma \cdot H_0 + q_s) / (S_u)_b$	K_a	$\gamma \cdot H_0$ or $(\gamma - \gamma_w) \cdot H_0$	$\gamma_w \cdot H_0$	P (kPa)
R			0,23	28,5		42,29
MPH	1,9		0,3	28,5		65,61
SO1	3,6		0,3	72		94,77
SO2	2,04		0,3	90	49,45	139,45
SB	24,61	3,04	0,89	82,02	71,90	586,58

3.3.3. Compression force on the struts

The force on the struts is obtained by applying the static equilibrium equation for each body diagram. And b_1 , b_2 and b_3 are the level arm of all the resultant force. The following table is an extract of excel sheet made to calculate the compression force in the struts.

Table 3.5. Presentation of the force obtains in each strut

Layer	b_1 (m)	b_2 (m)	b_3 (m)
R	9,25		
MPH	7,75	8,25	7,56
SO1	5	6,33	4,5
SO2	1,5	2,16	0,41
SB	4,5	7,5	3,375
1st strut (kN)		3370,28	
2nd strut (kN)		8729,08	

The force obtain in the button will be used by the structural engineer to find the section of steel to use.

CHAPTER 3: RESULTS AND INTERPRETATIONS

3.3.4. Deformation of the wall

The deformation of the wall is estimated with the finite difference method implemented in the excel software and the table below is an extract of this excel sheet that presented the displacement of the wall.

Table 3.6. Presentation of the maximum displacement of the wall

L (m)	10
h (m)	1
E (GPa)	33
ν (-)	0,3
λ (m)	2,5
D (m)	3021978
q (kPa)	586.58
$q^*(\lambda)^4/D$	0,0076
w (mm)	7.82

The value obtain here is the displacement of the wall and this is acceptable the maximum displacement was 40mm.

3.3.5. Calculation of the flow

Using the finite difference method describe in the previous chapter, the flow obtains by using an excel sheet is equal to 35.8 m³/h and this excel sheet is presented in annex 2.

3.3.6. Determination of the power of the pump

After having obtained the flow of water infiltrating in the station, it is possible to determine the power of the pump and the number of wells necessary to lower the water table connected to this pump.

CHAPTER 3: RESULTS AND INTERPRETATIONS

- The influence radius of a well equals:

$$L = C_r(H - h_0)\sqrt{K} = 1500 * (47.7 - 35.57) * \sqrt{(1.18 * 10^{-5})} = 62.5 \text{ m}$$

- The maximum level of water downstream the well:

$$h_d = h_0 \left(\frac{C_1 C_2 (H - h_0)}{L} + 1 \right) = 27 * (0.3 * 1.4 * (47.7 - 26) / 62.5 + 1) = 32.75 \text{ m}$$

this value is less than the required water level 35.57 NGF before the excavation and is satisfactory.

- The nominal flow of a well is:

$$Q_n = 2\pi * r_p * h_w * \frac{(k)^{0.5}}{15} = 2\pi * 0.2 * 12.13 * (0.0000118)^{0.5} * 3600 / (3 * 15) = 4.19 \text{ m}^3/\text{h}$$

- The minimum number of wells is: $n = Q_{\text{tot}} / Q_n = 35.8 / 4.19 = 8.54$

Where r_p is the radius of the well and h_w is the wet height of the well and is estimated to be the third of the total height of the water

For this project, to be in safety conditions the number of wells to be use is 10.

- The power of the pump connected to the wells:

$$P = \gamma * H * Q = 9.81 * (57 - 27) * 35.8 / 3600 = 2.93 \text{ kW.}$$

3.3.7. Minimum height of the raft

Because the pump will be stop at the end of the construction of the raft, there is a risk of lifting of the excavation bottom because the pore pressure below the impermeable bottom remains very high. We can determine the minimum height of the raft:

$$FS = \gamma_{\text{sat}} * D' / \gamma_w * H \text{ and for the } FS = 1$$

$$D' = \gamma_w * H / \gamma_{\text{sat}} = 9.81 * 12.13 / 21 = 5.67 \text{ m}$$

This height is the minimum height of the height to be constructed in the Aulnay-sous-Bois train station to be safe against uplift.

CHAPTER 3: RESULTS AND INTERPRETATIONS

3.4. Numerical results

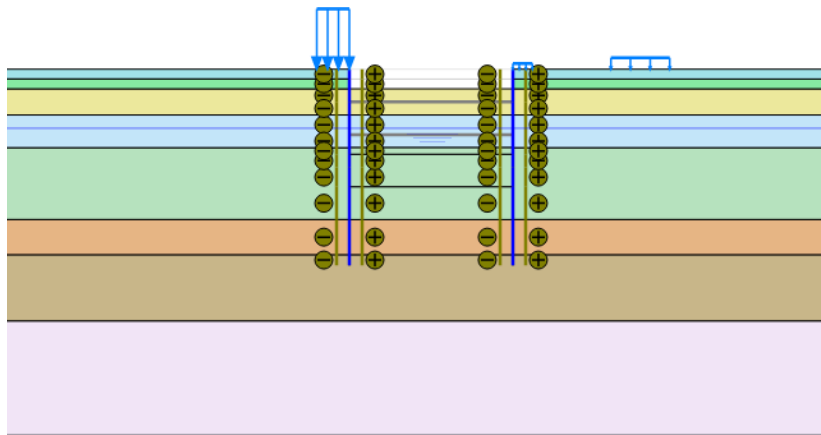
3.4.1. Hypothesis

Since there is no exact analytical solution for this problem, the main goal is to obtain the reliable and consistent results for the model. In this numerical model, the diaphragm wall is modelled by the plate element.

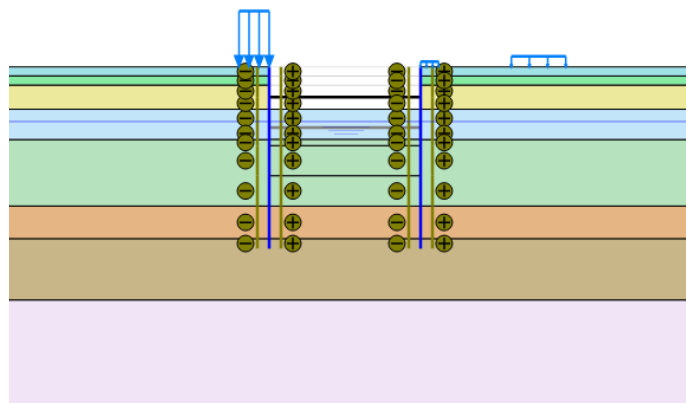
3.4.2. Calculation steps

The calculation steps are as follows:

- Step 1: first excavation (until elevation 50NGF)

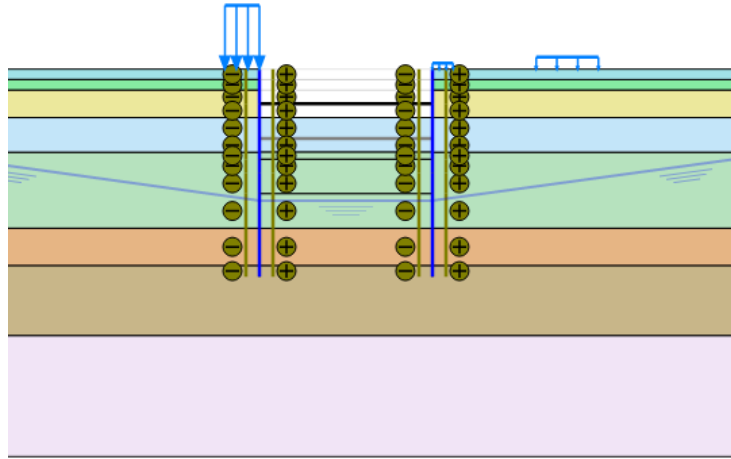


- Step 2: activation of the first row of struts

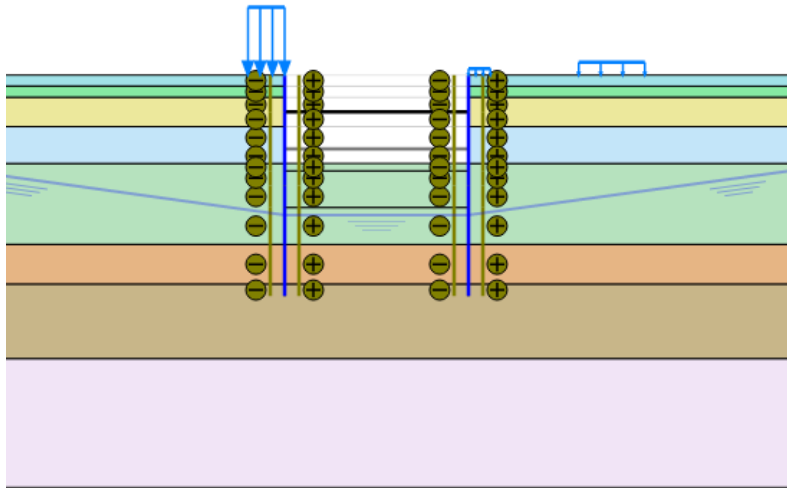


- Step 3: lowering of the water table to the elevation 35.67 NGF

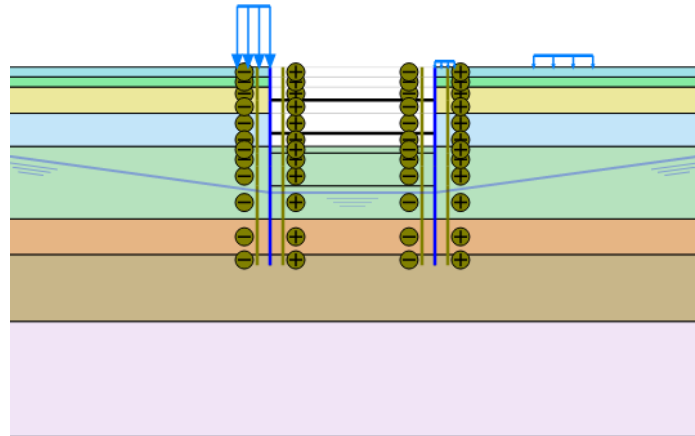
CHAPTER 3: RESULTS AND INTERPRETATIONS



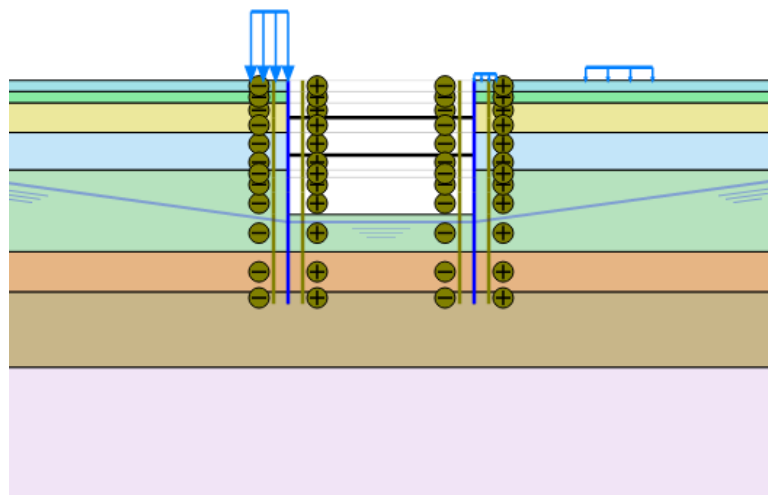
- Step 4: second excavation (up to elevation 45 NGF)



- Step 5: activation of the second row of the struts



- Step 6: third excavation (up to elevation 36.67NGF)



3.4.3. Mesh generation

Generating a proper Finite Element mesh is an important intermediate step between the definitions of the geometry and the construction stages. In order to have a smooth and accurate calculation, the finite element mesh has to fulfil several criteria. For the numerical stability of the calculation, the mesh should have a good quality, that is, the elements should be regular without being excessively long and thin. For the accuracy of the calculation, the elements should be small enough, especially in those areas where significant changes in stress or strain can be expected during the analysis. In order to obtain a precise result, the mesh is refined

CHAPTER 3: RESULTS AND INTERPRETATIONS

around the excavation where the stresses and deformation are high and to do this, the option choose in Plaxis is fine mesh.

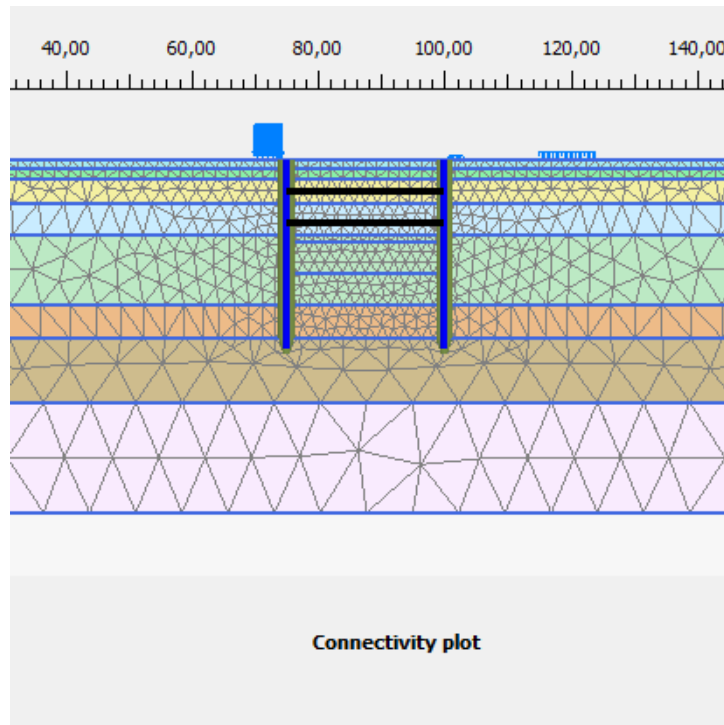


Figure 3.11. Meshing system of the station on initial state soil

3.4.4. Principal result

Before presenting the result, the curve represents the stage construction is presented to prove that all phases run in the Plaxis code.

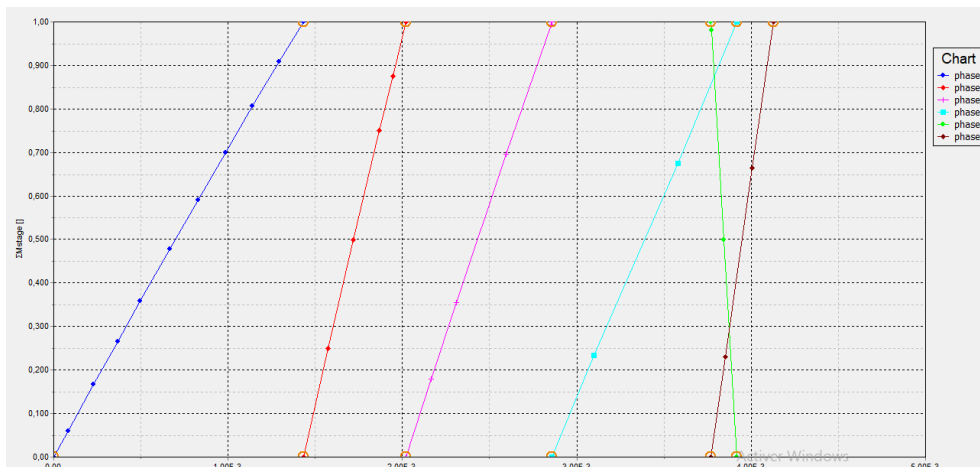


Figure 3.12. Phase construction of the project

DESIGN OF A RETAINING STRUCTURE AND ITS PUMPING SYSTEM FOR AN UNDERGROUND STRUCTURE CONSTRUCTION Presented by TCHINDA KENGNE Franck Junior

CHAPTER 3: RESULTS AND INTERPRETATIONS

The initial state of the model is presented by the figure 3.13 which is the phase at which Plaxis generates the initial state of the soil.

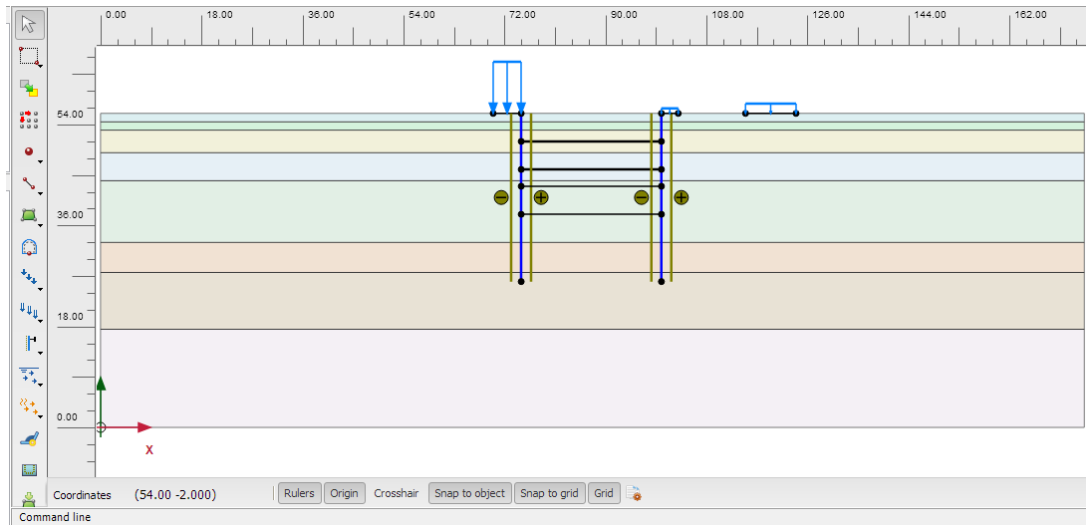


Figure 173.13. Model of the constructed wall at initial state

3.4.4.1. Deformation of the wall

The deformation of the model shows a vertical displacement of the soil at the bottom of the excavation which can be linked to the release of the stresses induced by the uplift of the soil located below the bottom of the excavation and the horizontal displacement is due to the pressure of the earth and the hydrostatic pressure.

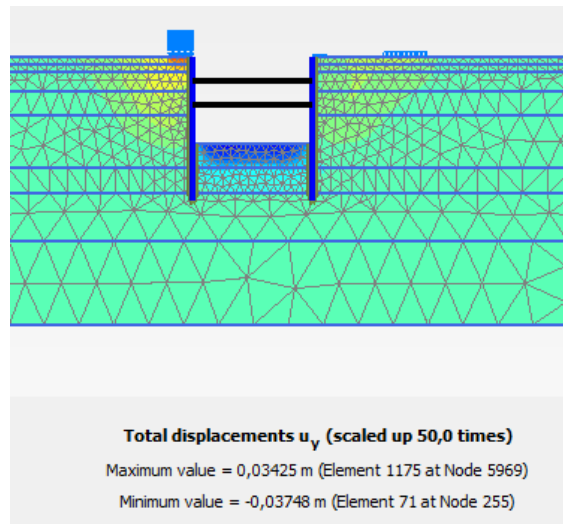


Figure 3.14. Deformation of the model

DESIGN OF A RETAINING STRUCTURE AND ITS PUMPING SYSTEM FOR AN UNDERGROUND
STRUCTURE CONSTRUCTION Presented by TCHINDA KENGNE Franck Junior

CHAPTER 3: RESULTS AND INTERPRETATIONS

This maximum of 37.48mm value represents the maximum settlement on the ground level near the top of the wall is due the presence of the machine during the construction of the wall.

The maximum displacement of the wall is obtained at the last phase of excavation in the Plaxis code and is presented in the figure below.

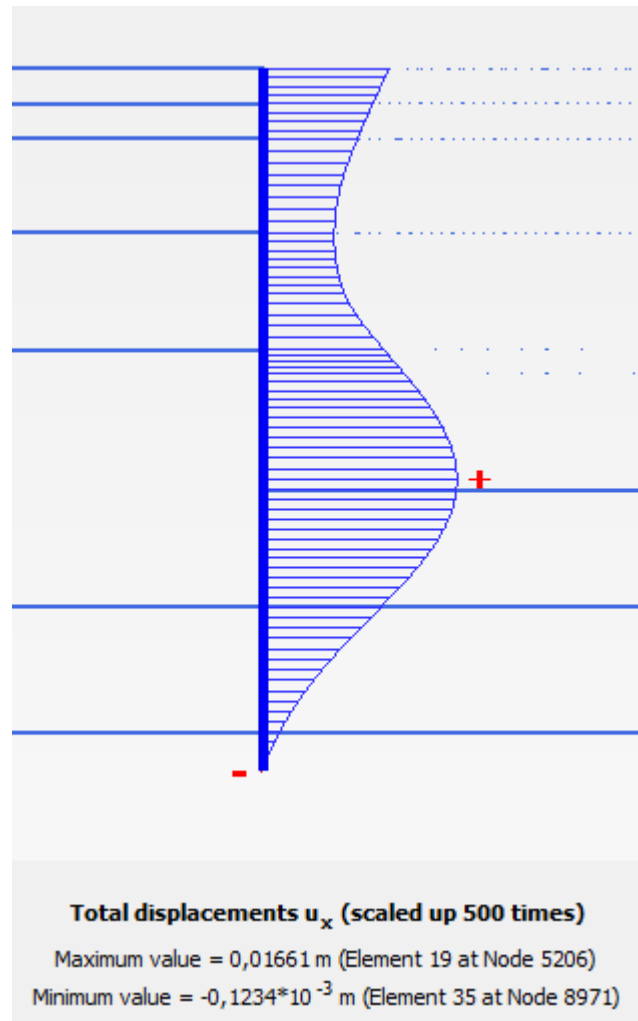


Figure 3.15. Deformation of the wall

The deformation of the wall obtain by the analytical method is less than the deformation obtains with the numerical method and this may be due to the behaviour of the soil which is correctly simulated in the Plaxis software which takes into account certain parameters not taken into account in the analytical method.

CHAPTER 3: RESULTS AND INTERPRETATIONS

This value of the displacement of the wall is less than the admissible value that was 40 mm.

3.4.4.2. Compression force in the struts

The figure 3.16 is the Plaxis output which presents the compression force of the struts due to the lateral pressure on the wall

2D PLAXIS 2D Output - [wall - Calculation results, Node-to-node anchor, third excavation [Phase_6] (6/71), Table of node-to-node anchors]

2D File View Project Deformations Forces Tool Options Expert Window Help

third excavation [Phase_6] (Step 71)

Output Close

Structural element	Node	Local number	X [m]	Y [m]	N [kN]	N _{min} [kN]
NodeToNodeAnchor_1_1	497	1	75,000	51,000	-2544,125	-3329,139
Element 1-1 (Node-to-node anchor)	6105	2	100,000	51,000	-2544,125	-3329,139

2D PLAXIS 2D Output - [wall - Calculation results, Node-to-node anchor, third excavation [Phase_6] (6/71), Table of node-to-node anchors]

2D File View Project Deformations Forces Tool Options Expert Window Help

third excavation [Phase_6] (Step 71)

Output Close

Structural element	Node	Local number	X [m]	Y [m]	N [kN]	N _{min} [kN]
NodeToNodeAnchor_2_1	2415	1	75,000	46,000	-8292,019	-8292,019
Element 2-2 (Node-to-node anchor)	6583	2	100,000	46,000	-8292,019	-8292,019

Figure 3.16. Force on the struts in Plaxis code

We observe that these compression force obtain using the numerical method are close to that obtain using the analytical method. The fact that these two values are close gives us confidence in the reliability of the results.

3.4.4.3. Bending moment diagram on the wall

The following figure is the bending moment diagram of the wall obtain with the Plaxis code and this is the maximum moment obtain in all the phase of excavation.

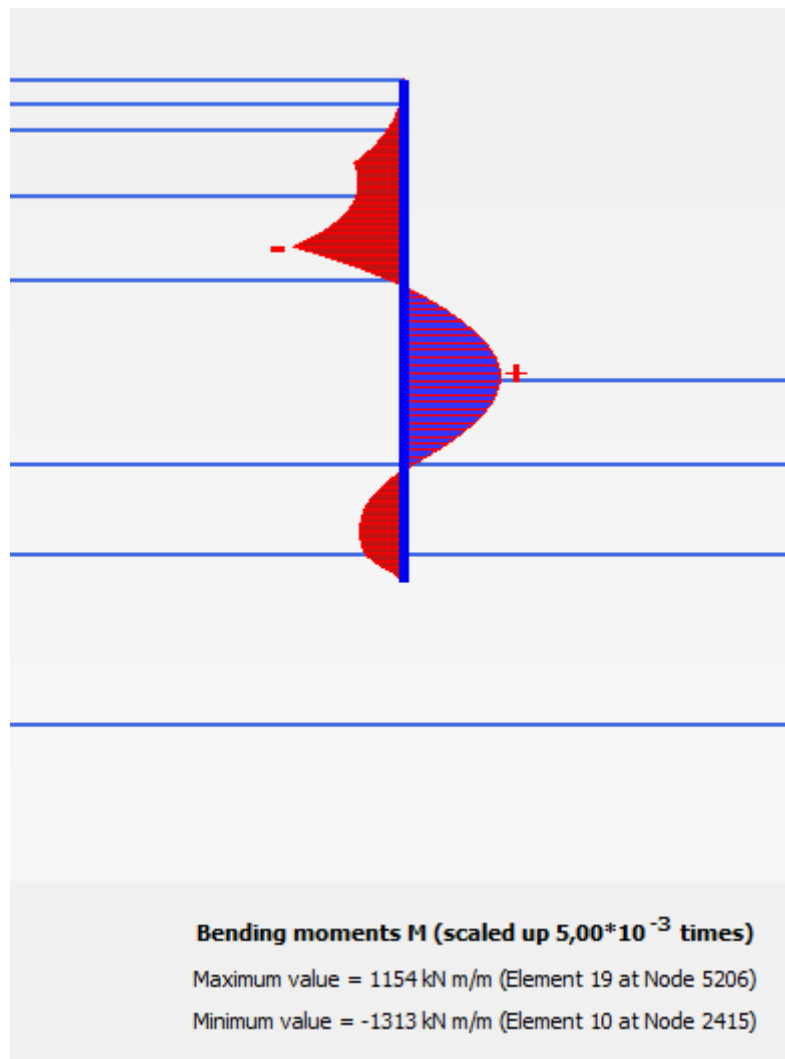


Figure 3.17. Bending moment diagram of the wall

The negative moment is due to the presence of the struts that is going in compression and at the bottom, the change of the concavity means that it exists a point in which the moment is equal to zero.

3.4.4.4. Shear force diagram

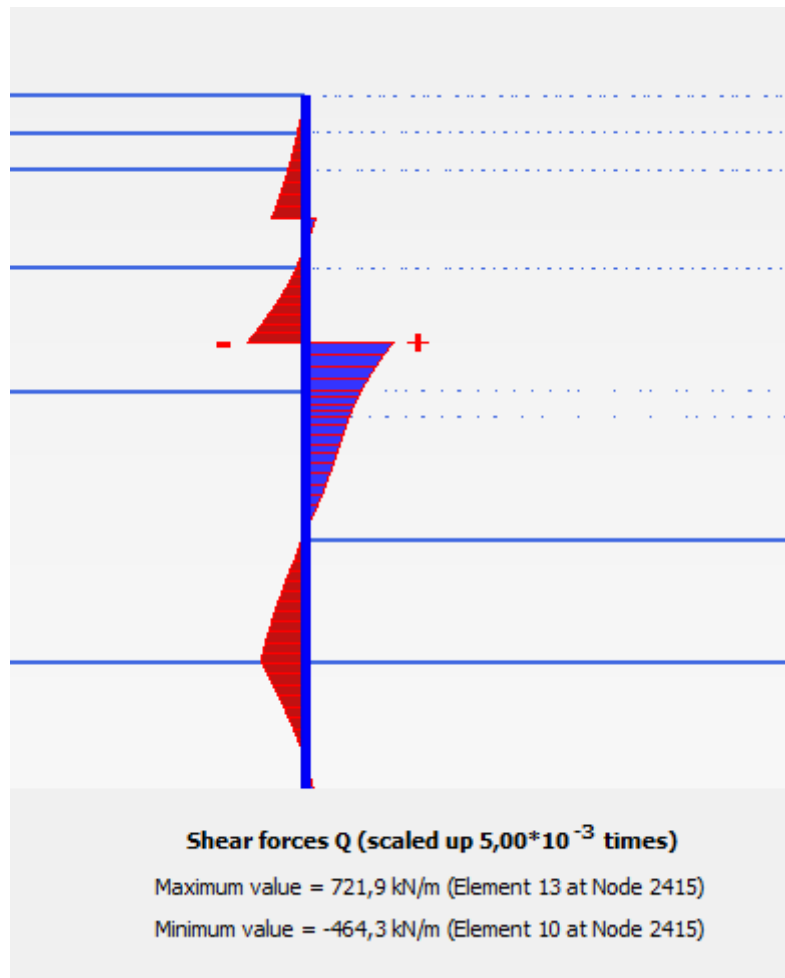


Figure 3.18. Shear force diagram of the wall

The presence of the struts influences the evolution of the shear and in the deeper layer the change of slope of the shear is due to the variation of the load which is different from one layer to another.

Remark: the previous diagram is used by structural engineers to do the structural design of the wall. This result is obtained by increasing a button to those originally planned in the project.

3.4.4.5. Flow on the station

The following figure represents the flow calculated by the Plaxis software and this is the total flow in the station before the realization of a raft.

CHAPTER 3: RESULTS AND INTERPRETATIONS

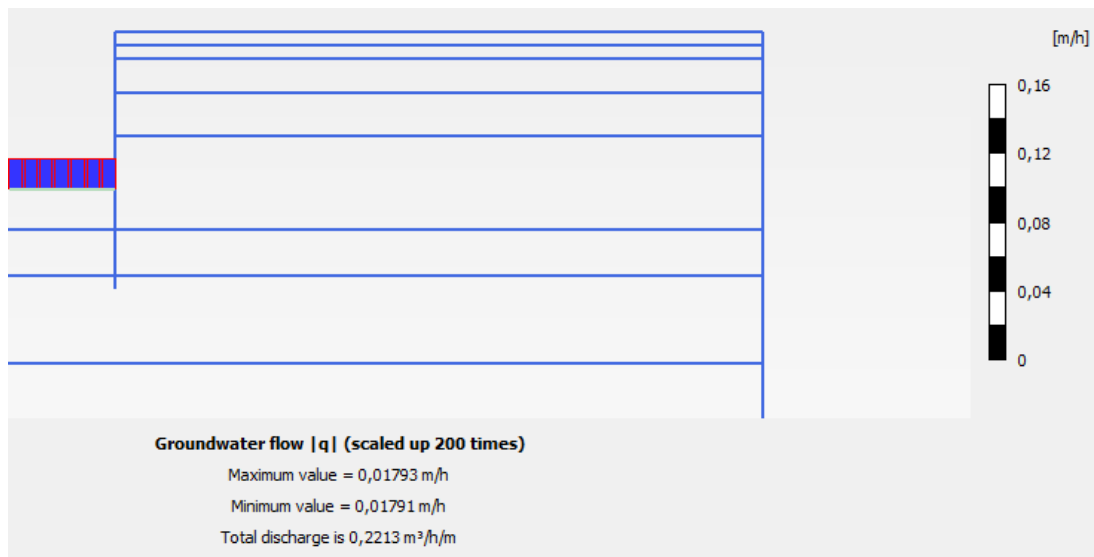


Figure 3.19. Ground water flow in the station

The total discharge display by the software is $0.2213 \text{ m}^3/\text{h}/\text{m}$ and this will be multiplied by the total perimeter of the station in order to have the real flow in the station.

$$Q = 0.2213 * 2 * (60.6 + 25.4) = 38.06 \text{ m}^3/\text{h}$$

This value is close to the value obtain by using the finite difference solution this means that all the conclusions drawn from the analytical results remain valid.

Conclusion

The main objective of this chapter was to present the result of the analytical and numerical design of the diaphragm wall used to construct the Aulnay-sous-Bois station. Then the analytical solution was obtaining by using the approximation presented in the literature review that shows that the pressure formula on the wall differ depending on the type of soil. The numerical result was close to the analytical result and this gives a high level of confidence on the calculation made in this work

GENERAL CONCLUSION

The subject of this work was entitled design of a retaining structure and its pumping system for an underground structure construction. The main objectives were to determine the pressure acting on the wall, the maximum displacement of the wall, the force that compressed the struts and the flow entering in the train station using the analytical method and the numerical method to confirm the results in order to come up with a reliable solution. The stability of the diaphragm wall is a very complex phenomenon that involves several geotechnical or site parameters such as soil, water table, road or surrounding buildings. The first chapter of this work focused on the state of arts of the main terms of the subject that was retaining walls and pumping system. It consists of the classification of the retaining wall in general and in particular to present the technologies used for the installation of the type of wall use in the train station of Aulnay-sous-Bois and the system used to pump the water under the ground. The second chapter presented the method use in order to obtain the result presented in chapter three and the third chapter present the result obtain with the analytical method using excel software and the result obtain with the numerical method using Plaxis software. The approach adopted was to do all the verification and calculation needs to study the stability of the wall using the analytical method and numerical method with the Plaxis software that use the finite element. After the analysis, we obtain that the compression forces are equal to 3370 kN and 8729kN in the strut on the first and second row respectively and the water flow that has to be pumped is 38.06 m³/h.

As perspective, a structural analysis can be done in order to determine the quantity of reinforcement need to overcome the bending moments, the shear force and to determine the section of steel use as strut.

Bibliography

BUDHU, M. (2011). *SOIL Mechanics AND Foundations*.

CFMS. (s.d.). *Guide méthodologique pour le rabattement de la nappe*.

CFMS, & SFEG. (s.d.). *Guide méthodologique pour le rabattement de nappe*.

Clayton, C. R., Woods, R. I., Bond, A. J., & Milititsky, J. (2013). *EARTH PRESSURE AND EARTH RETAINING STRUCTURES*. Taylor & Francis Group, LLC.

CSTC. (juillet 2014). *Exécution des parois moulées*.

Eurocode, 7. (1997). *Geotechnical design*.

Gragnano, C. (2019). *Shear strenght in soil*.

LOMBARDI. (2019). *NOTE D'HYPOTHESES GEOTECHNIQUES PARTICULIERES GARE ALN*. France.

LOMBARDI. (s.d.). *NOTE D'HYPOTHESE GEOTECHNIQUE PARTICULIERE GARE ALN*. France.

MAJORANA, P. C. (s.d.). *Theory of Elasticity*.

MINIERE, B. D. (s.d.). *UTILISATION DES POINTES FILTRANTES POUR L'UTILISATION DES ACQUIFERES*. Orléans.

Prof. Teatini, & L.Di Micco. (2019). *Dimensioning the drainage systems*.

R.F.Craig. (2004). *CRAIG'S SOIL MECHANICS*.

Riadh, S. (s.d.). *MODELISATION NUMERIQUE D'UNE PAROI DE SOUTÈNEMENT EN ZONE URBAINE*.

SIMONINI, P. (2019). *Shear strenght in soil*.

SIMONINI, P. P. (2019). *Seepage in porous media*.

DESIGN OF A RETAINING STRUCTURE AND ITS PUMPING SYSTEM FOR AN UNDERGROUND STRUCTURE CONSTRUCTION Presented by TCHINDA KENGNE Franck Junior

Ventsel, E., & Krauthammer, T. (2001). *Thin Plates and Shells*.

EN 1997-1:2004 Eurocode 7: Geotechnical design - Part 1: General rules. PN-83/B-03010 Retaining walls. Static calculation and design.

Webography.

<https://tkraghu.tripod.com/Page12.html>

<https://fr.m.wikipedia.org/wiki/Mur-de-sout%c3%A8nement>

<https://en.m.wikipedia.org/wiki/Plaxis>

<https://fr.weatherspark.com/y/48246/M%C3%A9t%C3%A9o-moyenne-%C3%A0-Aulnay-sous-Bois-France-tout-au-long-de-l'ann%C3%A9e>

ville-data.com. (2022, february 14). *ville-data.com*

Aulnay-sous-bois.fr. (2022). *ma-ville*.

APPENDICES

APPENDIX 1: This appendix is a picture of a excel sheet use for the determination of the pressure on the wall with the analytical method

DONNEES DU PROBLEME										
couche	c (kPa)	phi(°)	E (Mpa)	poisson coef	Kh(m/s)	Kv (m/s)	Yuns (kN/	Ysat (kN/	Su (kPa)	
R	0	28	27		0,3	0,00001	0,000004	19	19	0
MPH	5	34	60		0,3	0,00001	0,000015	19	19	15
SO1	10	33	60		0,3	0,000029	0,000012	18	18	20
SO2	10	33	120		0,3	0,000029	0,000012	18	18	20
SB	5	33	200		0,3	0,000031	4,1E-06	21	21	5
MC1	20	30	120		0,3	0,00013	0,000052	20	20	50
MC2	50	35	800		0,3	0,00013	0,000052	20	20	50
CG	100	35	1493		0,3	2,1E-06	8,4E-07	21	21	100
calcul de la poussée des terres et de l'eau en utilisant l'EC7 DA1 Comb1 (A1+M1+R1)										
	Y*H0/Su	(Y*H0+qs)	Ka	Y*H0 or (Y-Yw)*H0	Yw*H0	P (kPa)				
R			0,234672	28,5		42,29372				
MPH	1,9		0,3	28,5		65,61				
SO1	3,6		0,3	72		94,77				
SO2	2,0475		0,3	90		131,22				
SB	24,618	3,0412	0,893061	82,0227	71,9073	586,589				
calculation of the force on the button step by step										
en considerant la somme des moments nul au niveau de la deuxième rangée de boutons, on obtient										
couche	b1 (m) rec	b2 (m) tri	b3 (m)rect		A (kN/m)	B1 (kN/m)	B2 (kN/m)			
R	9,25				561,7145	251,9718	1202,875			
MPH	7,75	8,25	7,5625							
SO1	5	6,333333	4,5							
SO2	1,5	2,166667	0,416667							
SB	4,5	7,5	3,375							
	distance entre le bouton dans le plan (m				6					
	1st button (kN)			3370,287062						

APPENDIX 2: This appendix presents the iteration need to determine the flow

Données du problème																					
couches	Kh(m/s)	Kv (m/s)	épaisseur de la couche																		
SO2	0,000029	0,000012	5																		
SB	0,000031	4,1E-06	11																		
MC1	0,00013	0,000052	5,37																		
MC2	0,000013	0,000052	10,13																		
CG	0,000021	8,4E-07	17,5																		
calcul de la perméabilité equivalente																					
Keh (m/s)	2,76029E-05		a																		
Kev (m/s)	5,0614E-06		5,453606 L (m)																		
Ke (m/s)	1,18199E-05		l (m)																		
coordonnées des points de la grille																					
	0	3	6	9	12	15	18	21	24	27	30	33	36	39	42	45	48	51	54	57	60
14	0	11,43	11,43	11,43	11,43	11,43	11,43	11,43	11,43	11,43	11,43	11,43	11,43	11,43	11,43	11,43	11,43	11,43	11,43	11,43	11,43
15	3	11,4	11,3	11,25	11,2	11,15	11,1	11,05	11	10,9	10,8	10,7	10,6	10,6	10,5	10,5	10,4	10,3	10,2	10,1	10,1
16	6	11,3	11,25	11,2	11,1	11	10,9	10,8	10,7	10,6	10,5	10,4	10,3	10,2	10,1	10	9,9	9,8	9,7	9,6	9,5
17	9	11,1	10,9	10,7	10,5	10,3	10,1	9,9	9,7	9,5	9,3	9,1	8,9	8,7	8,5	8,3	8,1	7,9	7,7	7,5	7,3
18	12	10,8	10,7	10,6	10,4	10,2	10	9,8	9,6	9,4	9,2	9	8,8	8,6	8,4	8,2	8	7,8	7,6	7,4	7,2
19	15	10,5	10,4	10,3	10,2	10,1	9,9	9,7	9,5	9,3	9,1	8,9	8,7	8,5	8,3	8,1	7,9	7,7	7,5	7,3	7,1
20	18	10,2	10	9,8	9,6	9,4	9,2	9	8,8	8,6	8,4	8,2	8	7,8	7,6	7,4	7,2	7	6,8	6,6	6,4
21	21	9,9	9,7	9,5	9,3	9,1	8,9	8,7	8,5	8,3	8,1	7,9	7,7	7,5	7,3	7,1	6,9	6,7	6,5	6,3	6,1
22	24	9,6	9,4	9,2	9	8,8	8,6	8,4	8,2	8	7,9	7,8	7,7	7,4	7,3	7	6,9	6,6	6,4	6,2	6,1
23	27	9,3	9,2	9,1	9	8,7	8,6	8,4	8,2	8	7,8	7,6	7,4	7,2	7	6,8	6,6	6,4	6,3	6,2	6,1
24	30	9	8,8	8,6	8,4	8,2	8	7,8	7,6	7,4	7,2	7	6,8	6,6	6,5	6,5	6,4	6,3	6,2	6,1	5,715

APPENDIX

exécution des étapes de la méthodologie (étape 1)		0	3	6	9	12	15	18	21	24	27	30	33	36	39	42	45	48	51	54	57	60
26																						
27	0	11,43	11,43	11,43	11,43	11,43	11,43	11,43	11,43	11,43	11,43	11,43	11,43	11,43	11,43	11,43	11,43	11,43	11,43	11,43	11,43	11,43
28	3	11,365	11,32732	11,26007	11,21007	11,16007	11,11007	11,06007	10,98895	10,91782	10,84665	10,77548	10,70431	10,63314	10,56197	10,49080	10,41963	10,34846	10,27729	10,20612	10,13495	10,06378
29	6	11,325	11,22676	11,14401	11,06126	10,95739	10,85351	10,74964	10,64577	10,53802	10,43027	10,32252	10,21477	10,11178	10,00703	9,907029	9,799281	9,691534	9,583786	9,476038	9,374505	9,272072
30	9	11,1	10,91162	10,73099	10,53874	10,34649	10,15423	9,961981	9,769728	9,577476	9,385224	9,192971	9,000719	8,808466	8,616214	8,423962	8,231710	8,039458	7,847205	7,654953	7,462701	7,270448
31	12	10,9	10,69225	10,54225	10,39225	10,2	10	9,8	9,6	9,4	9,2	9	8,8	8,6	8,4	8,2	8	7,8	7,6	7,4	7,2	7,0
32	15	10,6	10,39225	10,2845	10,16901	10,01126	9,853514	9,653514	9,453514	9,253514	9,053514	8,853514	8,653514	8,453514	8,253514	8,053514	7,853514	7,653514	7,453514	7,253514	7,053514	6,853514
33	18	10,25	10,00775	9,815495	9,623243	9,43099	9,23099	9,03099	8,83099	8,63099	8,43099	8,23099	8,03099	7,83099	7,63099	7,43099	7,23099	7,03099	6,83099	6,63099	6,43099	6,23099
34	21	9,95	9,7	9,5	9,3	9,1	8,9	8,7	8,5	8,3	8,107748	7,915495	7,723243	7,531000	7,338748	7,146495	6,954243	6,761990	6,569738	6,377485	6,185233	5,992980
35	24	9,65	9,407748	9,215495	9,023243	8,815495	8,623243	8,423243	8,223243	8,023243	7,823243	7,623243	7,423243	7,223243	7,023243	6,823243	6,623243	6,423243	6,223243	6,023243	5,823243	5,623243
36	27	9,4	9,184505	9,06901	8,96901	8,873514	8,783514	8,693514	8,603514	8,513514	8,423514	8,333514	8,243514	8,153514	8,063514	7,973514	7,883514	7,793514	7,703514	7,613514	7,523514	7,433514
37	30	9,05	8,85	8,7	8,5	8,45	8,3	8,1	7,9	7,7	7,5	7,3	7,1	6,95	6,775	6,675	6,525	6,4	6,3	6,2	6,08275	5,975
38																						
39																						
40	exécution des étapes de la méthodologie (étape 2)																					
41	0	11,43	11,43	11,43	11,43	11,43	11,43	11,43	11,43	11,43	11,43	11,43	11,43	11,43	11,43	11,43	11,43	11,43	11,43	11,43	11,43	11,43
42	3	11,37866214	11,31499	11,27153	11,21558	11,16528	11,11498	11,05576	10,99653	10,91915	10,84177	10,77332	10,68701	10,65486	10,56856	10,53641	10,45011	10,38165	10,3132	10,22689	9,360252	8,249576
43	6	11,29587859	11,21668	11,121	11,02338	10,92576	10,81921	10,71267	10,60285	10,49303	10,37993	10,26684	10,16029	10,0472	9,947196	9,834102	9,727555	9,61446	9,501366	9,44882	9,384791	9,316126
44	9	11,183107	10,92231	10,7436	10,56787	10,38247	10,19646	10,01046	9,824451	9,638445	9,451839	9,265354	9,079228	8,893523	8,707218	8,521512	8,335207	8,148901	7,962596	7,75437	7,546152	7,337927
45	12	10,8961262	10,71041	10,53691	10,36845	10,19345	10,0006	9,801201	9,601801	9,402401	9,203001	9,003601	8,804202	8,604802	8,405402	8,206003	8,006603	7,807203	7,607803	7,408403	7,209003	7,009603
46	15	10,6461262	10,42796	10,26486	10,12617	9,980927	9,79878	9,616633	9,416633	9,216633	9,016633	8,816633	8,616633	8,416633	8,216633	8,016633	7,816633	7,616633	7,416633	7,216633	7,016633	6,816633
47	18	10,3038738	10,03482	9,827389	9,640483	9,44703	9,253577	9,053577	8,853577	8,653577	8,45178	8,254778	8,055378	7,854778	7,655378	7,454778	7,255378	7,054778	6,854778	6,654778	6,454778	6,254778
48	21	9,975	9,722327	9,502401	9,303602	9,103602	8,904202	8,704202	8,504202	8,310749	8,117296	7,93039	7,73039	7,543484	7,33039	7,143484	6,93039	6,73039	6,53039	6,30511	6,028818	5,715
49	24	9,678873803	9,43422	9,226188	9,026188	8,839283	8,632735	8,439283	8,257135	8,074988	7,929746	7,748799	7,621141	7,384505	7,258316	7,089636	6,842265	6,594663	6,347506	6,20032	5,987122	5,715
50	27	9,417252393	9,229758	9,027685	8,90357	8,81243	8,539275	8,321423	8,139275	7,945222	7,75237	7,565464	7,365464	7,189979	6,981095	6,815031	6,63021	6,470242	6,332147	6,156267	5,964731	5,715
51	30	9,2	9,067252	8,959505	8,759505	8,626757	8,393131	8,226757	8,026757	7,826757	7,630631	7,434505	7,250879	7,053255	6,902376	6,711126	6,576498	6,435124	6,303874	6,182188	5,96854	5,715
52																						
53	exécution des étapes de la méthodologie (étape 3)																					
54	0	11,43	11,43	11,43	11,43	11,43	11,43	11,43	11,43	11,43	11,43	11,43	11,43	11,43	11,43	11,43	11,43	11,43	11,43	11,43	11,43	11,43
55	3	11,3724954	11,32483	11,26687	11,21969	11,16723	11,1127	11,05817	10,99194	10,92571	10,85533	10,77741	10,72665	10,64496	10,61004	10,52835	10,47759	10,40344	10,32928	9,906565	9,346648	8,055063
56	6	11,2976124	11,19453	11,10259	11,00298	10,89845	10,79388	10,68346	10,57904	10,45842	10,34381	10,23127	10,11458	10,10143	9,983735	9,79558	9,627895	9,560354	9,342208	8,990353	7,791803	6,241141
57	9	11,10909659	11,03954	10,95809	10,85856	10,75903	10,65950	10,56000	10,46050	10,36100	10,26150	10,16200	10,06250	9,96300	9,86350	9,76400	9,66450	9,56500	9,46550	9,36600	9,26650	9,16700
58	12	10,91435794	10,7101	10,53396	10,36237	10,18409	9,997372	9,803113	9,604705	9,406273	9,207841	9,009409	8,810978	8,612547	8,414116	8,215775	8,017344	7,818912	7,52355	7,157095	6,483846	5,715
59	15	10,66204194	10,40625	10,26236	10,14054	9,940435	9,772176	9,579766	9,387356	9,187402	8,987495	8,787588	8,587681	8,387774	8,187867	7,987960	7,788053	7,588146	7,292827	6,935742	6,36751	5,715
60	18	10,34047342	10,11173	9,844777	9,649246	9,461787	9,265983	9,070132	8,870132	8,670132	8,470132	8,270132	8,070132	7,870132	7,670132	7,470132	7,270132	7,070132	6,870132	6,540132	6,158894	5,715
61	21	10,01310025	9,738053	9,515106	9,307702	9,109984	8,909984	8,710745	8,514895	8,319044	8,131632	7,939221	7,752658	7,54222	7,36105	7,144359	6,95704	6,74526	6,54041	6,296074	6,022414	5,715
62	24	9,704610197	9,456174	9,235603	9,043714	8,839218	8,652059	8,455453	8,267146	8,09884	7,915448	7,71294	7,563751	7,428454	7,288902	7,180809	7,039284	6,834261	6,402768	6,215161	5,963721	5,715
63	27	9,454316127	9,226849	9,070721	8,860412	8,72322	8,503131	8,338306	8,134912	7,946605	7,759446	7,563989	7,368532	7,180345	7,014144	6,8131	6,652979	6,486402	6,322154	6,155073	5,942172	5,715
64	30	9,242252393	9,154755	8,970532	8,848351	8,628781	8,483016	8,265683	8,083016	7,872558	7,6915	7,503109	7,304672	7,132803	6,934143	6,777234	6,604168	6,455214	6,320402	6,146237	5,956662	5,715
65																						
66	exécution des étapes de la méthodologie (étape 4)																					
67	0	11,43	11,43	11,43	11,43	11,43	11,43	11,43	11,43	11,43	11,43	11,43	11,43	11,43	11,43	11,43	11,43	11,43	11,43	11,43	11,43	11,43
68	3	11,377413	11,31853	11,27133	11,21696	11,16589	11,11258	11,053	10,99343	10,92683	10,85704	10,79713	10,72065	10,67638	10,59831	10,55404	10,47165	10,41765	10,19081	9,895641	9,078448	8,051662
69	6	11,28351157	11,18932	11,08539	10,9852	10,88139	10,77239	10,66331	10,54905	10,43479	10,31929	10,2044	10,09194	9,972927	9,86255	9,749243	9,639739	9,478444	9,261823	8,91307	7,685996	5,975482
70	9	11,11687073	10,93649	10,76882	10,59918	10,42742	10,25495	10,07865	9,901701	9,724107	9,546513	9,369254	9,191325	9,013349	8,837433	8,661457	8,485452	8,303082	7,972889	7,519976	6,354683	4,81229
71	12	10,90960035	10,71876	10,5327	10,35671	10,17912	9,994725	9,803079	9,602870	9,410997	9,215751	9,016505	8,819338	8,622085	8,424997	8,227744	8,030577	7,792369	7,516703	7,04007	6,458167	5,715
72	15	10,67850502	10,4508	10,26055	10,08658	9,920476	9,740201	9,557586	9,369395	9,164362	8,964501	8,764919	8,56508	8,365402	8,165405	7,965727	7,765723	7,528202	7,249143	6,835736	6,324751	5,715
73	18	10,36457511	10,09227	9,86255	9,66147	9,468088	9,2776	9,08002	8,883004	8,685495	8,485978	8,286508	8,088488	7,887551	7,690149	7,487559	7,289524	7,072280	6,626096	5,516072	4,139649	5,715
74	21	10,03926212	9,763722	9,52556	9,317803	9,115298	8,917904	8,720242	8,523222	8,328809	8,13772	7,945555	7,752128	7,571532	7,375105	7,174222	6,987117	6,765054	6,536013	6,296625	6,014179	5,715
75	24	9,734637253	9,472019	9,256602	9,044638	8,858534	8,656512	8,469662	8,284547	8,097732	7,916667											

APPENDIX

110	exécution des étapes de la méthodologie (étape 7)																					
111	0	3	6	9	12	15	18	21	24	27	30	33	36	39	42	45	48	51	54	57	60	
112	0	11,43	11,43	11,43	11,43	11,43	11,43	11,43	11,43	11,43	11,43	11,43	11,43	11,43	11,43	11,43	11,43	11,43	11,43	11,43	11,43	11,43
113	3	11,37376497	11,31841	11,26238	11,21095	11,15659	11,10134	11,04462	10,98505	10,92321	10,86402	10,80735	10,75322	10,69354	10,63203	10,53995	10,46428	10,2759	10,04645	9,543626	8,912703	7,946053
114	6	11,27445405	11,16396	11,06091	10,9534	10,84686	10,73795	10,62554	10,51226	10,39701	10,27944	10,16623	10,04602	9,936683	9,812435	9,695272	9,509579	9,290353	8,806236	8,194145	7,10634	5,815447
115	9	11,10883452	10,94766	10,78279	10,62375	10,4623	10,29959	10,13521	9,968235	9,800249	9,631958	9,462448	9,295164	9,125212	8,958508	8,773553	8,576978	8,252469	7,846564	7,05202	6,041014	4,431552
116	12	10,91811605	10,71949	10,53498	10,35091	10,17195	9,989587	9,805273	9,616245	9,42596	9,23416	9,040837	8,84761	8,654974	8,458583	8,258317	8,024007	7,758244	7,367483	6,908795	5,295776	5,715
117	15	10,68693545	10,46556	10,25642	10,0653	9,877199	9,694425	9,504712	9,314729	9,118426	8,922226	8,723465	8,525482	8,326046	8,124996	7,916938	7,688033	7,426301	7,096842	6,908795	6,225773	5,715
118	18	10,40965685	10,14295	9,906486	9,690332	9,489546	9,292943	9,099767	8,903037	8,708252	8,509451	8,314539	8,113572	7,911917	7,714489	7,514183	7,293713	7,057626	6,708653	6,462831	6,101225	5,715
119	21	10,10034156	9,82004	9,574829	9,349015	9,143953	8,942767	8,747359	8,554962	8,359183	8,173976	7,979739	7,793788	7,585003	7,405504	7,18884	6,999297	6,768644	6,545277	6,280896	6,00766	5,715
120	24	9,797875739	9,53816	9,294564	9,080821	8,879642	8,693874	8,498166	8,311012	8,13058	7,961599	7,770119	7,562471	7,404162	7,183677	7,024254	6,800441	6,626451	6,398693	6,192445	5,922118	5,715
121	27	9,544919981	9,309321	9,125557	8,90821	8,744885	8,535609	8,365491	8,167126	7,982629	7,799031	7,602614	7,415117	7,227243	7,064145	6,862886	6,70004	6,508154	6,329814	6,131202	5,927588	5,715
122	30	9,365923908	9,262933	9,064089	8,908664	8,696694	8,537348	8,33053	8,154264	7,96113	7,770413	7,591424	7,390901	7,22273	7,020312	6,858725	6,668357	6,502079	6,318279	6,128252	5,926741	5,715
123																						
124	exécution des étapes de la méthodologie (étape 8)																					
125	0	11,43	11,43	11,43	11,43	11,43	11,43	11,43	11,43	11,43	11,43	11,43	11,43	11,43	11,43	11,43	11,43	11,43	11,43	11,43	11,43	11,43
126	3	11,37420712	11,31481	11,2617	11,20673	11,1534	11,09803	11,04081	10,98193	10,92282	10,85929	10,80276	10,73572	10,68316	10,60899	10,5466	10,41751	10,27161	9,942049	9,531098	8,82593	7,943176
127	6	11,26886313	11,16232	11,05309	10,94822	10,84006	10,73066	10,61965	10,50591	10,39056	10,27461	10,15762	10,04646	9,924602	9,812072	9,660348	9,497123	9,174376	8,773899	8,009456	7,077943	5,749611
128	9	11,11105808	10,94518	10,78761	10,62713	10,46907	10,30883	10,14654	9,982699	9,817356	9,65073	9,4825	9,317535	9,150322	8,978223	8,800136	8,552335	8,260198	7,720933	7,03795	5,891771	4,417977
129	12	10,91416365	10,72458	10,53498	10,35208	10,17017	9,989911	9,805633	9,619624	9,430254	9,240169	9,048639	8,857577	8,664335	8,469833	8,257403	8,02753	7,717793	7,354932	6,838407	6,225773	5,715
130	15	10,69234031	10,46541	10,25893	10,05965	9,87225	9,683256	9,49651	9,303537	9,110517	8,913274	8,716701	8,517912	8,319321	8,116075	7,903374	7,668502	7,394839	7,061813	6,665105	6,204217	5,715
131	18	10,41494309	10,15881	9,916484	9,699432	9,494572	9,298366	9,102336	8,908788	8,711289	8,517083	8,312759	8,123461	7,92046	7,724181	7,511661	7,294854	7,046316	6,648265	6,448265	6,093223	5,715
132	21	10,11502849	9,838046	9,587158	9,364223	9,151888	8,953056	8,756628	8,5616	8,372983	8,175192	7,992938	7,788459	7,609252	7,396553	7,212754	6,989393	6,783095	6,534827	6,284397	6,002407	5,715
133	24	9,819250882	9,549108	9,320023	9,093535	8,900416	8,696696	8,510808	8,321605	8,130918	7,955951	7,753339	7,591093	7,378195	7,217403	6,997297	6,829121	6,605584	6,413802	6,180266	5,958766	5,715
134	27	9,553598533	9,345358	9,119699	8,945219	8,732176	8,564551	8,361126	8,183137	7,992806	7,802033	7,625423	7,424509	7,257998	7,053886	6,891296	6,693904	6,522572	6,326071	6,136305	5,926019	5,715
135	30	9,403926688	9,262164	9,105678	8,894301	8,733946	8,52461	8,355648	8,156478	7,972484	7,787654	7,591649	7,419297	7,216425	7,052436	6,853611	6,690221	6,500736	6,32249	6,127306	5,924607	5,715
136																						
138	exécution des étapes de la méthodologie (étape 9)																					
139	0	11,43	11,43	11,43	11,43	11,43	11,43	11,43	11,43	11,43	11,43	11,43	11,43	11,43	11,43	11,43	11,43	11,43	11,43	11,43	11,43	11,43
140	3	11,37240261	11,31458	11,25779	11,20469	11,14969	11,0945	11,03763	10,97967	10,91901	10,86131	10,79693	10,74223	10,67312	10,61583	10,5182	10,41754	10,19875	9,932436	9,436013	8,817221	7,921483
141	6	11,26826108	11,15617	11,05053	10,94198	10,83507	10,72576	10,61447	10,50158	10,38789	10,27114	10,15873	10,03887	9,927533	9,79265	9,657506	9,427831	9,155716	8,629039	7,981487	6,953805	5,741074
142	9	11,10702215	10,94834	10,78721	10,63172	10,47374	10,31593	10,15613	9,99447	9,831233	9,667881	9,502571	9,339726	9,170594	9,002049	8,795277	8,56614	8,184584	7,713432	6,920248	5,875653	4,347748
143	12	10,91729701	10,72066	10,53555	10,35022	10,17094	9,989163	9,807364	9,621844	9,435171	9,24604	9,056946	8,869596	8,674934	8,474238	8,264653	8,006629	7,712349	7,295652	6,824534	6,241264	5,715
144	15	10,68978652	10,47006	10,25666	10,05942	9,865398	9,678144	9,487289	9,297423	9,102574	8,908188	8,715335	8,51751	8,313183	8,109125	7,891087	7,650979	7,367775	6,830498	6,348264	6,189848	5,715
145	18	10,420407548	10,16355	9,926912	9,706521	9,50094	9,301507	9,10714	8,910804	8,7174	8,518916	8,326523	8,124178	7,930091	7,722298	7,51704	7,286725	7,041042	6,755197	6,43815	6,084992	5,715
146	21	10,12649432	9,851305	9,603787	9,373701	9,16466	8,960963	8,764958	8,572614	8,376563	8,19126	7,990266	7,809801	7,603111	7,402067	7,202477	7,007851	6,742731	6,427369	6,003549	5,715	
147	24	9,832068363	9,573056	9,326297	9,117115	8,902385	8,713854	8,516855	8,328844	8,145614	7,950176	7,790408	7,572921	7,4088	7,193553	7,027719	6,807603	6,626322	6,39874	6,188583	5,950202	5,715
148	27	9,582304581	9,347339	9,155757	8,936471	8,764538	8,565668	8,383045	8,186585	8,001745	7,818828	7,622603	7,451547	7,248202	7,083986	6,881542	6,715106	6,516335	6,334296	6,130344	5,926772	5,715
149	30	9,407881226	9,30008	9,098966	8,932515	8,720816	8,554674	8,350835	8,173601	7,982436	7,79205	7,614449	7,414273	7,246932	7,044452	6,881312	6,685134	6,514464	6,320046	6,128577	5,923586	5,715
150																						
151	exécution des étapes de la méthodologie (étape 10)																					
152	0	11,43	11,43	11,43	11,43	11,43	11,43	11,43	11,43	11,43	11,43	11,43	11,43	11,43	11,43	11,43	11,43	11,43	11,43	11,43	11,43	11,43
153	3	11,37228858	11,31169	11,25663	11,20099	11,14696	11,09122	11,03478	10,97638	10,9187	10,85682	10,80062	10,73493	10,67899	10,59809	10,52088	10,36939	10,19325	9,850252	9,426105	8,758262	7,919305
154	6	11,2642888	11,15506	11,04496	10,93899	10,83044	10,72174	10,61107	10,49899	10,38462	10,27196	10,15419	10,0428	9,916703	9,795064	9,617445	9,419817	9,053728	8,608011	7,849933	6,936456	5,699192
155	9	11,10830015	10,94577	10,79049	10,63289	10,47835	10,32152	10,16384	10,00422	9,843627	9,681109	9,519924	9,354532	9,191085	9,006257	8,811519	8,525151	8,18538	7,608245	6,888826	5,77561	4,33945
156	12	10,9138396	10,72376	10,53335	10,35206	10,16967	9,990375	9,808014	9,6													

APPENDIX 3 : Drilling machine for a large diameter drawdown well (CFMS, 2016)



APPENDIX 4: The limit between the different formations found in the cores and pressiometrics are presented in this appendix

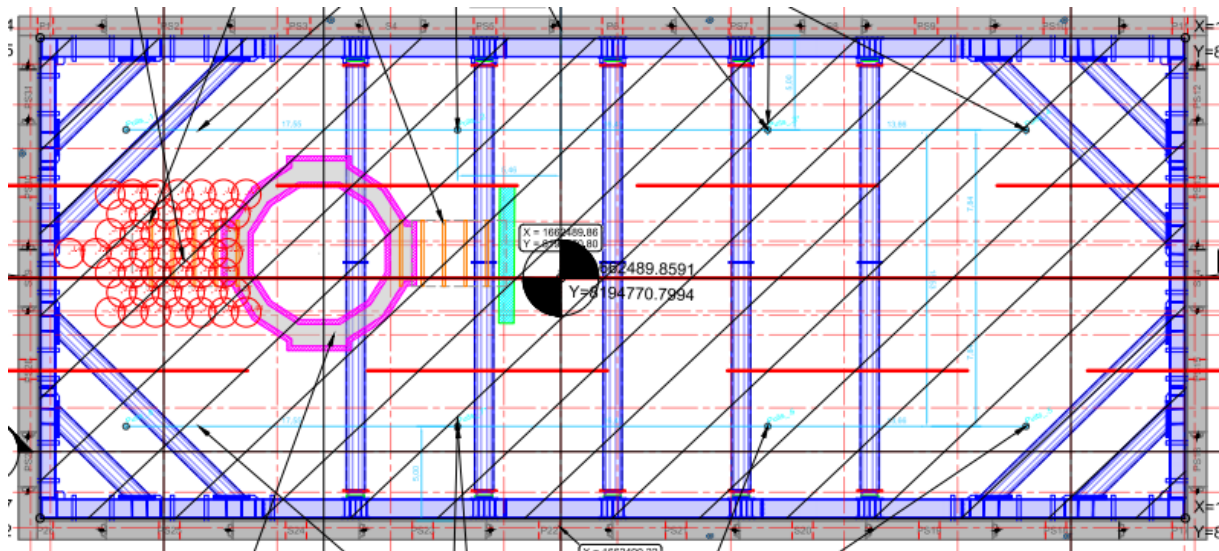
	Cote NGF du toit de la couche										
	AUL-AVP-FD1064*	AUL-AVP-SP1061	AUL-AVP-SC0876	AUL-AVP-FD1063*	AUL-AVP-FD1062*	AUL-AVP-FD2134*	AUL-AVP-FD2652*	AUL-AVP-FD1540*	AUL-AVP-FD1539*	AUL-AVP-SC0877	AUL-AVP-FD1538*
R, Am,	55.85	56.02	56.36	56.0	56.3	57.7	56.6	56.4	56.2	56.3	56.15
MPH (1) -SV	54.55	55.22	54.71	54.5	55	55.95	55.35	55.1	54.9	54.8	55.15
SO(1)	52.35	51.52	53.1	52.5	53	<54.7	53.6	53.7	53.2	53	53.65
SO(2)			49.81					48.9			
SB(1)	42.85	42.62	43.76	45	45.4		43.8	43.4	44.2	43.9	45.15
MC(2)	32.85	35.27		33.1	33.3		33.6	33.4	33.2	33.2	30.65*
MC(4)	26.85	31.20	32.16	29	27.3		28.6	27.4	27.2	28.8	
CG	<20.85	<27.52	16.36 17.91	<21	<20.8		<21.6	<21.4	<20.7	17.4	<17.65

	Cote NGF du toit de la couche										
	AUL-PRO-FD2917*	AUL-PRO-SP05441 (PR102)	AUL-PRO-SP05440 (PR101)	AUL-PRO-SC05432 (SC101)	Puit (7.5m de diamètre)	AUL-FAI-SP0018	AUL-PRO-SC05433 (SC102**)	AUL-PRO-SC05431 (SD/C106)	AUL-PRO-SC05434 (SC103**)	AUL-PRO-SP3279	AUL-PRO-SC3278
R, Am,	56.38	56.80	56.80	56.80	56.80	57			56.5	57.36	57.32
MPH (1) -SV	55.23	54.8	55.10	55.7	55.8	55.5		57.8	Marnes cimentées	-	
SO(1)	53.80	53.30	53.80	53.6	51.8	54.5 ?	Horizontal	54.3	indif.	54.76	54.72
SO(2)	47.88	49.60	49.80	49.60	47.8		Jet grouting	52.30		52.36	
SB(1)	45.68	46.0	46.80	46.8	44.8	47.3		46.30	46.00	47.36	47.17
MC(2)	33.58	34.80	34.30	35.10		33.3*		<36.0	34.20	34.86	34.72
MC(4)	28.6		30	32.0						30.86	
CG	16.18	<31.59	<28.6	<29.10					<31.40	20.36	20.22

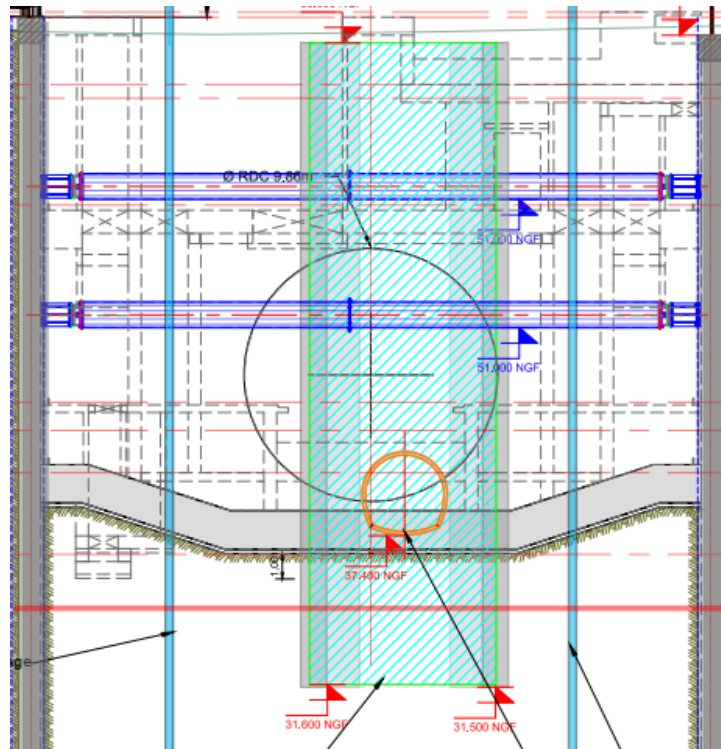
	Cote NGF du toit de la couche										
	AUL-AVP-SC2163	AUL-FAI-SC0015	AUL-AVP-SP2164	AUL-PRO-FD2918*	AUL-PRO-FD3280*	AUL-AVP-SP1060	AUL-FAI-SC0017	AUL-FAI-SP0019*	AUL-PRO-FD2919*	AUL-FAI-SC0016*	AUL-AVP-SC1585*
R, Am,	57.4	56.9	57.80	57.84	57.84	57.74	58.2	58	58.13	58.2	58.03
MPH (1) -SV	56.14	55.4	56.65	56.64	56.64	56.44	56.8	57.3 56.5 50.2	56.93	56.65	
SO(1)	53.9	53.9	54.8	55.34	55.84	53.74	55.5		54.13	54.6	55.33
SO(2)			50.8		51.84	51.04	50.2				
SB(1)	47.54	46.7	47.00	46.24	46.84	45.25	47.2	45.5	46.73	46.35	45.83
MC(2)	35.44	35.82	33.60	35.64	36.64	36.24	35.21	32.3	32.53	31.2	32.83
MC(4)						31.44	30.8				28.83
CG	19.24	20.9	18.00	16.04	18.2	<29.74	16.7	<31	17.73	19,0	17.23

	Cote NGF du toit de la couche				Lithologie moyenne <i>(Hors sondages marqué d'une étoile*)</i>	Lithologie cahier B	Lithologie retenue	
	AUL-EXE-SC06601 AUL-EXE-SC1	P1	P2	P3			Ouest	Est
R, Am,	57,6	57,6	57,6	57,6	57,2	57,8	56	58
MPH (1) -SV	56,4	56,8	56,4	55,6	55,8	55,8	54,5	57
SO(1)	55,4	55,6	55,6	54,4	54,2	53,3	53	55
SO(2)	-	-	-	-	50,4	50,3	49	51
SB(1)	45,6	46,6	47,6	47,1	46,2	47,0	44	46,5
MC(2)	34,1	36,1	35,8	36,1	34,8	35,0	33	35
MC(4)	-	-	-	-	30,5	30,8	27,5	30
CG	18,6	18,6	18,6	18,6	18,2	17,5	17,5	17,5

APPENDIX 5: The top view of the train station after the installation of the struts is presented in this appendix



APPENDIX 6: This appendix presented the cross section of the Aulnay-sous-Bois train station



APPENDIX 7: Drilling machine of diaphragm wall



APPENDIX 8: Hydraulic drilling machine of diaphragm wall



APPENDIX 9: Reinforcement cage of a panel of diaphragm wall

